Physicochemical Problems of Mineral Processing

Fizykochemiczne Problemy Mineralurgii

Index No. 32213X

ISSN 0137-1282

34

2000

Physicochemical
Problems
of Mineral Processing
34 (2000)

Instructions for preparation of manuscripts

It is recommended that the following guidelines be followed by the authors of the manuscripts:

- Original papers dealing with the principles of mineral processing and papers on technological aspects of mineral processing will be published in the journal which appears once a year.
- The manuscript should be sent to the Editor for reviewing before February 15 each year.
- The manuscript should be written in English. For publishing in other languages the approval of the editor is necessary.
- Contributors whose first language is not the language of the manuscript are urged to have their manuscript competently edited prior to submission.
- The manuscript should not exceed 10 pages.
- Two copies of the manuscript along with an electronic copy on a floppy disc should be submitted for publication before April 15.
- There is a 80 USD fee for printing the paper. No fee is required for the authors participating in the Annual Symposium on Physicochemical Problems on Mineral Processing.
- Manuscripts and all correspondence regarding the symposium and journal should be sent to the Editor.

Address of the Editorial Office
Technical University of Wrocław
Wybrzeże Wyspiańskiego 27, 50-370 Wrocław, Poland
Institute of Mining Engineering
Laboratory of Mineral Processing

Location of the Editional Office:
Pl. Teatralny 2, Wrocław, Poland
Phone: 344 12 01, 44 12 02
Fax: 3448123, telex: 0712254 pwr.pl
E-mail: Andrzej.Luszczkiewicz@.ig.pwr.wroc.pl
Jan.Drzymala@.ig.pwr.wroc.pl
http://www.ig.pwr.wroc.pl/conference/conf_uk.html

Orders from abroad can be placed with
Ars Polona, Krakowskie Przedmieście 7, 00-950 Warszawa
Bank account number: Bank Handlowy SA, Warszawa 201061–0071–0000

Physicochemical Problems of Mineral Processing 34 (2000)

Z. SADOWSKI
(EDITOR)

Wrocław 2000

Streszczenia prac publikowanych w *Fizykochemicznych Problemach Mineralurgii* ukazują się w *Chemical Abstracts, Metals Abstracts, Реферативный Журнал* oraz w innych wydawnictwach abstraktujących
The papers published in *Physicochemical Problems of Mineral Processing* are abstracted in *Chemical Abstracts, Metals Abstracts, Реферативный Журнал* and other sources

Adres Redakcji
Zakład Przeróbki Kopalin i Odpadów, Instytut Górnictwa Politechniki Wrocławskiej
Politechnika Wrocławska, Wybrzeże Wyspiańskiego 27, 50-370 Wrocław
tel. 3441201, 3441202, fax: 3448123, telex: 0712254 pwr.pl
E-mail: Andrzej.Luszczkiewicz@ig.pwr.wroc.pl; Jan.Drzymala@ig.pwr.wroc.pl
http://www.ig.pwr.wroc.pl/conference/conf_uk.html

Siedziba Redakcji
Budynek Wydziału Górniczego Politechniki Wrocławskiej, pl. Teatralny 2, 50-051 Wrocław

ISSN 0137-1282

OFICYNA WYDAWNICZA POLITECHNIKI WROCŁAWSKIEJ, WYBRZEŻE WYSPIAŃSKIEGO 27, 50-370 WROCŁAW

LIST OF CONTENTS

Physicochemical Problems of Mineral Processing, 34 (2000), 5–16
Fizykochemiczne Problemy Mineralurgii, 34 (2000), 5-16

Abdel Tawab NEGM*, Abdel Zaher ABOUZEID*, Tawfik BOULOS**, Hussin AHMED**

NEPHELINE SYENITE PROCESSING FOR GLASS AND CERAMIC INDUSTRIES

Received March 15, 2000; reviewed and accepted May 15, 2000

There are several localities in the Eastern Desert in Egypt where nepheline syenite has been located. Among these localities are: Gabal Elkahfa, Gabal Abuikhrug, Gabal Nigrub Elfogani, Gabal Elnaga, and Gabal Mishbih. One of these ores, El-Kahfa nepheline ore, was selected for beneficiation to produce a product suitable for ceramic and glass manufacturing. An ore sample from El-Kahfa was characterized chemically and mineralogically. The chemical analysis of the sample was 57.8% SiO_2, 17.1% Al_2O_3, 5.3% Fe_2O_3, 9.2% Na_2O, and 5.5% K_2O. Mineralogically, it was found that the ore consists mainly of: orthoclase, andesite, nepheline, biotite, hornblend, and augite. The main objective of this research work was to reduce the iron content of the ore to a permissible limit to be used in glass and ceramics. Using a dry high intensity magnetic separator, a product assaying 0.5% Fe_2O_3 (about 0.35% Fe) from a size fraction -0.125+0.045 mm was obtained. When a wet high gradient magnetic separator was used at solid/liquid ratio of 1:9, the iron content was reduced down to 0.32% Fe_2O_3 using feed of -0.045 mm size fraction. By reverse flotation technique, a concentrate containing 0.4% Fe_2O_3 was obtained. Combining flotation with magnetic separation, i.e., subjecting the nonmagnetic fraction from the high gradient magnetic separator to anionic flotation, it was possible to get a final product assaying 0.21% Fe_2O_3 at a recovery of 70% using feed of - 0.075 mm.

Key words: nepheline, syenite, ceramic raw material, processing, flotation, magnetic separation.

INTRODUCTION

Feldspathoid rocks e.g. nepheline syenite, aplite and feldspar are indispensable raw

* Cairo University, Faculty of Engineering, Dept. of Mining, Egypt
** Centeral Metallargical Research & Development Institute, Egypt

materials in glass, ceramics and fillers production. However, nepheline is the most common of all due to its higher alkalis and alumina content per unit weight, it has been a formidable competitor to feldspar in North America and parts of Western Europe.

The low fusion point of nepheline syenite lowers the melting temperature, promoting faster melting, higher productivity and fuel savings in glass industry (Guillet 1994). In ceramics industry, the high fluxing capacity of nepheline allows it to act as a good vitrifying agent and permits a lower flux content in the ceramic body, lower firing temperatures and faster firing schedules.

In plastic, it is used as an inert, low cost filler in PVC, epoxy and polyester resin systems. Because it exhibits a low resin demand, high filler loadings are possible, permitting reduced requirements for more expensive components. In PVC resins, it exhibits a low tinting strength, has a refractive index close to that of vinyl resin and has a very low optical dispersion, all of which allows it to be used in nearly transparent stock. Finely ground nepheline syenite is especially employed as an inert filler in paints, both latex and alkaloid systems, as metal primers, wood stains, etc. it contributes a high dry brightness, high bulking value and easy wetting and dispersion in paint formulation.

Environmentally, nepheline syenite, which contains no free silica, is less health hazardous than feldspar, particularly in ultrafine grinding for fillers and extenders production in both plastics and paint fields.

In Egypt, research and development projects were not able to confirm the techno-economic feasibility of the Red Sea nepheline syenites in production of alumina and Portland cement (Ismail 1976). Nevertheless, direct utilisation of beneficiated rock in glass and ceramics production might be another option for making the most of 90 million tons of ore reserves in the different localities of the Eastern Desert (El-Ramly 1970).

For all these reasons, this research will be devoted to the study of the amenability of nepheline syenite from Gabal El-Kahfa locality of the Eastern Desert in Egypt, to beneficiation for different industrial applications. Characterisation of the samples by routine chemical analysis, thermal analysis and ore microscopy will be carried out prior to concentration. Both dry and wet magnetic separation methods will be demonstrated. Reverse flotation of iron bearing contaminants will, also, be employed either separately or in combination with magnetic separation for the objective of producing high quality nepheline concentrates.

ORIGIN, TYPES AND CHARACTERISTICS

Nepheline syenite is a light-coloured igneous rock, not a mineral, which is similar in its medium to coarse-grained appearance to granite. In an alkali-rich rock magma

deficient in silica, nepheline will form instead of albite feldspar (Minnes 1983; Guillet 1994). However some nepheline gneisses and other nepheline rocks may also have formed by metasomatic nephelinization process.

Nepheline rocks are composed essentially of nepheline, sodic plagioclase (usually albite or oligoclase) and microcline but in varying proportions, with small amounts of biotite, hornblende, magnetite, pyroxene, muscovite, sodalite, garnet, zircon, apatite, ilmenite, calcite, pyrite and zeolites as impurities or colouring minerals (Hewitt 1961).

The structural formula of nepheline is $Na_3KAl_4Si_4O_{16}$. Potassium is always present in nepheline, most frequently, in a ratio of Na/K =3:1, although ratios of 4:1 and 6:1 are known (Minnes 1983 and Guillet, 1994). It crystallises in the hexagonal system and frequently forms 6 to 12 sided prisms. It has a distinct and imperfect cleavage and a subconchoidal fracture. It is brittle with hardness of 5.5-6 in Mohs' scale and specific gravity of 2.5 to 2.7.

MAJOR WORLD DEPOSITS, POTENTIAL AND PRODUCTION

Nepheline Syenite deposits are rarely of great areal extent. However, although size is not a very important criterion in commercial considerations, more important are the purity and the location of the deposit.

Nepheline syenite reserves are considered limitless in the former USSR, Norway, Canada and recently Turkey. The largest potential nepheline syenite deposits are those of the Kola Pennisula, Russia, about 100 billion ton covering two areas of 450 and 250 square miles (Notholt 1983). In Norway, at Norsk Nefelin, the volume of proven nepheline syenite exceeds 135 million cubic meter representing nearly 400 million tons of a nature the company considers suitable for mining. In Canada, Idusmin Co. has published a reserve figure of 240 million tons of nepheline syenite found in Blue Mountain area. The Canaan deposit of Brazil extending in two localities 300 and 100 square miles was found to represent only 120 million tons (de Ferran 1983). Reserves of the rock in Turkey, was recently estimated and was found over 1 billion ton (Gulsoy 1993). Most other countries are typically much smaller.

The principal producing countries of glass and ceramic grades of nepheline syenite are Canada and Norway, where 70% of their production is directed towards the glass industry, 28 % to manufacturers of ceramic bodies and 2% for use in fillers (Harben 1995). The combined production of the two countries has grown from 250,000 ton in 1961 to 740,000 ton in 1972 (Minnes 1983). The total production of both Canada and Norway represented 26% of the world production in 1995 taking into consideration that Republic of Russia production in the same year reached 70% of the world production (2.5 million tons) (Harben 1995). Former USSR production in the years 1980 – 1994 range between 2.3 – 2.45 million tons / year.

NEPHELINE SYENITE DEPOSITS OF EGYPT

The presence of nepheline syenite in Egypt is confined to the ring complexes. These complexes are circular igneous structures formed after magma solidification. They are located in the southern sector of the Eastern Desert, south Idfu - Mersa Alam road in a square limited by the longitudes 33°and 36°and latitudes 22° and 25°. The nepheline syenite localities were studied from the geological point of view by the „Egyptian Geological Survey". Photogeological maps were prepared. The various rock types were identified, also mineralogical and chemical compositions were determined. (Ramely et.al. 1969).

MATERIALS AND METHODS

SAMPLE CHARACTERIZATION

A grab sample from El Kahfa locality of the Eastern Desert was crushed in a jaw crusher to less than 1 inch and then in a roll crusher to less than 3 mm. The sample was thoroughly mixed and divided into small bags for grinding. Chemical analyses and petrographic examination were carried out on representative sample of the ore. Granulometric analysis of the crushed sample was carried out, and each size fraction was chemically analysed. Sink and float tests were conducted on the different size fractions of the crushed samples using bromoform (2,889 g/cm^3). The Frantz isodynamic tester was used to separate magnetic heavy contaminants of the nepheline syenite sample.

PROCESSING TECHNIQUES

High intensity magnetic separation was carried out using different types of dry and wet separator that vary in field intensity and mode of operation. The „Dings" cross belt separator used in this investigation is a dry pick up type with an auxiliary permanent magnet for the separation of ferro-magnetic material ahead of the electromagnet at a minimum air gap of 3 mm. The „Carpco" induced roll magnetic separator was also used. It is a free – fall separator that is widely used with dry sand size materials. On the other hand, wet methods were investigated using high intensity high gradient magnetic separate the laboratory „Boxmag Rapid" magnetic separator consists of a canister packed with magnetized stainless steel wool matrix. The main parameters affecting the process are feed size, type of matrix, deep rate and packing density. Reverse floatation of heavy minerals contaminants of the nepheline syenite

samples was carried out in a „Denver D – 12" flotation cell using different collectors and constant pH. Combined magnetic separation followed by reverse flotation of the non magnetic fraction was also conduced to ensure ultimate removal of the iron bearing mineral.

RESULTS AND DISCUSSIONS

CHEMICAL ANALYSIS OF THE ORIGINAL SAMPLES

Results of the complete chemical analysis of the original nepheline syenite sample is shown in Table (1) which indicate that the sample is low in alumina high in iron content, and out of market specifications for glass and ceramics production.

Table 1. Complete Chemical Analysis of Gabal El – Kahfa Nepheline Syenite Ore

Consitituent	SiO_2	Al_2O_3	Fe_2O_3	CaO	MgO	Na_2O	K_2O	TiO_2
%	57.82	17.08	5.30	0.87	0.20	9.18	5.46	0.13
Consitituent	P_2O_5	S	Cl	CO_2	Humidity	L.O.I	Total	
%	0.01	0.02	0.05	0.15	0.48	0.53	97.28	

PETROGRAPHIC EXAMINATION

Microscopic examination of both thin and polished sections of the nepheline syenite samples shows that they are composed mainly of perthitic orthoclase and albite (oligoclase and andesine) from 50 to 70 %, nepheline from 15 to 25 % and green hornblende from 4 to 6%. Other minerals include small amounts of augite, biotite and hornblende with traces of free silica.

X-ray diffraction analysis of the bulk samples confirms the above conclusions for the major components. Oligoclase, andesine orthoclase and nepheline minerals are abundant with minor hornblende, biotite and augite. On the other hand XRD analysis of the sink fraction (separated by bromoform) depicts peaks for biotite, hornblende and augite, and feldspar.

GRANULOMETRIC ANALYSIS OF THE CRUSHED SAMPLES

Size distribution curve of the secondary crushed sample is shown in Table 2. A general unimodal representation is exhibited for the sample with d_{50} equals 1.85 mm.

Table 2. Dry Size Analysis and Chemical Analysis of El-Kahfa Nepheline Syenite Crushed Sample

Size, mm	Wt., %	Cum. Wt. % passing	Fe_2O_3 %	Al_2O_3 %	Distribution, %	
					Fe_2O_3	Al_2O_3
+6.68	4.93	100	5.28	17.31	4.89	4.99
-6.68 + 4.67	7.05	95.07	5.18	17.26	6.86	7.13
-4.67 + 2.40	28.89	88.02	5.27	17.27	28.61	29.23
-2.40 + 1.67	12.99	59.13	5.3	16.86	12.94	12.83
-1.67 + 0.85	16.95	46.14	5.23	16.96	16.66	16.84
-0.85 + 0.58	6.83	29.19	5.21	17.28	6.69	6.91
-0.58 + 0.40	6.54	22.36	5.26	16.86	6.47	6.46
-0.40 + 0.20	5.28	15.82	5.28	16.79	5.24	5.19
-0.2 + 0.106	4.23	10.54	5.43	16.96	4.32	4.20
-0.106 + 0.074	1.82	6.31	5.86	16.89	2.00	1.80
-0.074	4.49	4.49	6.20	16.86	5.23	4.43
Total (Calc.)	100		5.42	17.36	100	100
Head	100		5.30	17.08	100	100

LIBERATION STUDIES

Evidently, a gradual decrease in the iron content is exhibited with the corresponding decrease in size. From an average of 5.25 % Fe_2O_3 in the head sample, it reaches 0.85 % in the float of size -0.106+0.075 mm. The problem of such high iron content in the float fraction can not be attributed to the liberation of the different mineral phases only, but also to the presence of biotite which is a light iron bearing mineral (sp.gr. 2.7-3.2). This agreed with the phases encountered in the float fraction studied by XRD.

It is clear that the sink-float technique is not the most appropriate technique for studying the degree of liberation of these types of samples due to the presence of light iron bearing minerals, such as biotite, which joins the desired species in the float fraction. Consequently, the Frantz isodynamic high intensity magnetic tester was used for the liberation studies as discussed below.

Results of the magnetic separation of the different size fractions is depicted in Fig. 1. Obviously, the results are quite different, concerning concentrate iron content than in sink-float tests. The percentage of Fe_2O_3 in the - 0.053 + 0.045 mm fraction reached 0.1 % but with an alumina recovery of 77.5%.

Table 3 shows the sink-float results for the different size fractions of the ground sample using bromoform (2.889 g/cm^3).

Table 3. Sink-float results of the nephelme syenite of Gabal El-Kahfa ground sample using bromoform (2.889 g/cm^3)

Size, mm	Product	Wt., %	Fe_2O_3 %	Al_2O_3 %	Distribution, %	
					Fe_2O_3	Al_2O_3
-0.25 + 0.211	Float	89.8	1.38	19.03	23.03	97.54
	Sink	10.2	40.6	4.20	76.97	2.46
	Total	100	5.38	17.52	100	100
	Head	17.54	5.46	17.46	100	100
-0.211 + 0.125	Float	86.5	1.2	19.68	19.89	97.89
	Sink	13.8	30.33	3.08	8.01	2.11
	Total	100	5.22	17.39	100	100
	Head	42.6	5.32	17.5	100	100
-0.125 + 0.106	Float	83.4	0.96	19.93	15.60	96.18
	Sink	16.6	26.08	3.97	84.40	3.82
	Total	100	5.13	17.28	100	100
	Head	10.05	5.10	17.20	100	100
-0.106 + 0.075	Float	79.6	0.85	20.06	12.86	91.24
	Sink	20.4	22.47	7.51	87.14	8.76
	Total	100	5.26	17.5	100	100
	Head	12.53	5.32	17.35	100	100
-0.075 + 0.053	Float	81.3	1.43	19.78	22.39	93.77
	Sink	18.7	21.6	5.71	77.64	6.23
	Total	100	5.2	17.15	100	100
	Head	8.18	5.25	17.35	100	100
-0.053 + 0.045	Float	83.4	2.06	19.3	32.30	94.40
	Sink	16.6	21.7	5.81	67.70	5.60
	Total	100	5.32	17.06	100	100
	Head	5.21	5.12	17.10	100	100

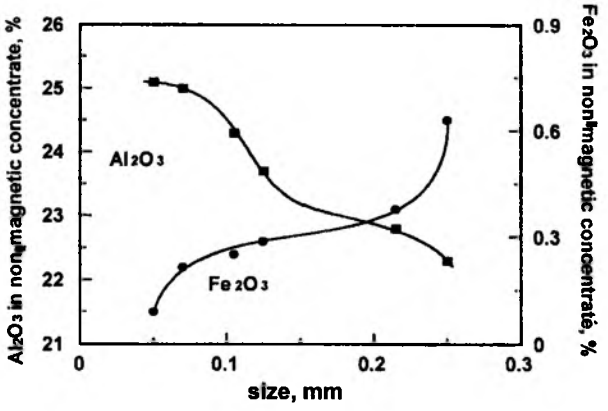

Fig. 1. Effect of the degree of fineness on the alumina and iron assays of El-Kahfa ground sample separated by Frantz Isodynamic Tester.

The cross belt 'Dings' dry magnetic separator was used under predetermined optimum conditions. A non magnetic concentrate having 0.98% Fe_2O_3 was obtained. Better results were achieved with the size fraction –0.25 + 0.045 mm feed, as shown in Table 4.

Table 4. Separation of Nepheline Syenite Using the „Dings" Magnetic Separator

Feed size mm	Product	Wt., %	Fe_2O_3	
			Ass. %	Dist. %
-0.25 + 0.125	Conc.	72.46	0.98	13.68
	Tail	27.54	16.27	86.32
	Total	100	5.19	100
	Head	94.2	5.25	92.6
-0.125 + 0.045	Conc.	73.69	0.58	8.38
	Tail	26.31	17.76	91.62
	Total	100	5.10	100
	Head	87.7	5.20	74.80

On the other hand, using the „Carpco" induced roll separator a non-magnetic concentrate assaying 0.58 Fe_2O_3 was achieved as shown in Table 5.

Table 5. Results of Magnetic Separation Using The „Carpco" Induced Roll Magnetic Separator

Feed size mm	Product	Wt., %	Fe_2O_3	
			Ass. %	Dist. %
-0.25 + 0.125	Conc.	70.86	1.03	14.14
	Tail	29.14	15.2	85.86
	Total	100	5.16	100
	Head	94.2	5.25	92.6
-0.125 + 0.045	Conc.	71.68	0.61	8.36
	Tail	28.32	16.92	91.64
	Total	100	5.23	100
	Head	87.7	5.20	74.8

Regardless of the improved results obtained with the induced roll magnetic separator the nepheline syenite concentrates did not satisfy the requirements for glass and/or ceramics production.

Wet high gradient magnetic separation of Gabal EI-Kahfa sample gave relatively better results. Using 1.5 mm iron spacing as a magnetic matrix a systematic decrease in the iron content of the non magnetic concentrate was obtained with decrease in feed

size. The iron content reached 0.4 % and 0.32 % Fe_2O_3 with the -0.075 mm and the -0.045 mm feed, respectively, using the steel wool matrix as shown in Table 6.

Table 6. Effect of Feed Size on the Wet High Gradient Magnetic Separation of Nepheline Syenite

Feed size mm	Magnetic Matrix	Product	Wt., %	Assay, %		Distribution, %	
				Fe_2O_3	Al_2O_3	Fe_2O_3	Al_2O_3
-0.075	Stainless	Conc.	63.6	0.41	23.48	4.86	87.23
	Steel	Tail	36.4	14.0	6.00	95.14	12.77
	Wool	Total	100	5.36	17.12	100	100
	Matrix	Head	100	5.30	17.08	100	100
-0.045 at 10%	Stainless	Conc.	58.6	0.32	23.82	3.57	81.39
solid no	Steel	Tail	41.4	12.25	7.70	96.43	18.61
soduim	Wool	Total	100	5.26	17.15	100	100
silicate (S.S)	Matrix	Head	100	5.30	17.08	100	100
-0.045 at	Stainless	Conc.	49.6	0.20	23.76	1.86	68.91
5% solid	Steel	Tail	50.4	10.34	10.55	98.14	31.09
and 0.2	Wool	Total	100	5.31	17.10	100	100
kg/t S.S	Matrix	Head	100	5.30	17.08	100	100

When the -0.074 mm size feed was used in flotation, with the collector „Cyanamid" Aeropromotors mixture, the best nepheline syenite concentrate was obtained (Table 7). From 5.3 % Fe_2O_3 and 17.1 % Al_2O_3 in the feed, the flotation concentrate had 0.4 Fe_2O_3 % and about 23.5 % Al_2O_3 with alumina recovery of 93 %.

Table 7. Results of Reverse Anionic Flotation of El-Kahfa Sample(100 % -0.075 mm Feed) Using Cyanamid collector

Collector Dose	Product	Wt., %	Assay %		Distribution %	
			Fe_2O_3	Al_2O_3	Fe_2O_3	Al_2O_3
2.25 kg/t	Conc.	67.86	0.40	23.46	5.37	92.99
	Tail	32.14	15.63	3.73	94.73	7.01
	Total	100	5.31	17.12	100	100
	Head	100	5.30	17.08	100	100

Combined Magnetic Separation–Flotation of the Finely Ground Nepheline Syenite Samples

It was interesting to investigate the amenability of cleaning the -0.075 mm finely ground non magnetic concentrates obtained by using the wet „Boxmag Rapid" high gradient separator through anionic flotation in view of the unsatisfactory results achieved with each process separately. However, the same technique was successfully

employed by Golsoy et al. (1993) for the treatment of the Turkish nepheline syenite deposit of Kirsehir Kaman District. Results shown in Table 8 indicate that from the non magnetic nepheline syenite concentrate of El Kahfa sample assaying 0.41% Fe_2O_3 and 23.48% Al_2O_3, a clean flotation concentrate having 0.21 % Fe_2O_3 and 23.63% Al_2O_3 was obtained at a total recovery of about 81%.

Table 8. Magnetic Separation–Flotation Results of El–kahfa Nepheline Sample (100%-0.075 Feed)

Process	Product	Wt., %	Assay, %		Distribution, %	
			Fe_2O_3	Al_2O_3	Fe_2O_3	Al_2O_3
Magnetic Separation Using Boxmag Wet Separator	Conc.	63.6	0.41	23.48	4.86	87.23
	Tail	36.4	14.00	6.00	95.14	12.77
	Total	100	5.36	17.12	100	100
	Head	100	5.30	17.08	100	100
Reverse Anionic Flotation Using „Cyanamid" 0.4 kg/t	Conc.	58.47	0.21	23.63	2.32	80.8
	Tail	5.31	2.94	22.14	2.84	6.64
	Total	63.6	0.43	23.51	5.16	87.44
	Head	63.6	0.41	23.48	4.86	87.23

CONCLUSIONS

Optimisation of the dry high intensity magnetic separation of the ground samples using the „Ding's" cross-belt separator at a maximum magnetic field intensity of 13 kGauss, minimum air gap of 3mm, and feed size -0.125+0.045 mm gave nepheline concentrate having 0.58% Fe_2O_3.

Using the „Carpco" induced roll magnetic separator, a free-fall device, a concentrate having 0.61% Fe_2O_3 was obtained with the same size fraction –0.125 + 0.045 mm feed.

Using the wet „Boxmag Rapid LHW" high gradient magnetic separator with a field intensity of 14 kGauss at a pulp density of 10 % solid, and feed rate of 6 kg/h solids (1 lit./min. suspension) it was possible to obtain cleaner nepheline syenite concentrates from finely ground feed, i.e. 100% less than 0.045 mm by using the stainless steel wool magnetic matrix. Product having 0.32% Fe_2O_3 was obtained with an alumina content of about 24 %.

When separation was conducted at a diluted pulp density (5% solid instead of 10%) in presence of sodium silicate as a dispersing agent, a nepheline concentrate assaying 0.2% Fe_2O_3 and 23.76% Al_2O_3 was obtained from a feed having 5.3 % Fe_2O_3 and 17.1

% Al_2O_3 of El-Kahfa sample at alumina recovery of 68.9%.

Optimisation of the reverse flotation process for minimising the iron bearing contaminants, a concentrate was obtained with El-Kahfa nepheline sample using the „Cyanamid" Aeropromoter, reaching 0.4% Fe_2O_3 and 23.5% Al_2O_3 from a feed having 5.3% Fe_2O_3 and 17.1% Al_2O_3.

Combined magnetic separation flotation of the finely ground samples yielded cleaner concentrates having 0.21% Fe_2O_3 and 23.63 % Al_2O_3 at recoveries of 81%. This means that combined magnetic separation – flotation technique improved the alumina recovery almost the same grade as the high gradient magnetic separation.

Microscopic studies of the nepheline syenite concentrates shows a brownish tinge of iron-bearing minerals which can be a surface coating which were not separated by mechanical attrition or disseminated fine grains in a matrix of syenite. This might explain the difficulty of obtaining high quality products that satisfy the international specifications for glass and ceramics production. However, these concentrates can be used in the local ceramics industry.

REFERENCES

AHMED H.A. (1998), *Beneficiation of some Egyptian Nepheline Syenite Ores for Ceramics and Glass Industries,* M. Sc. Thesis, Faculty of Engineering, Cairo University

DE FERRAN A. (1983), *The Canaan Nepheline Syenite Venture*, Proceedings of 5th Industrial Minerals International Congress, B. M. Coope and G.M. Clarke eds. Plc ., London, p. 101

EL-RAMLY M.F., DERENIUK N.E., ARMAMUS L. K. (1970), *Assessment and Technological Testing of the Nepheline Syenite of Gabal Abu-Khrug*, Extract From Studies on Some Mineral Deposits of Egypt, Article 9. A Geological Survey of Egypt publication, Editor O. Moharram,.

EL- RAMLY M.F. (1969), *The Three Ring Complexes of Gabal El-Kahfa, Gabal Nigrub El-Fogani ,and Gabal El -Naga*, A geological Survey of Egypt Publication.

EL-RAMELY M.F, BUDAROUV V., HUSSIEN A. A. (1971), *Alkaline Rocks Of South Eastern Desert*, Geol. Surv. Cairo, Egypt,.

GUILLET R. G. (1994), *Nepheline Syenite Benificiation for Different Industrial Applications*, Industrial Minerals and Rocks, 6th Edition, Senior Editor Carr. D. D. Society of Mining, Metallurgy & Exploration Inc. Colorado.

GULSOY O. Y., ERGNN S. L., KULAKSIZ S. (1994), *Beneficiation of Nepheline Syenites in Turkey*, Proceeding of the Mining, Petroluem and Metallurgy Conference, Assuit University, Assuit, Egypt.

HARBEN P.W. (1995), *The Industrial Minerals Handbook*, Second Edition, Metal Bulletin, London.

HEWITT D.F. (1961), *Nepheline Syenite Deposits of Southern Ontario*, Vol.49, Pt. 8, Ontario Department of Mines Toronto p.194.

ISMAIL A. K. (1976), *A Contribution to the Extractive Metallurgy of local Nepheline syenite Deposits for Alumina Production*, Ph.D. Thesis Faculty of Science, Cairo Univ.

MINNES D., G. LEFOND J., BLAIR R. (1983), *Nepheline Syenite*, Industrial Minerals and Rocks 5th Edition, AIME, New York P.931.

MOBARAK H. A. (1996), *The Mineralogy of Some Egyptian Alkaline Rocks, Beneficiation and Utilization Ceramic Industry,* Ph.D. Thesis Faculty of Science, Cairo University.

NOTHOLT A. G. L. (1983), *Igneous Phosphate Resources: Their Growing Contribution to World Markets*, Phosphates What Prospects For Growth, Metal Bulletin London, p.43.

A.T. Negm , A.Z. Abouzeid, T. Boulos, H.Ahmed, Przeróbka nefelinowych sjenitów dla przemysłu szklarskiego i ceramicznego, Fizykochemiczne Problemy Mineralurgii 34 (2000), 5-16, (w jęz. ang.)

W Egipcie istnieje kilka złóż sjenitu nefelinowego, wśród nich Gabal El-Kahta, G. Abuikhrug, G. Nigrub Elfogani oraz G. Mishbih. W tej pracy do badań użyto surowiec z El-Kahta, który dokładnie scharakteryzowano pod względem chemicznych i mineralogicznym. Badany materiał zawierał 57.8% SiO_2, 17.1% Al_2O_3, 5.3% Fe_2O_3, 9.2% Na_2O i 5.5% K_2O, a jego głównymi minerałami były ortoklaz, andezyn, nefelin, biotyt, hornblenda i augit. Głównym celem pracy było zredukowanie zawartości żelaza w rudzie do poziomu dopuszczalnego dla surowców do produkcji szkła i ceramiki. Przez zastosowanie separatora magnetycznego o dużym polu uzyskano produkt zawierający 0.5% Fe_2O_3, czyli około 0.35% Fe dla frakcji o uziarnieniu 0.045 - 0.125 mm. Z kolei stosując separator działający na mokro, przy stosunku zawartości części stałych do cieczy jak 1:9, zawartość żelaza została zredukowana do 0.32% dla nadawy o wielkości ziarn -0.045 mm. Za pomocą odwrotnej flotacji uzyskano zaś koncentrat o zawartości 0.4% Fe_2O_3. Łącząc flotację z separacją magnetyczną, tj. poddając produkt niemagnetyczny separacji magnetycznej o wysokim gradiencie pola oraz flotacja w obecności anionowych kolektorów uzyskano końcowy produkt zawierający 0.21% Fe_2O_3 z uzyskiem 70% dla nadawy o uziarnieniu -0.075 mm.

Physicochemical Problems of Mineral Processing, 34 (2000), 17–24
Fizykochemiczne Problemy Mineralurgii, 34 (2000), 17–24

Beata CWALINA*, Heike FISCHER**, Stanisław LEDAKOWICZ***

BACTERIAL LEACHING OF NICKEL AND COBALT FROM PENTLANDITE

Received March 15, 2000; reviewed and accepted May 15, 2000

The influence of *Thiobacillus ferrooxidans* bacteria on efficiency of nickel and cobalt leaching from natural pentlandite $(Ni,Fe)_9S_8$ have been examined. The effect of pulp density, particle size and initial ferrous ion concentration in leaching solution on the leaching yield was also evaluated. It has been demonstrated that the presence of *T.ferrooxidans* bacteria in leaching system induced considerable increase in nickel and cobalt leaching from pentlandite. The decrease in efficiencies of nickel and cobalt bacterial leaching processes have been denoted in systems containing high amounts of ferrous ions. Initial Fe^{2+} concentration of 4.5 g/dm^3 seems to be the most favourable for pentlandite bioleaching. The 20% pulp density may be admitted to be optimum regarding both satisfactory yields of bioleaching process and high nickel and cobalt concentrations in leaching solutions. The obtained results showed that particle size of 90-125 μm was optimum for nickel and cobalt bioleaching from pentlandite.

Key words: thiobacillus ferrooxidans, bacterial leaching, nickel ions, cobalt ions

INTRODUCTION

Bacterial leaching is a method used in many countries for metals recovery from variety of materials, including low-grade ores and metaliferrous wastes (Lundgren and Silver, 1980; Karavaiko, 1985). During bioleaching, metals are extracted from

* Department of Molecular Biology, Biochemistry and Biopharmacy, Medical University of Silesia, 41-200 Sosnowiec, Narcyzów 1
** TU Bergakademie Freiberg, Institut für Technische Chemie, Freiberg, Germany
*** Department of Bioprocess Engineering, TU Łódź, 90-924 Łódź, Wólczyńska 175

insoluble compounds such as sulphides and oxides, which are transformed (mainly through oxidation processes) into soluble forms such as sulphates.

Microorganisms that are most often used in bioleaching processes are acidophilic, autotrophic sulphur bacteria belonging to *Thiobacillus ferrooxidans* species. This bacteria group derives energy for growth and multiplication from oxidation processes, in which both ferrous ions and/or inorganic sulphur compounds (including metal sulphides) may serve as substrates being oxidised.

Bacterial oxidation of ferrous ion to ferric form is very important because of oxidative agent (Fe(III)-ion) regeneration by this way. Bioleaching processes are usually carried out in acid environment, preferably at pH 1.7-2.4, where metal ions remain in solution (Karavaiko 1985). Important features of *T.ferrooxidans* bacteria are their abilities to tolerate high acidity as well as high concentrations of metal ions (Cwalina et al. 1998). Under such conditions, bacteria must be resistant to metal ions (Groudev 1979; Karavaiko 1985; Cwalina and Dzierżewicz, 1989, 1991). This resistance may be achieved, among others, by bacteria selection during adaptation processes (Cwalina 1994; Cwalina et al. 1998a).

Pentlandite $(Ni,Fe)_9S_8$ is one of the main nickel-containing minerals (Chodyniecka and Zawiślak 1987). Except nickel and iron, pentlandite often contains also cobalt. Its concentration in ore may achieve 25% and usually is 25-50-times lower than nickel concentration (Torma 1988).

Pentlandite leaching in the presence of bacteria *T.ferrooxidans* may proceed according to the reaction (Torma 1972):

$$(Ni,Fe)_9S_8 + 17{,}625\ O_2 + 3{,}25\ H_2SO_4 \rightarrow 4{,}5\ NiSO_4 + 2{,}25\ Fe_2(SO_4)_3 + 3{,}25\ H_2O \quad (1)$$

The aim of the present study was to examine the efficiency of nickel and cobalt leaching (in sterile systems and in the systems inoculated with *T.ferrooxidans* bacteria) from natural pentlandite. The influences of pulp density, particle size, and initial iron concentration in leaching solution on the leaching yield have also been evaluated.

MATERIALS AND METHODS

In the present study, the natural pentlandite ore containing 5.21% Ni, 51.10% Fe and 0.25% Co, originated from Sudbury (Canada) has been used. Using X-ray diffraction method it has been demonstrated that in this ore pentlandite $(Ni,Fe)_9S_8$ was accompanied by non-stoichiometric pyrrhotite Fe_7S_8 (Fischer 1997).

Bioleaching processes have been carried out using the strain *T.ferrooxidans* 583 obtained from the German collection of microorganisms and cell cultures (DSM;

Deutschen Sammlung von Mikroorganismen und Zellkulturen GmbH, Braunschweig, Germany). The strain was cultured in 9K nutrient medium (Silverman and Lundgren 1959) containing Fe^{2+} at concentration of 9 g/dm^3 (pH 2.5). Actively growing bacterial populations were used for inoculation the leaching systems.

To evaluate the efficiency of nickel leaching from pentlandite, the sulphide samples (particle size 36-63 μm, 90-125 μm, 200-250 μm or 63-200 μm) were introduced into Erlenmeyer flasks in amounts needed to obtain pulp densities of 1%, 5% or 20% w/v (weight per volume). The flasks were placed on thermostated (32°C) rotary shakers. As leaching solutions, the liquid medium 9K or its modifications (iron-free solution or liquid media containing Fe^{2+} at concentrations of 4.5 or 13.5 g/dm^3), both sterile (supplemented with 5 cm^3 of 2% thymol acting bacteriostatically) and inoculated with *T.ferrooxidans* bacteria (10^7 cells in 1 cm^3 of the leaching solution) have been used.

The concentrations of nickel and cobalt in the leaching solutions were determined by means of an atomic absorption spectrophotometer (AAS UNICAM 939).

RESULTS AND DISCUSSION

The changes in yields of nickel and cobalt leaching from pentlandite have been investigated under sterile conditions and in systems inoculated with *T.ferrooxidans* bacteria. Obtained results have been shown in Fig. 1 and Fig. 2, respectively for nickel and cobalt ions liberated into leaching solutions.

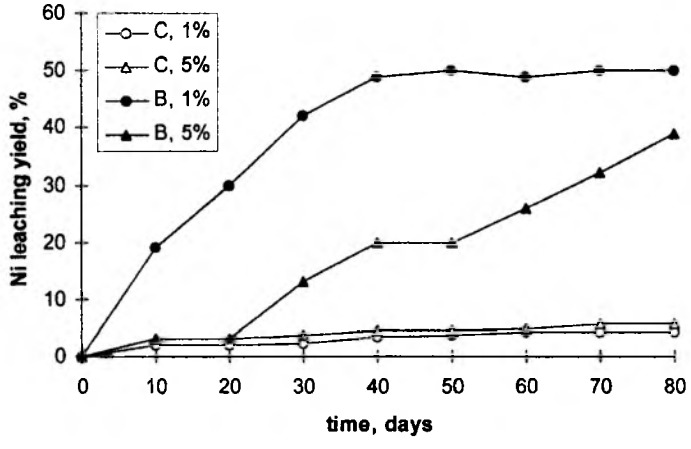

Fig. 1. The influence of pulp density (1%, 5%) on dynamics of chemical (C) and bacterial (B) leaching of nickel from pentlandite.

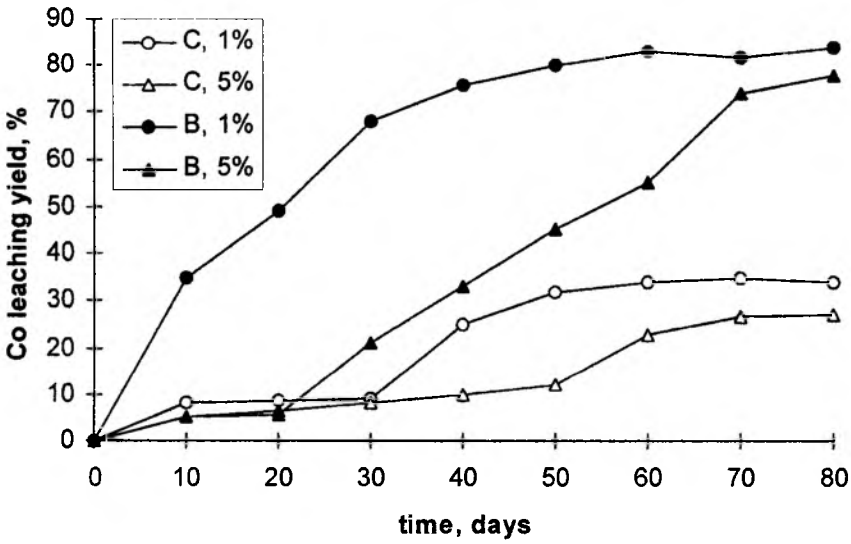

Fig. 2. The influence of pulp density (1%, 5%) on dynamics of chemical (C) and bacterial (B) leaching of cobalt from pentlandite.

It may be noticed that the maximum yields of nickel and cobalt leaching from pentlandite were usually obtained in slurries containing 1% w/v of ore, both sterile and containing microorganisms (Figs 1, 2). Only the nickel chemical leaching effects were very similar at pulp densities used (Fig.1). *T.ferrooxidans* bacteria caused considerable increase in the leaching efficiency (Figs 1, 2). The influences of bacteria and pulp densities on leaching yield were specially visible in case of the nickel solubilization, where the bacterial leaching processes proceeded with effectiveness 7-12-times higher as compared with respective processes carried out in the sterile systems (Fig. 1). After 80 days of process run, the 4% and 6% yields of nickel chemical leaching were attained at 1% and 5% pulp densities, respectively. Using the same the pulp densities, the bacterial leaching of nickel from pentlandite proceeded with the yields of about 50% and 40% (Fig. 1). Respective yields of cobalt leaching were 34% and 27% in the sterile systems as compared with 84% and 78% in the systems inoculated with bacteria (Fig. 2).

The influence of pulp density on nickel and cobalt concentrations in the solutions obtained after chemical and bacterial leaching of pentlandite is shown in Fig. 3.

The results presented in Fig. 3 indicate that the concentrations of both leached metals were considerable higher in the leaching solutions obtained in the systems with higher the pulp densities, although increased the pulp densities caused decrease in the

bioleaching yields (Figs. 1 and 2)

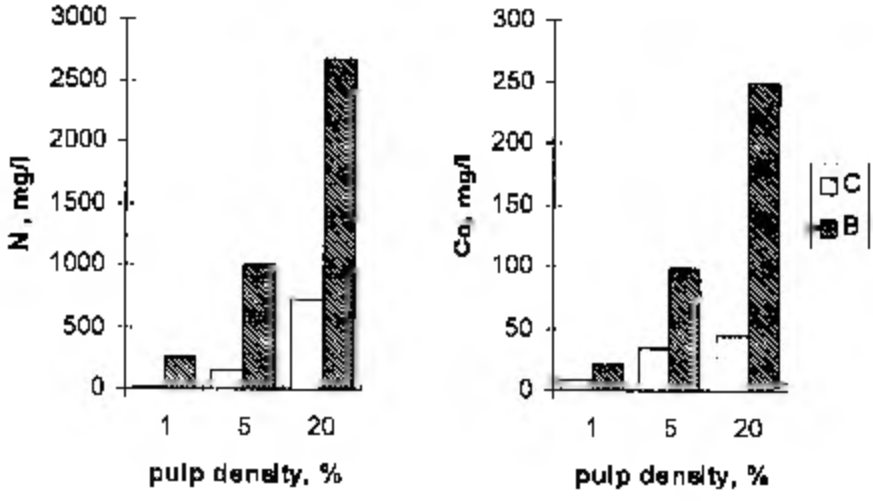

Fig. 3. The influence of pulp density on nickel and cobalt concentrations in the solutions obtained after chemical (C) and bacterial (B) leaching of pentlandite

The results of investigations carried out to evaluate the effect of ore break-up on nickel and cobalt bioleaching yields are presented respectively in Fig. 4 and Fig. 5.

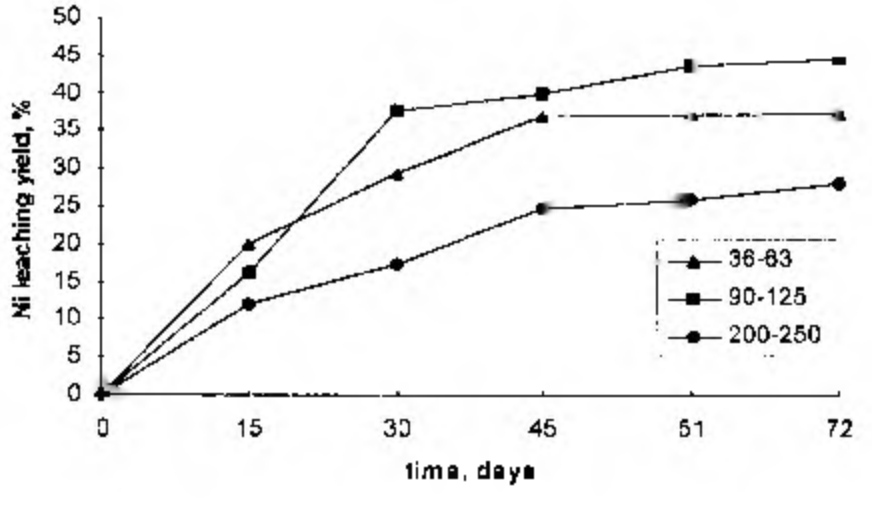

Fig. 4. The influence of particle size (36-63 μm, 90-125 μm, 200-250 um) on nickel bacterial leaching from pentlandite.

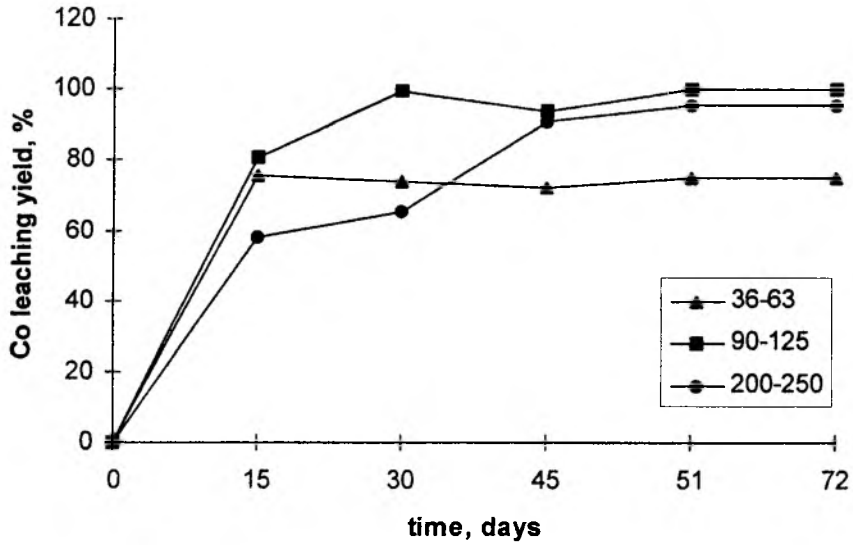

Fig. 5. The influence of particle size (36-63 μm, 90-125 μm, 200-250 μm) on cobalt bacterial leaching from pentlandite.

It may be seen that the bioleaching process was the most effective when the ore particle sizes were in range of 90-125 μm. All early described experiments have been carried out in 9K solution containing Fe^{2+} at concentration of about 9g/dm^3. It was interesting to examine the influence of this ion concentration on bioleaching yield. Results have been presented in Table 1.

Table 1. The influence of Fe^{2+} initial concentrations in the leaching solutions on the efficiency of nickel and cobalt leaching from pentlandite; C - control systems (sterile); B - bacterial systems (inoculated with *T.ferrooxidans*).

Fe^{2+} [g/dm^3]	Leaching yield [%]			
	Ni^{2+}		Co^{2+}	
	C	B	C	B
0	4,6	49,6	38,5	87,9
4,5	9,2	49,2	21,4	100,0
9,0	16,8	38,4	43,3	79,2
13,5	18,3	16,9	38,3	39,8

It may be stated that the efficiency of chemical leaching of nickel was higher with

higher ferrous ion initial concentration in the leaching solution. Similar dependence was not observed in the case of chemical leaching of cobalt. Bioleaching efficiencies of both tested metals decreased with increasing Fe^{2+} initial concentrations. Using X-ray diffraction method it has been found that under such conditions, the formation of insoluble hydroxy-compounds, such as goethite FeO(OH), from hydroxy-sulphates $Fe_3(SO_4)_2(OH)_5 \cdot 2H_2O$, $(NH_4)Fe_3(SO_4)_2(OH)_6$ and jarosites $KFe_3(SO_4)_2(OH)_6$ took place (Fischer, 1997). These compounds covered surface of leached ore and thus lowered bioleaching efficiency.

CONCLUSIONS

It has been demonstrated that the presence of *Thiobacillus ferrooxidans* bacteria in the leaching system induced considerable increase in nickel and cobalt leaching from pentlandite. The decrease in efficiencies of nickel and cobalt bacterial leaching processes have been noticed in the systems containing higher initial amounts of Fe^{2+}. This ion concentration of 4.5 g/dm^3 seems to be the most favourable for the pentlandite bioleaching.

The 20% pulp density can be assumed as the optimum value as far as satisfactory yield of the pentlandite bioleaching process as well as the highest nickel and cobalt concentrations in the leaching solutions are concerned.

The obtained results have shown that the particle size of 90-125 μm was optimum for nickel and cobalt bioleaching from the pentlandite.

REFERENCES

CWALINA B. (1994), *Sulphur metabolism of Thiobacillus ferrooxidans in the process of metals leaching from sulphide minerals* (in Polish). Wyd.US, Katowice

CWALINA B., DZIERŻEWICZ Z. (1991), *Adaptation dependent metabolic activity of bacteria Thiobacillus ferrooxidans*. Acta Biol. Cracov. Bot., 33: 1-11.

CWALINA B., FISCHER H., LEDAKOWICZ S. (1998), *Thiobacillus ferrooxidans resistance to nickel ions*. In: Proc. Int. Conf. Trace Elements. Effects on Organisms and Environment. Eds. Migula P., Doleżych B., Nakonieczny M., EcoEdycja, Katowice. pp. 137-141.

CWALINA B., LEDAKOWICZ S., FISCHER H. (1998), *Effect of pH-adjustment in leaching solution on chemical and bacterial extraction of nickel from pentlandite* (in Polish). Fizykochem. Probl. Mineralurgii, 32: 125-133

FISCHER H. (1997), *Untersuchungen zur Adaption von Thiobacillus ferrooxidans an Nickelionen und zur mikrobiellen Laugung von Pentlandit*. Dr. Diss., TU Bergakademie Freiberg, Germany

KARAVAIKO G.I. (1985), *Microbiological Processes for the Leaching of Metals from Ores*. Ed. Torma A.E., UNEP, Moscow.

LUNDGREN D.G., SILVER M. (1980), *Ore leaching by bacteria*. Annu. Rev. Microbiol., 34: 263-283.

SILVERMAN M.P., LUNDGREN D.G. 1959. *Studies on the chemoautotrophic iron bacterium Ferrobacillus ferrooxidans*. I. An improved medium and a harvesting procedure for securing high cell yields. J. Bacteriol., 77: 642-647.

TORMA A.E. (1972), *Biohydrometallurgy of cobalt and nickel*. TMS Paper Select., Metal. Soc. A.I.M.E., Paper No. 72-77.

TORMA A.E. (1988), *Leaching of metals*. In: Biotechnology; V. 6b: Special Microbial Processes. Eds: Rehm H.J. & Reed G., VCH Verlagsgesellschaft, Weinheim

Cwalina B., Fischer H., Ledakowicz S., Bakteryjne ługowanie niklu i kobaltu z pentlandytu. Fizykochemiczne Problemy Mineralurgii 34 (2000), 17 – 24, (w jęz. angielskim)

Badano wpływ bakterii *Thiobacillus ferrooxidans* na efektywność ługowania niklu i kobaltu z naturalnego pentlandytu $(Ni,Fe)_9S_8$, zawierającego 5.21% Ni, 51.10% Fe i 0.25% Co. Oceniano także wpływ gęstości pulpy (1%, 5%, 20%), rozmiaru ziaren (36-63 μm, 90–125 μm, 200–250 μm, 63-200 μm) i początkowego stężenia jonu żelazawego Fe(II) w roztworze ługującym (4.5 g/dm^3, 9.0 g/dm^3, 13.5 g/dm^3) na wydajność ługowania. Wykazano, że obecność bakterii *T. ferrooxidans* w układzie ługującym powodowała istotne zwiększenie wyługowania niklu i kobaltu z pentlandytu. W układach zawierających wysokie stężenia jonów żelazawych (≥9 g/dm^3) odnotowano zmniejszenie efektywności procesów bakteryjnego ługowania niklu i kobaltu. Wydaje się, że najbardziej korzystne dla bioługowania pentlandytu jest początkowe stężenie Fe(II) wynoszące 4.5 g/dm^3. Biorąc pod uwagę zarówno satysfakcjonujące wydajności procesów bioługowania, jak i wysokie stężenia niklu i kobaltu w roztworach ługujących, można przyjąć 20%-ową gęstość pulpy jako optymalną. Wielkość ziaren pentlandytu, optymalna dla bioługowania niklu i kobaltu z tego minerału, powinna mieścić się w zakresie 90–125 μm.

Physicochemical Problems of Mineral Processing, 34 (2000), 25–33
Fizykochemiczne Problemy Mineralurgii, 34 (2000), 25–33

S. ŞENER*, G.ÖZBAYOĞLU**

INVESTIGATION OF STRUCTURAL CHEMISTRY OF THERMAL PROCESSES APPLIED FOR IMPROVEMENT OF GRINDABILITY OF ULEXITE

Received March 15, 2000; reviewed and accepted May 15, 2000

In this investigation, mechanism of the thermal processes and effect of the mineralogical and structural modifications on the grindability of ulexite were investigated. The mechanism of the thermal reactions were examined by thermo-analytical methods including TGA and DTA. The mineralogical and structural modifications were investigated by XRD and SEM techniques, respectively. The results indicated that ulexite thermally decomposes within 60-500°C. The structure was first transformed into $NaCaB_5O_6(OH)_6.3H_2O$ and then $NaCaB_5O_6(OH)_6.H_2O$ and finally became as completely X-ray amorphous phase accompanied with the thermal processes in the sequence of two-stage dehydration and two-stage dehydroxylation reactions resulting in two endothermic DTA peaks at 151°C and 180°C. Further treatment caused two-stage recrystallization processes resulting in an exothermic DTA peak at 636°C and an endothermic peak at 855°C. The changes in the grindability of ulexite were determined in terms of work index by the Hardgrove Grindability Test. The results showed that work index of ulexite was found as 7.11kWh/shton and decreased to 3.5 kWh/shton level within 200-280°C for 60 minutes. Further heating lead to 8.49 kWh/shton at 640°C for 60 minutes.

Keywords: ulexite, thermal reaction, thermal decomposition, grindability

INTRODUCTION

Ulexite is Na-Ca hydrated borate consisting of both OH species and water of crystallization. Under heat treatment, some thermal reactions take place. The mineral

* Environmental Engineering Dept., Mersin University, İçel, Turkey.
** Mining Engineering Dept., Middle East Technical University, Ankara, Turkey.

ulexite ($NaCaB_5O_9.8H_2O$) first gradually removes its water of crystallization and then either becomes amorphous or recrystallizes into newly formed crystalline phase while the structure undergoes significant structural changes. It only exfoliates due to gradual removing of water vapor within inducing the structure as amorphous state having numerous numbers of microcracks and interstices throughout the structure. This makes the structure weak and easily grindable (Şener, 1991; Şener and Özbayoğlu, 1995). There is a strong relationship between heat treatment and grindability of minerals. The change in chemical and mineralogical composition, degree of discontinuity due to heating may cause to decrease strength of the structure in such a way that the chemical bonds are broken and the structure is more disordered (Şener 1997; Şener and Özbayoğlu 1999).

In this study, the nature and mechanisms of thermal reactions accompanied with the mineralogical and structural changes in the structure of ulexite during heat treatment were examined and effect of the structural chemistry of the thermal processes on grindability of ulexite were investigated.

MATERIALS AND METHODS

Ulexite samples used throughout the study were prepared from the ulexite concentrates taken from Balıkesir-Bigadiç Mine of Etibank. Hand picked coarse crystals were cleaned by dipping them in water and then washing to remove dispersed clay minerals. The cleaned and air dried samples were crushed, ground and screened, and –1.168+0.600 mm sized samples kept for the subsequent experiments. The purity of the sample was found to be around 96% on the basis of B_2O_3 content. The chemical analysis of the sample is given in Table 1.

Conventional thermo-gravimetric (TG), differential thermo-gravimetric (DTG) and differential thermal analyses (DTA) were performed to determine amount of H_2O removed, temperature, nature and mechanism of thermal decomposition and reconstitution reactions. The Thermal Science brand TG1500 model thermo-gravimetric analyzer equipped with a microbalance system was used in the TG and DTG analyses. The Rigaku brand Thermoflex TG8110 model differential thermal analyzer was used in the DTA analysis. All the experiments were performed in a Rh-Pt crucible with the heating rate of 10°C/min under the flow of N_2 to sweep out accumulated water vapor produced during the decomposition.

The calcination tests were performed in a Heraeus brand muffle furnace equipped with time proportioning temperature control system that provides ± 0.8 %/°C sensitivity from the set point of temperature. In the procedure, the furnace was first set to the desired temperature with the empty porcelain crucible in cylindrical shape with the volume of 340 cm^3 and then the experiment was started right after introducing the

sample into the preheated crucible. At the end of each experiment, the calcined sample was allowed to cool down to room temperature in a desiccator.

Table 1. The Chemical Analysis of Ulexite Sample

Chemical Compounds, %	Ulexite
B_2O_3	41.17
CaO	18.80 *
Na_2O	7.50
SiO_2	0.85
MgO	0.22
K_2O	0.02
Fe_2O_3	0.09
Al_2O_3+TiO_2	0.85
Loss of ignition at 800°C	33.83

* CaO content exceeds the theoretical value of ulexite (13.8%) due to most probably presence of Ca-bearing impurities such as colemanite, calcite and gypsum in the ulexite concentrate

Mineralogical and structural changes and the identification of crystalline structure of the phases were carried out by X-ray diffraction analysis (XRD). In the analyses, Philips PW 1840 and Rigaku Miniflex brand X-ray powder diffractometers with Ni filtered CuK_{α} radiation were used. The surface characterization were performed by Leitz brand AMR 1000 model scanning electron microscope (SEM).

The changes in the grindability were evaluated with respect to work index, W_i. The standard Hardgrove grindability test was employed with Neco brand Hardgrove machine in accordance to ASTM D 409-93a, 1971.

RESULTS AND DISCUSSIONS

The temperature of decomposition, nature and mechanism of the thermal reactions occurred in the structure of ulexite are given in Figure 1. As seen in the figure, three distinct reactions were observed. The first reaction was due to the thermal decomposition of ulexite and occurred in two stages dehydration and two stage dehydroxylation reactions within 60-500°C. The dehydration reactions occurred within 60-260°C resulting in two overlapped endothermic DTA peaks at 151 and 180°C. The first stage of the dehydration reaction proceeded up to 180°C with a new crystalline phase [$NaCaB_5O_6(OH)_6 3H_2O$] formation and the corresponding weight loss was about 8% (two moles of H_2O). The second stage of the dehydration reaction began at 151°C, then proceed up to 260°C (as being overlapped with the first stage of

the dehydration reaction within 151-180°C). The corresponding weight loss was about 17% (four moles of H_2O) at 180°C. A new crystalline phase which was identified as $[NaCaB_5O_6(OH)_6H_2O]$ was produced. The mineralogical transformation within 120-260°C is given in Figure 2.

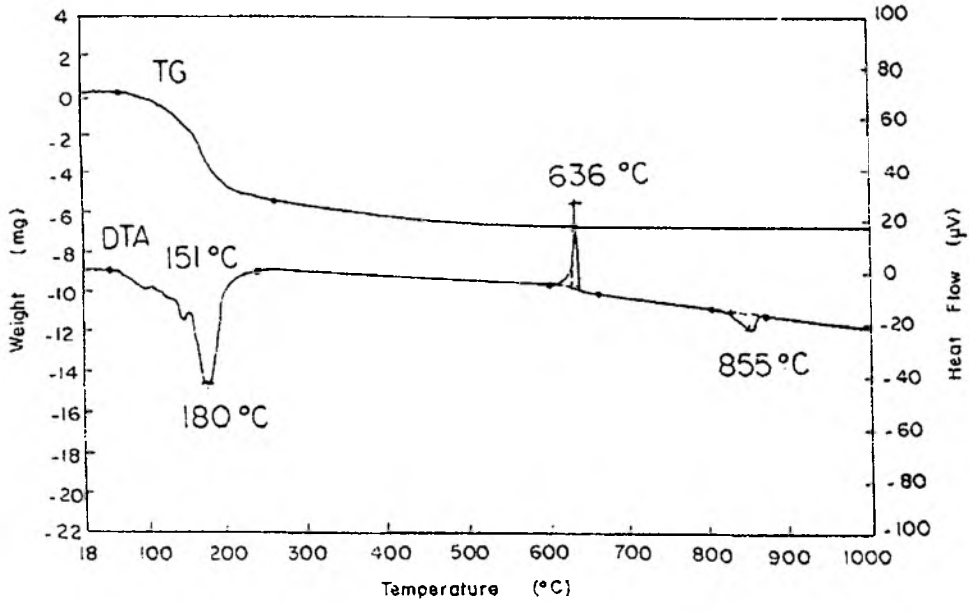

Fig. 1. TG and DTA curves of ulexite

The first stage of the dehydroxylation reaction took place within 180-260°C (as being overlapped with the second stage of the dehydration reaction) during which 26% weight loss (corresponds to 6 moles of H_2O; 5 moles by removing water of crystallization and 1 mole by splitting the OH groups) was obtained. The remaining 2 moles of water was gradually removed from the structure in a continuous way during the second stage of the dehydroxylation up to 500°C. The reaction did not give any peak but negative heat flow was observed along DTA curve up to 600°C, as seen in Figure 1. During the reaction, the structure was transformed into a completely X-ray amorphous state.

The gradual liberation of water vapour during the dehydration and dehydroxylation reactions has caused the structure having numerous numbers of microcracks and has exfoliated without decrepitating. The structural modifications were observed in the SEM microphotographs of ulexite calcined at 240°C given in Figure 3.

The second reaction in the DTA curve in Figure 1, was reconstitution reaction which was observed within 600-640°C giving an exothermic peak at 636°C. The

amorphous structure has been recystallized as $NaCaB_5O_9$ (Şener 1997). The structural modification was observed in the SEM microphotographs of ulexite calcined at 600°C given in Figure 4. As seen in the figure, the cavities along the microcracks and partings was reduced and folded and so the structure was transformed into reniform (kidney-like shape) texture due to rebuilding and shrinkage of the aggregates during the recrystallization.

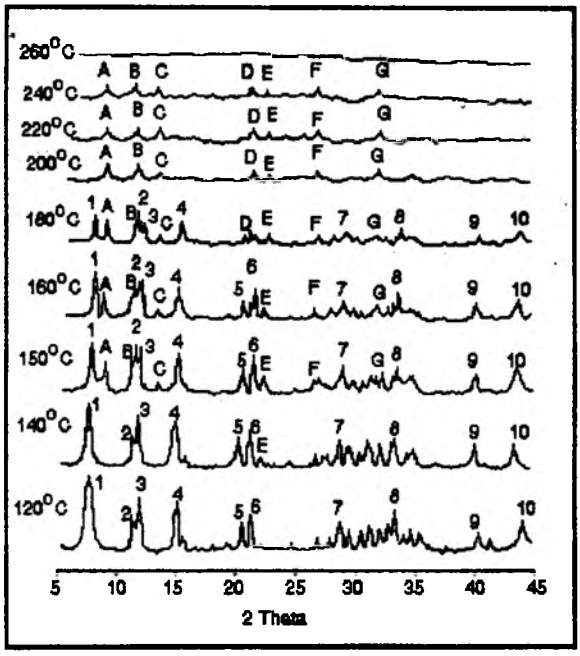

Fig. 2. Comparative results of the XRD patterns of ulexite calcined at 120-260°C

The third reaction in the DTA curve was again reconstitution reaction giving an endothermic peak at 855°C. The crystal $NaCaB_5O_9$ has been transformed into CaB_2O_4 remaining NaB_3O_5 in amorphous (Şener 1997). The SEM microphotographs of ulexite calcined at 850°C given in Figure 5 showed that the structure was in spongy texture containing open and closed pores due to partial fusion of the structure.

According to the results derived from the DTA and XRD examinations, the overall thermal reactions occurred in the structure of ulexite is given in equation (1).

Fig. 3. Microphotograph of the SEM image of ulexite calcined at 240°C (2000x)

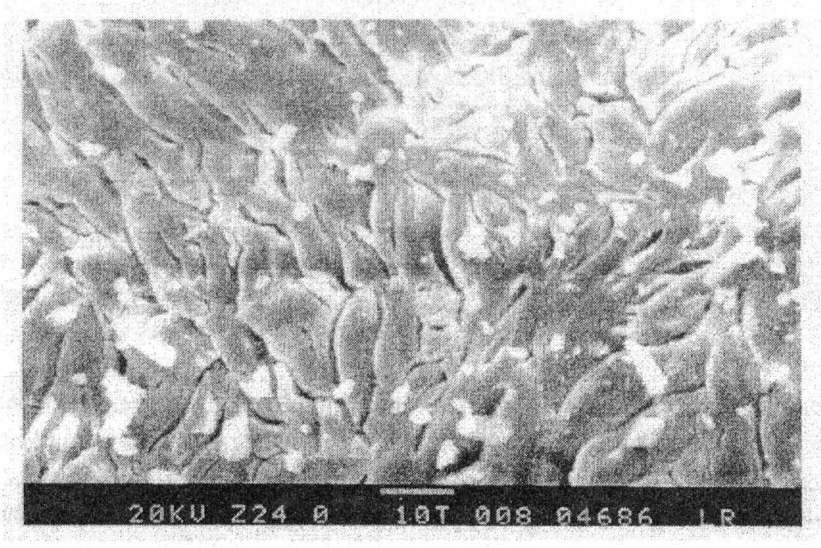

Fig. 4. Microphotograph of the SEM image of ulexite calcined at 600°C (2000x)

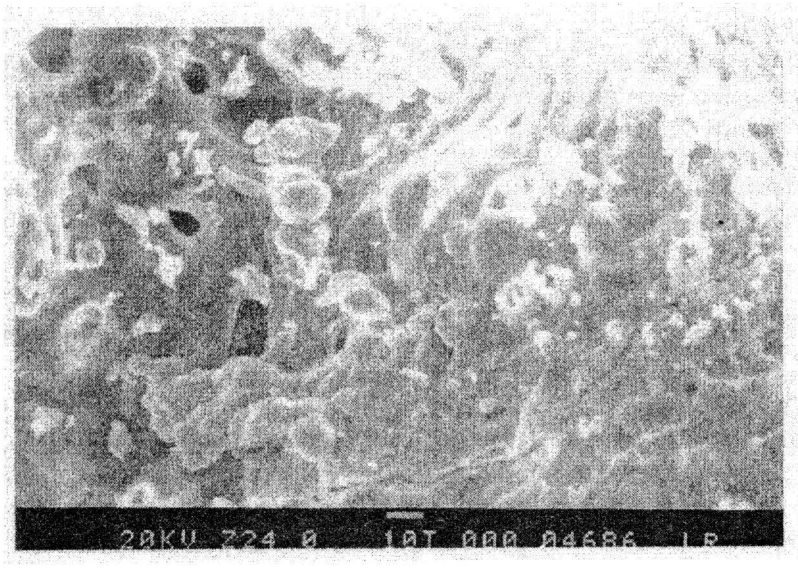

Fig. 5. Microphotograph of the SEM image of ulexite calcined at 850°C (1000x)

$$NaCaB_5O_6(OH)_6.5H_2O \xrightarrow[\text{(1. dehydration)}]{60\text{-}180^\circ C} NaCaB_5O_6(OH)_6.3H_2O + 2H_2O \xrightarrow[\text{(2. dehydration)}]{151\text{-}260^\circ C} NaCaB_5O_6(OH)_6.H_2O + 2H_2O$$

$$\xrightarrow[\text{(1. dehydroxylation)}]{180\text{-}260^\circ C} [NaCaB_5O_6(OH)_6.H_2O + \text{Amorphous matrix}] + 2H_2O \xrightarrow[\text{(2. dehydroxylation)}]{260\text{-}500^\circ C} [\text{Amorphous matrix}] + 2H_2O$$

$$\xrightarrow[\text{(Recrystallization)}]{636^\circ C} NaCaB_5O_9 \xrightarrow[\text{(Recrystallization)}]{855^\circ C} CaB_2O_4 + NaB_3O_5\ (\text{amorphous}) \qquad (1)$$

The effect of heat treatment on grindability of ulexite was measured in respect to work index (W_i). W_i of the uncalcined ulexite sample was found as 7.11 kWh/shton. The W_i of ulexite sharply decreased to 3.8 kWh/shton at 200°C and 3.5 kWh/shton at 280°C and reached to the minimum value of 3.45 kWh/shton at 320°C thereafter it sharply increased to 8.49 kWh/shton at 640°C.

The decrease in W_i was attributed to the mineralogical and structural changes in the structure. The gradual liberation of the produced water vapour due to heat treatment caused the structure to transform into chemically more disordered crystalline and amorphous phases and to form numerous microcracks and interstices throughout the structure (see Figure 3). This caused to increase the degree of discontinuity and porosity of the structure and makes it easily grindable. The reconstitution of the amorphous phase and the transformation of the structure into structurally more

ordered crystalline phase caused the increase in W_i. It was attributed to reducing and folding the microcracks and, shrinkage and partial fusion of the aggregates during the recrystallization, as seen in Figure 4 and 5. This gained the structure higher strength and made it hardly grindable.

CONCLUSIONS

Under heat treatment, ulexite loses its water of crystallization while undergoing different mineralogical and structural changes.

Thermal decomposition of ulexite has occurred within 60-500°C with two-stage dehydration proceeded by two-stage dehydroxylation reactions. Crystal structure has been transformed first into multi-domain heterogeneous matrix containing both crystalline and amorphous phases and then into completely X-ray amorphous state. Amorphization process has taken place along with dehydroxylation reaction.

Thermal reconstitution of the amorphous phase has taken place above 600°C. The amorphous structure has been first recystallized as $NaCaB_5O_9$ at 636°C and then it has been transformed into CaB_2O_4 remaining NaB_3O_5 in amorphous at 855°C.

Different structural modifications has also occurred in the structure during heat treatment. The gradual liberation of water vapour during the decomposition processes has caused the structure having numerous numbers of microcracks and has exfoliated without decrepitating. During the thermal reconstitution processes, the cavities along the microcracks and partings have first reduced and folded and then, has transformed into spongy texture containing open and closed pores due to partial fusion and shrinkage of the aggregates.

The mineralogical and structural modifications in the structure have affected the work index of ulexite. The heat treatment within 200-360°C improved the grindability.

REFERENCES

ŞENER S. (1991), *.Beneficiation of Balıkesir-Bigadiç ulexite concentrate by calcination*, M.Sc. Thesis, METU, Ankara, Turkey.

ŞENER S. (1997), *Determination of mechanisms of thermal reactions in the structure of ulexite and its use in the separation of ulexite from colemanite*, Ph.D. Thesis, METU, Ankara, Turkey.

ŞENER S. , ÖZBAYOĞLU G. (1995), *Separation of ulexite from colemanite by calcination*, Minerals Engineering, 8:6, 697-704.

ŞENER S. ÖZBAYOĞLU G. (1999). *Effect of structural changes on grindability of some boron minerals*. SME Annual Meeting. 99-13, Denver, Colorado.

S. Şener, G.Özbayoğlu, Badanie strukturalne ulexytu poddanego procesom termicznym dla mielenia, Fizykochemiczne Problemy Mineralurgii 34 (2000), 25 – 33, (w jęz. ang.)

W pracy badano mechanizmy procesów termicznych i wpływu przemian mineralogicznych i strukturalnych na rozdrobialność ulexytu. Badania mechanizmów reakcji prowadzono metodą analizy termicznej w tym TGA i DTA, a zmiany mineralogiczne i strukturalne za pomocą technik XRD i SEM. Wyniki wskazują, że ulexyt ulega termicznemu rozkładowi w zakresie 60-500°C. Najpierw powstaje $NaCaB_5O_6(OH)_6*3H_2O$ a potem $NaCaB_5O_6(OH)_6*H_2O$) ostatecznie stając się amorficzny. Towarzyszą temu procesy termiczne, kolejno, dwustopniowe odwodnienie i dwustopniowa dehydroksylacja powodujące dwa endotermiczne piki na krzywej DTA przy 151°C i 180°C. Dalsze ogrzewanie powoduje dwustopniową rekrystalizację powodującą egzotermiczny pik przy 636°C oraz endotermiczny pik przy 855°C. Zmiany rozdrabialności ulexytu określono za pomocą testu rozdrabialności Hardgrove'a. Stwierdzono, że indeks rozdrabialności ulexytu wynosi 7.11 KWh/krótką tonę i maleje do 3.5 KWh/krótką tonę dla próbek wygrzewanych w zakresie 200-280°C przez 60 minut. Dalsze ogrzewanie w temp. 640°C przez 60 minut podnosi wartość indeksu do wartości 8.49 KWh/krótką tonę.

Physicochemical Problems of Mineral Processing, 34 (2000), 35–45
Fizykochemiczne Problemy Mineralurgii, 34 (2000), 35–45

Nagui A. ABDEL-KHALEK*

FACTORIAL DESIGN FOR COLUMN FLOTATION OF PHOSPHATE WASTES

Received March 15, 2000; reviewed and accepted May 15, 2000

A factorial design was used to study effects, and their interactions, of the main parameters affecting column efficiency to recover phosphates from their wastes. Three-phase experiments were performed using a mixture of fatty acid and fuel oil as a collector for phosphate while pine oil was used as a frother. Meanwhile, 2-phase experiments were conducted to correlate the results of 3-phase experiments with that of bubble diameter and air holdup.

The results show that application of statistical design reveals very interesting information about the interaction between the studied parameters. For example, it is shown that the interaction (X_1X_2) between superficial gas velocity (X_1) and frother concentration (X_2) has a beneficial effect on grade but aversely affect recovery.

Key words: column flotation, phosphate, frother, collector

INTRODUCTION

Large quantities of fines are generated, as slimes, during beneficiation of phosphate ores. Such slimes are discarded due to the lack of a suitable method for their treatment and consequently the total recovery of phosphate is decreased (Abdel-Khalek et al. 2000). For example, about 1/3 of run-of-mine of Florida phosphate, below 150 mesh, is discarded as slimes. In addition, the presence of these slimes causes, in some areas, an environmental problem.

* Central Metallurgical Research and Development Institute, P.O.Box 87 Helwan, Cairo, Egypt. e-mail: naa_khalek@frcu.eun.eg, or naguialy@hotmail.com

Meanwhile, column flotation is becoming more popular as a flotation technique (Dobby and Finch 1991, Tuteja et al 1995, Abdel-Khalek and Stachurski 1993). The performance of column flotation depends on a number of operating parameters. To get the best metallurgical performance from a column, it is necessary to optimize column parameters. The conventional practice in mineral processing research is to perform tests as a function of one - variable - at - a - time. However, this can be deceptive, because this method does not provide information on the interaction of variables within the system (Griffith 1962). Studying interaction between variables is useful for a good understanding of the flotation column variables (El-Shall et al 1999, Patil et al. 1996).

Among the several approaches that can be used to optimize experiments, the statistical designed approach is found to be the most useful. A recent review of mathematical models in column flotation processes shows that, compared to kinetic models, not much attention has been given to statistical models (Tuteja et al. 1994).

This paper discusses the results of column flotation of phosphate wastes using a statistical design. The main parameters that affect phosphate flotation were investigated. Also, 2-phase experiments were conducted to correlate the results of 3-phase experiments with that of bubble diameter and air holdup.

MATERIALS AND METHODS

A sample of phosphate wastes (-0.106 mm) was used in this study. The sample contained about 7.8 % P_2O_5 and 78.5 % acid insoluble. A mixture of fatty acids and fuel oil with a ratio of 1:1 by weight was used as a collector. Pine oil was used as a frother.

Flotation tests were conducted using a 14.6cm diameter by 1.8m high Plexiglas flotation column. The feeding point was located at 30 cm from the column top. In each 3-phase experiment, a sample was conditioned with the pre-determined dosage of collector at pH 9.5. Frother-containing water and air were first introduced into the column through the sparger (Eductor type) at a fixed flow-rate. After every parameter was set and two-phase system was in a steady state, the phosphate material was fed, at a fixed flow-rate, to the column. Timed samples of tailings and concentrates were taken after reaching steady state conditions. The collected samples were weighed and analyzed. In 2-phase experiments (air-water system), air holdup and bubble diameter were calculated. Air holdup was measured using manometers. The diameter of air bubbles was calculated using drift-flux method (Dobby et al. 1988).

RESULTS AND DISCUSSION

2^3 FACTORIAL DESIGN

In order to determine the effects and interactions between different parameters, a series of experiments using 2^3 factorial design has been performed. The variables are coded between "-" and "+", where "-" represents the low level and "+" represents the high level of the factor. The levels of the coding are indicated in Table 1. So, there are eight (2^3) possible combinations, each of which was replicated twice, as given in Table 2. Calculation of the effects and their interactions as well as analysis of variance (ANOVA) have been carried out using Yates' method (Myers and Montgomery 1995; Garcia-Diaz and Phillips 1995). This ANOVA technique can be used to determine whether several means are significantly different from one another when compared to the experimental error. The F-test is used to compare two variances, i.e. compare the precision of the two sets of data. $F=S_1^2/S_2^2$ where S_1^2 is always the larger variance. These F values are compared to standard tables of the F distribution at the 95% level. The null hypothesis is that there is no significant difference between variances with the alternate hypothesis that S_1^2 is greater than S_2^2. The main effect (E_i) of factor X_i is estimated as the difference between the two averages:

$$Y_i^+ = T_i^+/r2^{n-1} \text{ and } Y_i^- = T_i^-/r2^{n-1} \quad (1a)$$

that is:

$$E_i = 1/r2^{n-1}(T_i^+ - T_i^-) \quad (1b)$$

Where T_i is the sum of the $r2^{n-1}$ observations corresponding to the 2^{n-1} experimental conditions having $X_I = +1$ or -1 and r is the number of replications. The results of these analyses are shown in Table 3. The results in Table 2 show that it is possible to obtain concentrates with grade (23.4-29.0 % P_2O_5) and recovery (54.9-80.2%) depending on the applied operating conditions.

Table 1. Levels of variables for 3-phase experiments

Variable	Code	Level	
		(-)	(+)
Superficial Air Velocity, cm/s	A	0.46	0.94
Frother Concentration, ppm	B	5	25
Superficial Wash Water Velocity, cm/s	C	0.4	1.2

Table 2. Results of treatments combinations for 2^3 design for 3-phase experiments

#	Factors			% P_2O_5			% Recovery		
	A	B	C	Replications		Total	Replications		Total
	X_1	X_2	X_3	1	2		1	2	
1	-	-	-	25.8	25.4	51.2	56.3	54.85	111.15
2	+	-	-	23.4	23.8	47.2	70.1	72.7	142.8
3	-	+	-	25.24	26.0	51.24	65.6	63.6	129.2
4	+	+	-	26.91	26.6	53.51	80.2	78.8	159.0
5	-	-	+	27.83	27.97	55.8	50.3	48.95	99.25
6	+	-	+	25.75	26.1	51.85	65.3	66.0	131.3
7	-	+	+	28.62	29.0	57.62	60.53	59.5	120.03
8	+	+	+	26.8	26.13	52.93	70.63	69.86	140.49

Table 3. Analysis of variance for effects and interactions between parameters

Source of Variance	Grade		Recovery	
	Net Effect	Computed F	Net Effect	Computed F
Main Effect:				
X_1	-1.29±0.38	62.22	14.25±1.25	690.91
X_2	1.15±0.38	49.50	8.03±1.25	219.41
X_3	1.88±0.38	131.05	-6.39±1.25	138.81
2-Factor Interaction:				
X_{12}	0.69±0.38	17.71	-1.68±1.25	9.61
X_{13}	-0.86±0.38	27.62	-1.12±1.25	4.24
X_{23}	-0.43±0.38	6.89	-0.54±1.25	0.97
3-Factor Interaction:				
X_{123}	-0.88±0.38	28.41	-1.22±1.25	5.05
$F_{(0.05,1,8)} = 5.32$				

EFFECT OF SUPERFICIAL AIR VELOCITY

Table 3 shows that the effect of (X_1) superficial air velocity (J_g) is statistically significant with respect to grade and recovery. Changing this parameter from its lower

level (0.46 cm/s) to higher level (0.94 cm/s) causes a remarkable improvement in recovery of P_2O_5 by 14.2 %. This is at the expense of reducing the grade by about 1.3 %. The effects of changing superficial air velocity on air holdup and bubble diameter are shown in Figures 1-2 respectively. Air holdup, at different levels of frother concentration, is expected to increase with rising superficial gas velocity (Figure 1). This may increase the probability of collision between particles and air bubbles and in turn will increase the number of particle-bubble aggregates, which will be reported to the concentrate. However, the results in Figure 2 reveal that bubble size is linearly related to the superficial gas velocity, at different levels of frother concentration. Similar results have been mentioned by other authors (El-Shall et al. 1999; El-Shall et al. 2000; Dobby and Finch 1986; Yianatos et al. 1986). Thus, the higher air rate produces larger bubbles, which implies a lower total surface area. For example, increasing J_g from 0.24 to 0.94 cm/s, at a frother concentration of 5 ppm, increased the bubble diameter from about 0.44 to 1.01 mm. Such larger bubbles will entrain more liquid throughout the cleaning zone of column. Consequently, the occurrence of particles of lower grade in the froth product will increase.

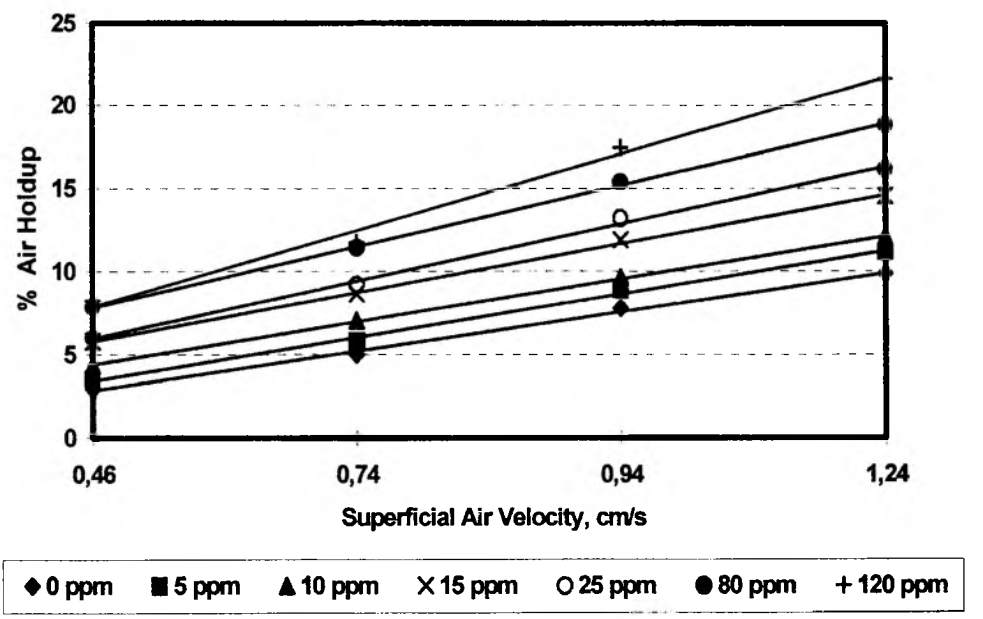

Fig. 1. Effect of superficial air velocity on air holdup at different frother dosages

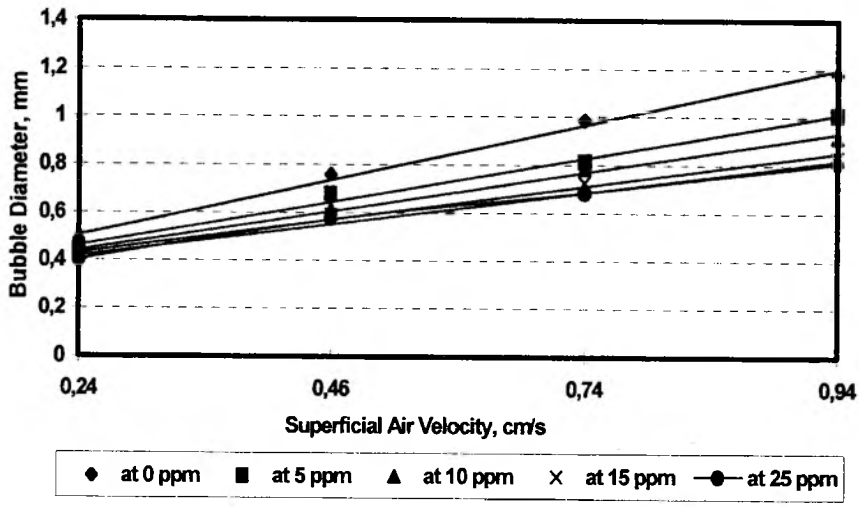

Fig. 2. Effect of superficial air velocity on air bubble diameter

EFFECT OF FROTH CONCENTRATION

The results in Table 3 depicts that increasing frother dosage (X_2) from 5.0 to 25.0 ppm, is accompanied by an improvement in grade of concentrate where the net increase in P_2O_5 content is +1.2. Also, it is interesting to note that the P_2O_5 recovery is also increased by about 8.0 %. It seems from these results that increasing concentration of frother in flotation of such fine phosphate particles is beneficial. On the contrary, it has been shown that in flotation of coarse (belt feed –1.18+0.425, coarse feed -0.85+0.425, and unsized feed –1.18+0.106 mm) particles of Florida phosphate, excessive addition of frother may affect adversely the recovery of concentrates (El-Shall et al 1999, El-Shall et al 1998). To investigate such behavior, the effect of frother concentration on air holdup and bubble diameter was studied in 2-phase experiments, the results of which are shown in Figures 3 and 4.

The results in Figure 3 show that there is a gradual increase in air holdup with increasing frother concentration in the range 5-120 ppm. The increase in air holdup is noticed at different J_g with increasing frother concentration. Such improvement in air holdup is accompanied by a significant reduction in bubbles diameter as shown in

Figure 4. Thus, bubble size will decrease with increasing frother dosage. The rising velocity of these smaller bubbles will be slower than that of larger ones. This will decrease the water recovered with concentrate and consequently will decrease the hydrophilic particles that can be reported with the concentrate. This might improve the grade (Table 3). At the same time, the rate of collision between particles and small air bubbles will increase at the higher frother dosage. This may lead to an increase in the collection rate (in terms of P_2O_5 recovery).

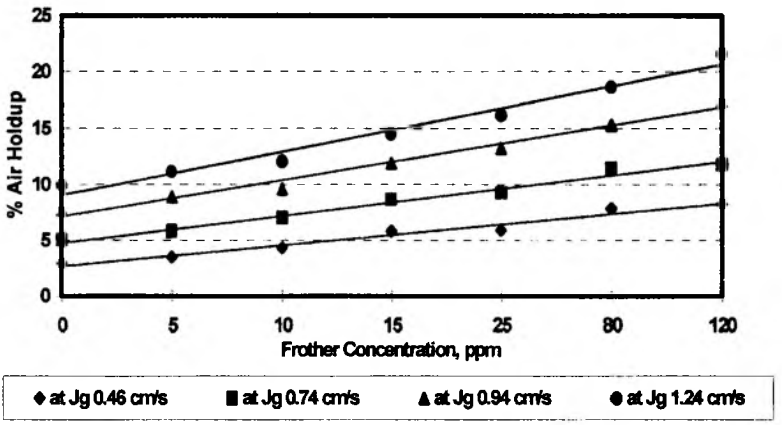

Fig. 3. Effect of frother concentration on air holdup at different superficial air velocity

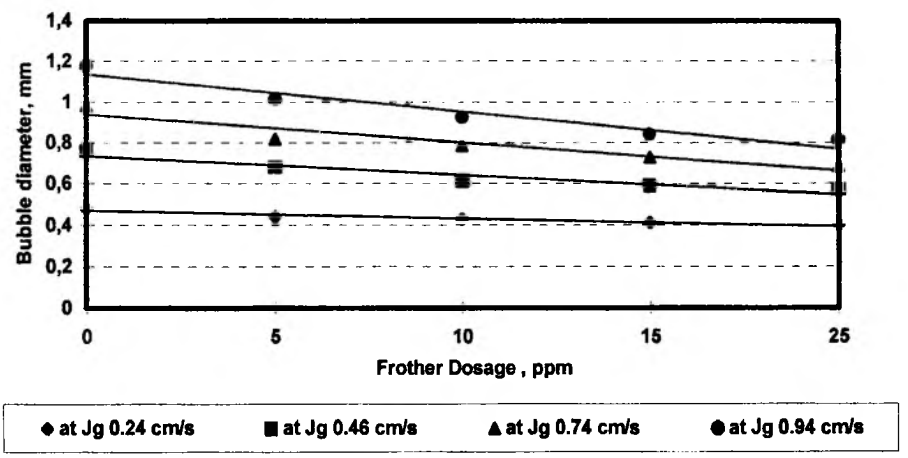

Fig. 4. Effect of frother dosage on air bubble diameter

This is because the collection rate constant (k) depends on bubble diameter (d_b) and superficial air velocity (J_g) according to the following equation (Finch and Dobby 1990).

$$K=1.5\ J_g\ E_K/\ d_b \qquad (2)$$

Where E_K is the collection efficiency.

EFFECT OF SUPERFICIAL WASH WATER VELOCITY

The main objective of applying the downward flow of wash water in the column is to minimize the entrained and entrapped non-floatable particles from the floatable bubble-particle aggregates (Choung et al 1993; Dobby and Finch 1985). This cleaning action is proved in Table 3. The net increase in P_2O_5 content is about +1.9 with increasing the superficial wash water velocity (X_3) from 0.4 to1.2 cm/s. This cleaning action has, also, been proved in column flotation of Egyptian phosphate ores (Abdel-Khalek et al. 2000).

The results shown in Table 3 also show that the recovery is significantly decreased by – 6.4 units with increasing the rate of wash water addition. It seems that at a low superficial wash-water velocity, hydrophilic particles of gangue minerals are washed at the froth zone and then returned to the recovery zone. The resulting product has good grade and high recovery. However, a higher superficial wash-water velocity may affect both the hydrophilic particles and the less hydrophobic particles. This may lead to a high-grade concentrate with lower recovery.

INTERACTIONAL EFFECTS

The interaction (X_1X_2) between superficial air velocity (J_g) and frother concentration is shown to be statistically significant for both grade and recovery as indicated from their average change. The computed F value also suggests the same conclusion. It is expected that the grade of concentrate can be positively affected due to the reduction of bubble diameter as a result of increasing frother dosage (Fig. 4).

On the contrary, the interaction (X_1X_3) between superficial air velocity (J_g) and superficial wash water velocity (J_{ww}) is statistically significant for grade but not for recovery. The computed F value also suggests the same conclusion. It is expected that wash water and air rates have more effect on the bias rate, because variations in these parameters significantly affect the performance of column flotation, as indicated by the main effect. This may lead to such slight reduction in grade (Table 3).

The interaction (X_2X_3) between frother concentration and superficial wash water velocity (J_{ww}) may or may not be significant with respect to grade but it is not

significant to recovery. The computed F value also shows the same trend. This is probably due to an increase of mixing in the cleaning zone as a result of increasing wash water flow rate. It may be concluded that there is no significant interaction between wash water flow-rate and frother concentration. In other words, whatever the level of frother concentration, when the wash water flow rate is increased from lower to higher level, the change in grade or recovery is not significant.

The interaction between the three parameters ($X_1X_2X_3$) is not significant to the recovery and may be significant to the grade as computed from F values. The change in grade is about –0.88 unit.

It is clear from the above discussion that application of such statistical design reveals very interesting information about the interaction between the studied parameters. It is shown that the interaction (X_1X_2) between superficial gas velocity and frother concentration has a beneficial effect on grade but aversely affect recovery. Meanwhile, interaction between superficial wash water and either frother concentration (X_2X_3) or superficial air velocity (X_1X_3) adversely affects the grade but it does not affect recovery.

Based on the above results the effects of the main parameters on the grade can be arranged in the following order: wash water > air flowrate > frother concentration. The order of significance of the main effects of variables for recovery is as follows: air flow rate > frother concentration > wash water.

CONCLUSIONS

Flotation column can be used to recover phosphate mineral from their wastes. It is possible to obtain concentrates with considerable grade and recovery depending on the applied operating conditions.

The effect of wash water or frother concentration is found to be statistically significant where each of them improves the grade of concentrate. On the contrary, effect of superficial air velocity decreases the grade. On the other hand, the effect of each of the studied parameters is found to be statistically significant with respect to the recovery. Both superficial air velocity and frother concentration increases the recovery. However, wash water decreases the recovery.

The interaction (X_1X_2) between superficial gas velocity and frother concentration has a beneficial effect on grade but aversely affect recovery. The interaction between superficial wash water and either frother concentration (X_2X_3) or superficial air velocity (X_1X_3) adversely affects the grade but it does not affect recovery.

REFERENCES

ABDEL-KHALEK N.A.; HASSAN F. & Arafa, M.A. (2000), *Recovery of valuable Phosphates from their slimes by column flotation,* Separation Science and Technology, Vol. 35, No. 7, pp. 1077-1086.

ABDEL-KHALEK N. A. & STACHURSKi J. (1993), *Benficiation of sulfur ore by conventional and column flotation,* Minerals and Metallurgical Processing, August, Vol. 10, 3, pp. 135-138.

CHOUNG J.W., LUTTRELL G.H., YOON, R.H. (1993), *Characterization of operating parameters in the cleaning zone of microbubble column flotation,* International J. Miner Process., Vol. 39, pp. 31-40.

DOBBY G.S., FINCH J.A. (1991), *Column flotation - A selected review, Part II.* Minerals Engineering, 4, 7-11, pp. 911-923.

DOBBY G.S., FINCH, J.A. (1986), *Flotation column scale-up and modeling,* CIM Bulletin, Vol. 79, No. 889, pp. 89-96.

DOBBY G.S., FINCH J.A. (1985), 17th Canadian Mineral Processors Operators Conference, Jan., 22-24.

DOBBY G.S., YIANATOS J.B., FINCH J.A, (1988), *Estimation of bubble diameter in flotation column from drift flux analysis,* Canadian Metallurgical Quarterly, Vol. 27, No.2, pp. 85-90.

EL-SHALL H., SVORONOS S., ABDEL-KHALEK N.A. (1999), *Bubble generation, design, modeling and optimization of novel flotation columns for phosphate beneficiation,* Reports to Florida Institute of Phosphate Research, FIPR, USA.

EL-SHALL H., ABDEL-KHALEK N.A., SVORONOS, S. (2000), *Frother-collector interaction of column flotation of phosphate,* Int. J. Miner. Process., Vol. 58, No. 1-4, pp. 187-199.

EL-SHALL H., CHENG Y.H., ABDEL-KHALEK N.A., SVORONOS S., GUPTA, S. (1998), *A parametric study of column flotation of Florida phosphate,* 2nd International Conference on Phosphate Beneficiation, Palm Coast, FL, USA, Dec.

FINCH J.A., DOBBY G.S. (1990), *Column Flotation,* Pergamon Press, New York, 180.

GARCIA-DIAZ A., PHILLIPS D.T. (1995), *Principles of Experimental Design and Analysis,* Chapman and Hall, New York, pp. 409.

GRIFFITH W.A. (1962), *The design and analysis of flotation experiments.* In: Flotation, (Editor) D.W. Fuerstenau, AIME, USA, pp 177.

MYERS R.H., MONTGOMERY D.C. (1995), *Response Surface Methodology,* John Wiley and Sons, New York, 705.

PATIL D.P., BORNWAL J.P., RAO T.C. (1996), *Column flotation of siliceous rock phosphate,* Minerals and Metallurgical Processing, Nov., pp. 147-150.

TUTEJA R.K., SPOTTISWOOD D.J., MISRA V.N. (1995), *Column parameters: their effect on entrainment in froth,* Minerals Engineering, Vol. 8,No. 11, pp. 1359-1368.

TUTEJA R.K., SPOTTISWOOD D.J., MISRA V.N. (1994), *Mathematical models of the column flotation process - A review,.* Minerals Engineering, Vol. 7, No. 12, pp. 1459.

YIANATOS J.B., FINCH J.A., LAPLANTE A.R., (1986), *Hold up profile and bubble size distribution of flotation column froths,* Canadian Metallurgical Quarterly, Vol. 25, No. 1, pp. 3023 - 29.

N.A.Abdel-Khalek, Planowanie czynnikowe procesu flotacji kolumnowej odpadów fosforowych. XXXVII Seminarium Fizykochemiczne problemy Mineralurgii, 34 (2000), 35-45, (w jęz. ang.)

Metoda planowania czynnikowego została zastosowana do opisania wpływu i współzależności miedzy podstawowymi parametrami procesu flotacji kolumnowej zastosowanej do odzysku fosforytu z

odpadów fosforytowych. Doświadczenia flotacyjne zostały przeprowadzone z wykorzystaniem kwasu olejowego i oleju napędowego jako kolektorów oraz oleju sosnowego jako spieniacza. Planowanie typu 2^3 zostało przeprowadzone w celu znalezienia korelacji między wynikami eksperymentu a średnicą pęcherzyków powietrza i parametrami urządzenia, które jej wytwarza. Otrzymane wyniki wskazują, że zastosowana metoda planowania dostarcza interesujących informacji o wzajemnej korelacji miedzy analizowanymi parametrami procesu. Dla przykładu , zostało pokazane, że korelacja X_1X_2 czyli miedzy prędkością przepływu gazu (X_1) a stężeniem spieniacza (X_2) na korzystny wpływ na wychód a niekorzystny wpływ na uzysk procesu flotacji.

Physicochemical Problems of Mineral Processing, 34 (2000), 47–56
Fizykochemiczne Problemy Mineralurgii, 34 (2000), 47–56

Zygmunt SADOWSKI*, Ewa JAŻDŻYK*, Teresa FARBISZEWSKA**, Jadwiga FARBISZEWSKA-BAJER**

BIOOXIDATION OF MINING TAILINGS FROM ZLOTY STOK

Received March 15, 2000; reviewed and accepted May 15, 2000

The biooxidation of gold-bearing arsenic concentrate from mining tailing was investigated. The strain of *Thiobacillus ferrooxidans* isolated from the Zloty Stok tailing heaps was used. The chemical and biooxidation processes were monitored by checking the ferrous, ferric and arsenic concentration in the leaching solution. Leaching experiments were conducted using both coarse (-0.5 +0.125 mm) and fine (-0.045 mm) fractions. The samples were examined by means of the specific surface area measurements and the X-ray diffraction analysis. The small differences were observed during the oxidation of coarse and fine fractions. The slow chemical dissolution of loellingite ($AsFe_2$) a main arsenic-bearing mineral, was supported by X-ray diffragrams. In the case of a fine fraction oxidation, the precipitation of ferric arsenate was responsible for the lower Fe and As readings. The production of new phase was also supported by the FTIR spectra. Obtained results suggest that the direct biooxidation mechanism was responsible for the arsenic-bearing concentrate biooxidation.

Key words: bioleaching, loellingite, arsenopyrite, Thiobacillus ferrooxidans, gold, ferric arsenate

INTRODUCTION

Biooxidation pre-treatment of refractory gold ores and flotation concentrates is an alternative method to roasting and pressure oxidation (Ehrlich, Brierley 1990; Rossi 1990; Barret et al. 1993; and Rawlings 1997). Refractory gold ores contain gold as

* Department of Chemistry, Wroclaw University of Technology, 50-370, Poland
** Department of Biology and Environment Engineering, University of Opole, 45-320 Opole, Poland

tiny inclusions in association with the sulphide, arsenosulphide and arsenic-bearing minerals (Wakao et al. 1988; Malatt 1999).

Bacterial oxidation of sulphide or arsenic refractory ores is mainly based on the action of the acidophilic, chemolithotrophic microorganisms such as *Thiobacillus ferrooxidans, Thiobacillus thiooxidans* and *Leptospirillum ferrooxidans*. These microorganisms are used to accelerate the rate of minerals oxidation by breaking down the crystal lattice and thus liberation of the microinclusions of native gold.

Generally, two broad mechanisms of bacterial oxidation have been proposed:

i. the "direct" mechanism in which microbial cells are attached to the mineral surface and used an enzyme system with oxygen.

ii. The "indirect" mechanism, in which the role of microorganism cells, is to produce ferric ions by oxidation of ferrous ions. The ferric ions participate in the chemical oxidation of minerals.

Most work with regard to the biooxidation has been done with pyrite and arsenopyrite (Adam et al. 1994; Nyashnu et al. 1999). The arsenopyrite was more rapidly and extensively destroyed than the pyrite. The biooxidation of arsenopyrite can be realised by the following way:

$$FeAsS + 5\ Fe^{3+} + 3\ H_2O \rightarrow 6\ Fe^{2+} + H_3AsO_3 + 3\ H^+ + S^0 \quad (1)$$

At the extreme oxidation condition, sulphur is completely oxidised to S(VI) and arsenic (III) is rapidly oxidised to arsenic(V):

$$FeAsS + 13\ Fe^{3+} + 8\ H_2O \rightarrow 14\ Fe^{2+} + H_3AsO_4 + 13\ H^+ + SO_4^{2-} \quad (2)$$

Wakao et al. (1988) have suggested that *Thiobacillus ferrooxidans* was not responsible for arsenate oxidation. According to Wakao's paper, the potential energy derived from the arsenate oxidation is not necessary for the growth of bacteria.

Chilean refractory gold ores containing both enargite (Cu_3AsS_4) and cobalt bearing sulphides (Co,Fe) $(AsS)_2$ as a gold matrix were also processed (Chimorro et al. 1998, Wiertz et al. 1999). The bioleaching process, in which the cobalt and arsenic were recovered, has been offered. It was found that bioleaching of energite is governed by the indirect mechanism.

The aim of this study was to determine factors affecting the efficiency of arsenic-gold concentrate biooxidation in shake flask studies systems. The mechanism of bioleaching of arsenic-bearing minerals is also investigated.

MATERIALS AND METHODS

Tailings from a closed arsenic mine at Zloty Stok (Lover Silesia, Poland) contain gold-bearing minerals (loellingite and arsenopyrite), and were hand collected and used in laboratory experiments. The tailing samples were ground and wet-screened to obtain the three fractions: 0.5-0.125, 0.125-0.040 and –0.040 mm. The arsenic tailing assayed 27.98 % Fe, 4.99 % As, 15.78 % SiO_2, 8.65 % S, 2.81 % Mg, 2.41 % Ca, and Au 3-7ppm. The carbonate minerals present in the feed material were dissolved using sulphuric acid.

The bacteria *Thiobacillus ferrooxidans* used in the biooxidation tests were isolated from slurries collected at the old arsenate mine Zloty Stok (Sadowski et al. 1998). The microorganism strain was initially adapted for growth in the presence of mineral feed prior to the biooxidation experiments.

Leaching and bioleaching experiments were performed in 250 ml Erlenmeyer flasks using 3 g of mineral sample in 100 ml of a nutrient solution. The slurry was conditioned in the medium 3K over 24 hours, then the inoculum was added to the bioleaching samples. Thymol, as a bacterial inhibitor was added to the chemical leaching samples. The flasks were shaken on a table shaker at the temperature equal to 30°C. Bacterial oxidation tests were performed at an initial pH = 2.

The flasks were periodically analysed for pH, iron(II) and total iron by the colorimetric method. The total arsenic concentration in the supernatant was determined by oxidation arsenic(III) to arsenic(V) and the concentration of molybdenum blue complex was measured at 865 nm.

Specific surface area of the mineral samples before and after of biotreatment was determined according to the BET method. Flow Sorb II 2300 (Micromeritics) was used to a surface area measurement.

The X-ray diffraction spectra of the mineral samples were obtained using Philips PW 1390 equipment, with CuK_a radiation and Ni filter.

Infrared spectra of sample obtained from after and before biooxidation were recorded on a Fourier Transformed Infrared Spectrometer Perkin Elmer Model 1600 FTIR. The sample was prepared by mixing 2 mg of mineral samples with 150 mg of KBr for transmission spectroscopy.

RESULTS

The initial bioleaching and chemical leaching experiments involving the arsenic bearing concentrate were carried at 12 % (w/v) of solid using –0.5+0.125 mm fraction. Figure 1 and 2 show the variation in the As, and Fe(III) concentrations during the leaching test. These data represent the average response of four particular tests. The

pH values were also recorded. The arsenic analyses were only performed on the liquid phase. In both cases, an increase of arsenic concentration was observed at the initial period. As can be seen from Fig. 1 and Fig. 2 the arsenic concentration in the bioleaching test was higher than that for the chemical leaching experiment.

Arsenic(III) is a primary product of the chemical and bacterial oxidation of loellingite and is normally oxidised by iron(III) to arsenic(V) in a secondary process. The predominance of arsenic(III) was observed at the early stage of oxidation period.

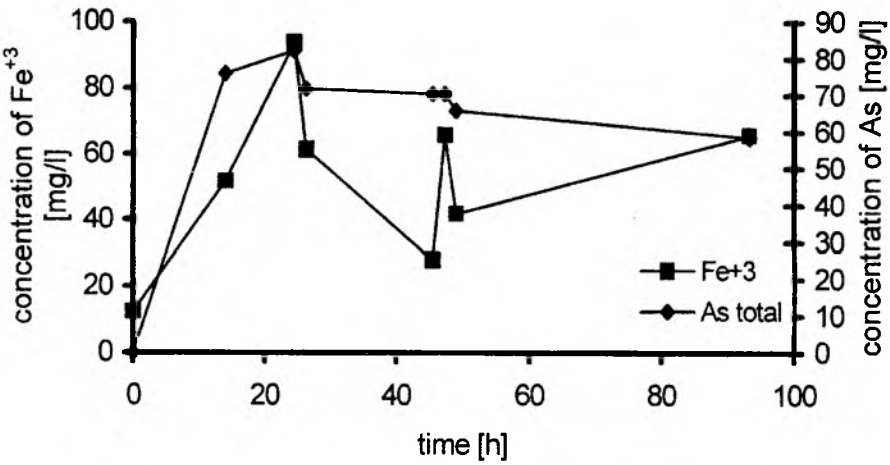

Fig. 1. Oxidation of arsenate concentrate (fraction –0.5 +0.125 mm)

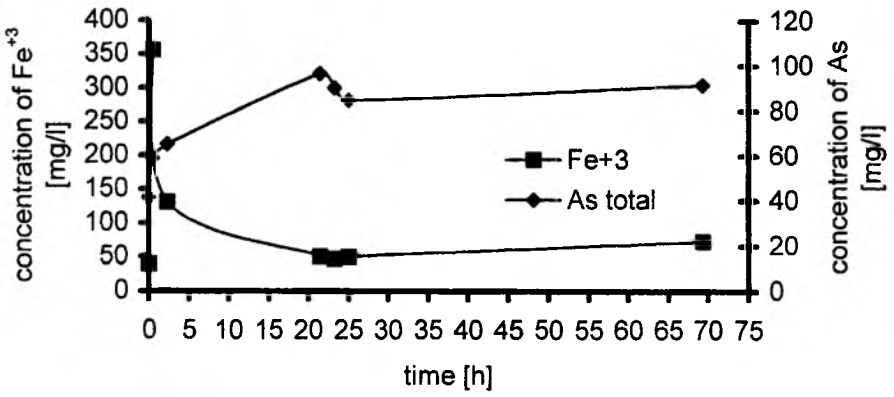

Fig. 2. Biooxidation of arsenate concentrate (fraction –0.5 +0.125mm)

The leaching results are confirmed in the Table 1, where the surface areas of bioleaching samples are higher than the surface areas of chemical leaching samples.

Table 1. The surface areas of arsenic concentrate samples after the both chemical and bioleaching

Sample size [mm]	Surface area [m^2/g]			Time of leaching [h]	Nature
	Without Leaching	Chemical Leaching	Bioleaching		
-0.5 +0.125 (30%)	0.32	1.02	2.94	24	2K
-0.5 +0.125(12%)	0.32	5.55	7.49	70	2K
-0.040 (6%)	6.64	27.6	28.8	65	2K
-0.040(12%)	6.64	12.54	16.18	65	2K
-0.040(18%)	6.64	11.77	11.87	65	2K
-0.040(12%)	17.64	58.64	60.45	32 days	9K

The effect of density on the rate of oxidation was investigated using a fine fraction (-0.040mm) of arsenic bearing concentrate. It was found, by analysing the surface areas of leaching samples that the optimal biooxidation conditions correspond to the concentration of 12 % (w/v). The surface areas achieved for the same time period of bioleaching are also shown in Table 1.

The high concentration of solid may induce a limitation in agitation of suspension and inhibits the leaching of mineral. Consequently the surface areas of samples at the higher concentrations have been lower that in the case of 5% of solid (Table 1).

A part of X-ray diffraction spectra of samples before and after of bio- and chemical leaching are shown at the Figure 3. They confirm that a biooxidation of loellingite is more extensive than chemical oxidation.

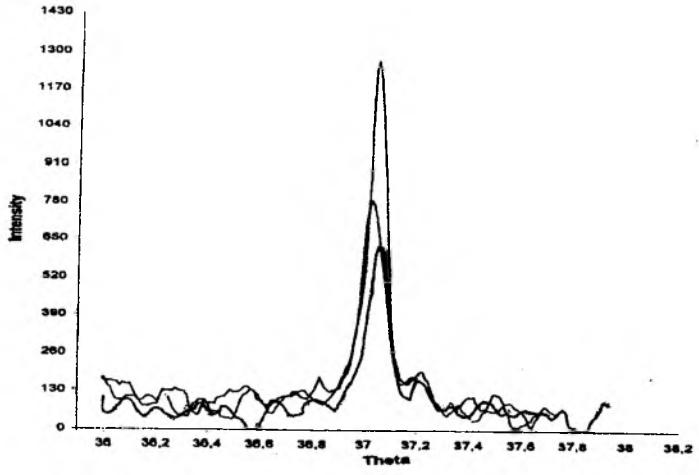

Fig. 3. A part of X-ray diffraction pattern of - 0.045 mm fraction of arsenate concentrate before and after both the chemical and bioleaching

As can be seen form Fig.4 and 5, the fine fraction showed a similar trend in the course of the bioleaching and chemical leaching like the coarse samples.

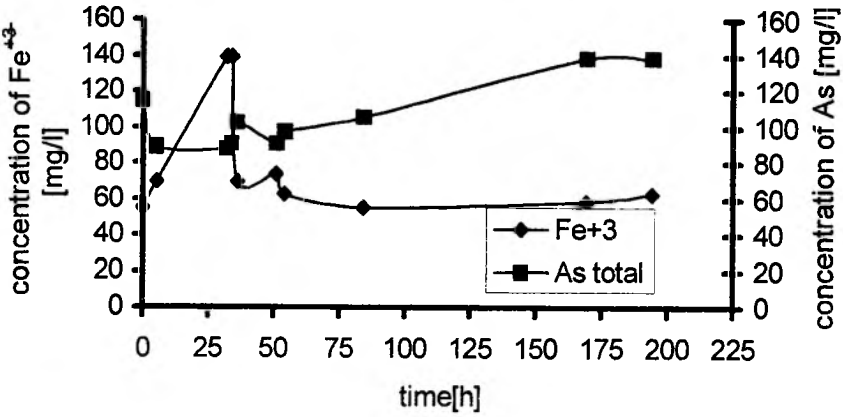

Fig. 4. Bioleaching of fine arsenate concentrate

Figure 5 indicates that the arsenic concentration in the solution slowly increased during the period of bioleaching. The evolution of arsenic concentrations, different from the leaching results of course fraction, can be attributed to the ferric arsenate precipitation.

$$3\ H_3AsO_4 + Fe_2(SO_4)_3 \rightarrow 2\ FeAsO_4 + 3\ H_2SO_4 \qquad (3)$$

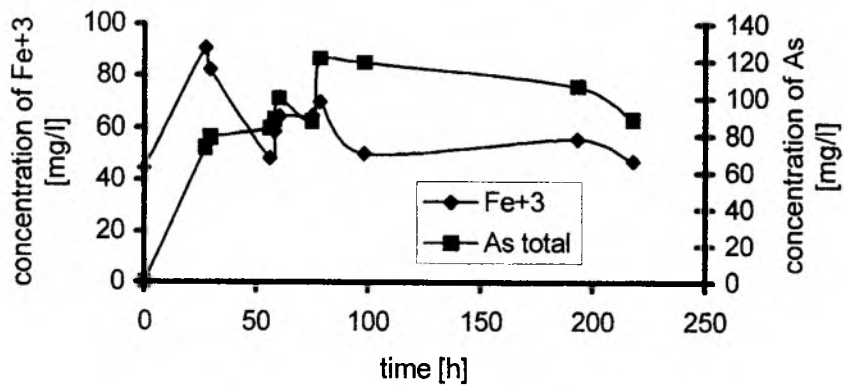

Fig. 5. Chemical leaching of fine arsenate concentrate

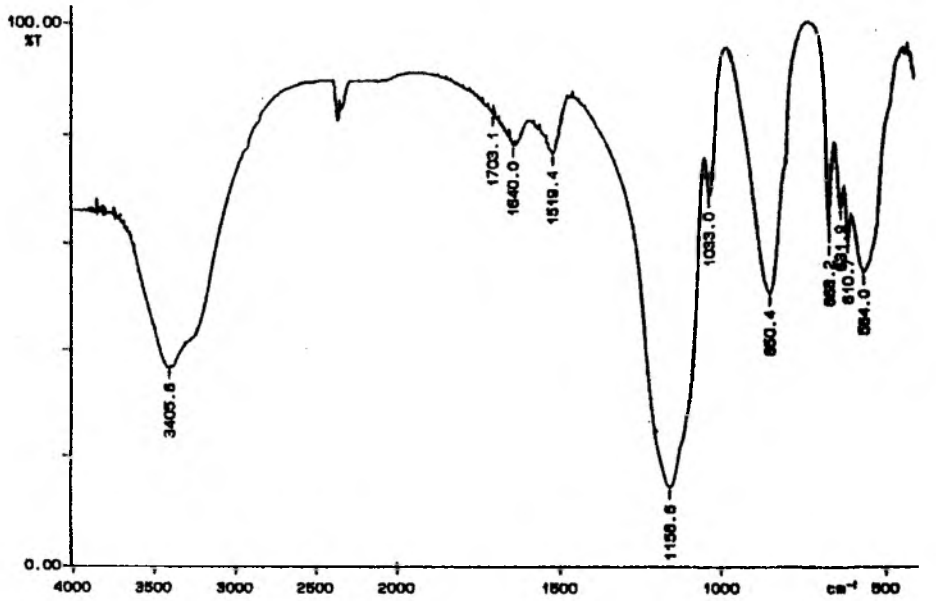

Fig. 6. FTIR spectra of ferric arsenate precipitated during the leaching tests

The precipitation of ferric arsenate was supported by the FTIR studies. From Fig. 6 it is apparent that the bands at 850 and 1033 cm^{-1} are assigned to the stretching vibration of ferric arsenate. The band at 1640 cm^{-1} corresponds to the stretching vibration of the structural water principally linked with ferric arsenate

DISCUSSION

The bacterial oxidation of mining tailing from Zloty Stok is not fully understood. It results from complex mineralogical composition of the tailings. According to early research (Norman, Snyman 1988; Komnitsas et al. 1994; Taxiarchou et al. 1994; Breed et al. 1996) the biooxidation of arsenic–bearing minerals results in a range of products with varying amounts of end forms of sulphur, iron and arsenic. Arsenic, for instance, may be present as As(III) or As(V). It was suggested that microbes did not oxidise arsenic (Fernandez et al. 1995, Cassity, Pesic 1999). The potential energy derived from the arsenic oxidation is not necessary for the growth of the micro-organisms. For this reason, the As(III) ions are chemically oxidised by ferric iron.

$$As(III) + 2\ Fe(III) \rightarrow As(V) + 2\ Fe(II) \quad (4)$$

The iron(II) produced in the above equation must be converted back to the iron(III) by bacterial oxidation process:

$$Fe(II) + 2\ H^{+} + 0.5\ O_2\ (bakteria) \rightarrow Fe(III) + H_2O \qquad (5)$$

The variation of arsenic speciation is caused by a precipitation of $FeAsO_4$. The precipitation of ferric arsenate can be realised at a Fe/As ratio higher than 3 (Reddy et al. 1987). During the bacterial leaching of arsenic-bearing mineral the Fe(III)/As ratio was changed. Arsenic ions were found to dominate in the initial stage of the biooxidation of fine fraction of arsenic-bearing ore. When the concentration of Fe(III) was suitable, the precipitation of iron arsenate occurs. The concentration of arsenic ions in solution decreases at the end period of leaching (Fig. 1 and Fig. 5). It is interesting to note, that the biooxidation process of the fine arsenic bearing solid waste in the presence of nutrient 9K medium can not be controlled by a change of arsenic ions concentration. The chemical analysis revealed that the leach solution was free from arsenic ions. The absence of arsenic ions is likely to be due to the ferric arsenate precipitation. On the other hand, the arsenic toxicity to *T.ferroodans* is well known (Cassity and Pesic 1999). In general, the toxicity decreases upon precipitation of $FeAsO_4$. It suggests that the bioleaching of arsenic bearing solid waste should be realised at a high ferric ion concentration. The concentration of arsenic ions in the leach solution can not be a parameter of biooxidation process.

CONCLUSIONS

1. Biooxidation of arsenic-bearing gold ore is a complex process, which occurs in a sequential way:
   i. the first stage corresponds to biooxidation of iron and leaching
   ii. in the second stage, arsenic(III) is oxidised to arsenic(V)
2. The recovery of arsenic was satisfactory for both coarse and fine fractions.
3. Concentration of As cannot be used to measure the extent of this process due to the precipitation of iron(III) arsenate during the fine fraction bioleaching.
4. The micro-organisms used for the biooxidation showed a good tolerance to the high arsenic concentration.

ACKNOWLEGEMENT

The authors with to acknowledge the financial support of Polish Science Foundation under grant number 9T 12B 028 14. We thank Ms. W. Jagiello for her assistance in determining the FTIR spectra.

REFERENCES

ADAM K., KOMNITSAS C., PAPASSIOPI N.L., KONTOPOULOS A.,POOLEY D.F., TIDY N.P. (1994), *Stability of Arsenical Bacterial Oxidation Products*, Hydrometallurgy, IMM, Chapman & Hall, pp..291-350.

BARRET J., HUGHES M.N., KARAVAIKO G.I., SPENCER P.A. (1993), *Metal Extraction by Bacterial Oxidation of Minerals*, Ellis Horwood, New York, pp. 1-75.

BREED A.,W., GLATZ A., HANSFORD G.S., HARRISON S. T.L. (1996), *The Effect of As(III) and As(V) on the Batch Bioleaching of a Pyrite- Arsenopyrite Concentrate*, Minerals Engineering , 9 (12), pp. 1235-1252.

CASSITY D.W., PESIC B. (1999), *Interaction of Thiobacillus ferrooxidans with arsenite, arsenate and arsenopyrite*, Biohydrometallurgy and the Environment Toward the Mining of 21st Century, R.Amils, A.Ballester (Eds.) Elsevier, Amsterdam, pp..521-532.

CHOIMORRO J., FRENAY J. (1998), *Bacterial Leaching of a Chilean Cobalt Arsenide.*, Environment & Innovation in Mining and Mineral Technology, M.A.Sunchez, F.Vergara, S.H.Castro (Eds.), University of Conception, Chile.

EHRLICH L.H., BRIERLEY L.C. (1990), *Microbial Mineral Recovery*, McGraw-Hill, New York, pp. 127-147.

FERNANDEZ, MONROY M.G., MUSTIN C., deDONATO P., BARRES O., MARION P., BARTELIN J. (1995), *Occurrences at Mineral-Bacterial Interface During Oxidation of Arsenopyrite by Thiobacillus ferrooxidans*, Biotech. Bioeng., 46, pp. 13-21.

KOMNITSAS C., POOLRY F.D. (1994), *Bacterial Oxidation of an Arsenical Concentrates*, Hydrometallurgy' 94, IMM, Chapman & Hall, pp. 351-359.

KRAUSE E., ETTEL V.A. (1989), *Solubility and Stabilities of Ferric Arsenate Compounds*, Hydrometallurgy, 22, pp..311-337.

MALATT K.A. (1999), *Bacterial Oxidation of Pure Arsenopyrite by Mixed Culture*, Biohydrometallurgy and Environment Toward the Mining of 21st Century, R.Amils, A.Ballester (Eds.), Elsevier, Amsterdam, pp.411-421.

NORMAN P.F., SNYMAN P.C. (1988), *The Biological and Chemical Leaching of an Auriferrous Pyrite/Arsenopyrite Flotation Concentrate*. Geomicrobilogy J., 6, pp. 1-10.

NYASHANU R.M., MONHENIUS A.J., BUCHNAN D.L. (1999), *The Effect of Ore Mineralogy on the Speciation of Arsenic in Bacterial Oxidation of Refractory Arsenical Gold Ores*, Biohydrometallurgy and Environment Toward the Mining of the 21st Century, R.Amils, A.Ballester, (Eds.), Elsevier, Amsterdam, pp.431-441.

RAWLINGS D.E. (ed.) (1997), *Biomining, Theory, Microbes and Industrial Process*, Springer-Verlog, Berlin, pp. 117-126.

REDDY R. G., HENDRIX J.I., QUENEAU P.B. (1987), *Arsenic Metallurgy Fundamentals and Application*, The Metallurgical Society Inc., Warrendale , pp. 199-211.

ROSSI G. (1990), *Biohydrometallurgy*, McGraw-Hill, Hamburg, pp. 493-520.

SADOWSKI Z., FARBISZEWSKA T., FARBISZEWSKA-BAJER J. (1998), *The Isolation of Bacteria Thiobacillus from Zloty Stok Deposit*, Physicochemical Problems of Mineral Processing 33, pp.191-199.

SPANCER P.A., BUDDEN R.J. SNEYD R. (1989), *Use of a Moderately Thermophilic Bacterial Culture for the Treatment of Refractory Arsenopyrite Concentrate*, Biohydrometallurgy, pp. 231-237.

TAXIARCHOU M., ADAM K., KONTOPOULOS A. (1994), *Bacterial Oxidation Conditions for Gold Extraction from Olympias Refractory Arsenical Pyrite Concentrate*, Hydrometallurgy, 36, pp. 169-185

WAKAO N., KOYATSU H., KOMAI Y., SHIMOKAWARA H., SAKURAI Y., SHIOTA H. (1988), *Microbial Oxidation of Arsenite Occurence of Arsenite-Oxidizing Bacteria in Acid Mine Water from a Sulfur-Pyrite Mine*, Geomicrobiology J., 6, pp. 11-24.

WIERTZ J.V., LUNAR R., MATURANA H., ESCOBAR B. (1999), *Bioleaching of Copper and Cobalt Arsenic-Bearing Ores: Chemical and Mineralogical Study*, Biohydrometallurgy and Environment Toward the Mining of the 21st Century, R.Amils, A.Ballester, (Eds.), Elsevier, pp..397-404.

Sadowski Z, Jażdżyk E, Farbiszewska T, Farbiszewska-Bajer J., Bioutlenianie odpadów górniczych ze Złotego Stoku, Fizykochemiczne Problemy Mineralurgii, 34 (2000), 47-56, (w jęz. ang.)

Przeprowadzone wcześniejsze badania wskazują, że odpady górnicze zgromadzone na Hałdzie Jan koło Złotego Stoku stanowią potencjalny surowiec do otrzymywania złota. Przestawiona praca zawiera wyniki badań nad procesem bioutleniania próbek mineralnych pobranych z hałdy Jan. W badaniach użyto homogenicznych bakterii *Thiobacillus ferrooxidans* wcześniej wyselekcjonowanych z tego złoża. Próbom bioługowania poddano grubo- i drobnoziarnistą frakcję surowca. Przebieg procesu bioutleniania analizowane przez kontrole zmian stężenia jonów Fe(II) , Fe(III), As oraz pH roztworu. Określono zmiany w powierzchni właściwej próbek mineralnych wywołane procesem bioutleniania. Zachowanie gruboziarnistej próbki mineralnej mało różni się od chemicznego i biologicznego utleniania materiału drobnoziarnistego. Badania rentgenowskie wskazują na łatwiejsze bioutlenianie loellingitu w porównaniu z procesem chemicznym. Zmniejszenie stężenia jonów arsenu w roztworze w końcowym okresie chemicznego ługowania należy tłumaczyć wytrąceniem się arsenianu żelaza. W przypadku zastosowanie pożywki 9K do bioługowania, stężenie arsenu w roztworze spadało do zera. Badania spektroskopowe potwierdzają powstanie arsenianu żelaza w procesie bioutleniania drobnoziarnistej frakcji odpadów górniczych z hałdy Jan.

Physicochemical Problems of Mineral Processing, 34 (2000), 57–66
Fizykochemiczne Problemy Mineralurgii, 34 (2000), 57–66

Tadeusz GLUBA*, Bogusław KOCHAŃSKI*

INTERPARTICLE DISTANCES IN THE CROSS SECTION OF GRANULES WITH DIFFERENT GRAIN SIZE DISTRIBUTIONS

Received March 15, 2000; reviewed and accepted May 15, 2000

Results of microscopic studies of interparticle distances in granules with different grain size distributions are presented in the paper. It was found on the basis of the analysis of luminance profiles of the image of the granule cross section that the granule consisted of multi-layer aggregates of grains placed at random in the granule volume. The range of changes in interparticle distances is related to the size of material grains.

Key words: granulation, granule, structure, configuration, distribution of particles

INTRODUCTION

A raw material for the process of agglomerative granulation is a fine-grained solid whose particles under the influence of binding liquid and mechanical interactions form cohesive agglomerates – granules. A granule is a system of n particles which are combined by the forces of mutual interactions (Strelkov 1982). It has a finite potential energy of potential interactions between the i-th and k-th particle belonging to the system. The extent and type of interactions depend on the following factors: the method of granulation, chemical and physical properties of a solid body and binding liquid, as well as on the process conditions. During the process, particles of fine-

* Technical University of Lodz, Faculty of Process and Environmental Engineering, Department of Process Equipment, ul. Wólczańska 175, 90-924 Łódź, Poland

grained solid with batch density corresponding to their position, transfer to the state resulting from the density of formed granules. The models of particle growth developed so far (Batterham et al. 1990) take into account neither changes of the density nor the structure of the granules being formed. In general, a predominating principle is to assume a defined mechanism of growth for a given method of granulation.

Many models of particle beds developed until present (Ouchiyama and Tanaka 1986, Yu and Standish 1987, Nolan and Kavanagh 1992) refer to systems consisting of a few components and built from spherical particles. The simplest elementary model of a granule is a system of two spherical particles of the same size, combined by interparticle forces. At the steady, average force of interactions between the two particles, the potential energy of the binary system depends on a distance from each other, so the determination of particle position within a granule is a vital problem.

Particles in a granule (the system of grains limited by the interfacial area) are arranged in some characteristic pattern. The closest neighbours of each grain reveals some order which decides about the granule microstructure. This order should refer both to the number of neighbours, as well as their location. In the case of grains of the same size the order should be the same for each grain. In a polydispersive system of particles, one may expect a significant differentiation depending on the particle size. The probability of finding a particle in the given point of granule volume depends on assuming a different position by another particle.

A probabilistic relationship between the position of particles can be described quantitatively by means of a bivariate distribution function of random variable X, which can assume only two values *x1* and *x2* with positive probability:

$$P(X = x1) = p \tag{1}$$

$$P(X = x2) = 1 - p \tag{2}$$

where $0 < p < 1$.

If a sphere of radius r limited by a layer of thickness dr is distinguished in a spherical granule, the number of particles in the layer surrounding the particle placed inside the granule is

$$dN = 4\pi(N/V)F(r)r^2dr \tag{3}$$

where: N – number of particles in volume V, and $F(r)$ – distribution function.

The aim of the study was to determine interparticle distances, the character and the parameters of distribution in granules formed from materials with different particle

size distribution. The values were determined on the basis of particle configuration in the system during experimental microscopic studies

EXPERIMENTAL

The structure was investigated in a set-up equipped with a reflecting microscope Olympus SZ11, with a camera, light source and a computer Pentium 133 equipped with an image analysis system "Lucia".

Granules formed from dolomite with three ranges of particle size (containing grains 0.16-20, 0.16-60 and 0.16-100 μm) and from glass balls (19-76 μm) of mean diameter 50 μm were tested. The tested granules were ground on a flat screen to approximately half their diameter in order to form a flat intersection. The obtained granule was the subject of microscopic studies

A fragment of the intersection field illuminated by a two-point light source was observed in the microscope and next, by means of a camera transmitted to the computer, where it appeared in the form of a rectangular image on the screen.

The position of five analysed images (in the form of rectangles 0.85 mm long and 0.65 mm high) along the longer axis of the intersection area is shown in Fig. 1.

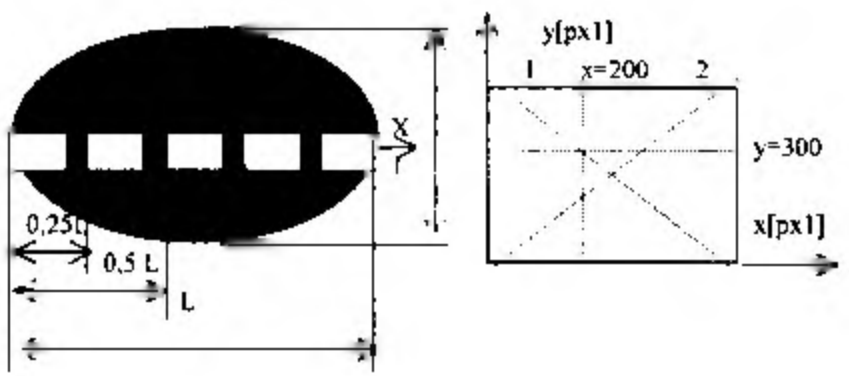

Fig. 1. Position of fields, coordinate axis and measuring points

Two of them include grains in the outer layer (X = 0, X = L), one in the middle and two others at a distance X = 0.25 L. In the measuring points of constant coordinates $y = 300$ pxl and $x = 200$ pxl the local image brightness (in the form of an abstract number) was determined. For the applied calibration the distance of measuring points was 0.00119 mm. One measuring length included a hundred points. The defined values of brightness of particular image points corresponded to the characteristic positions of grains and interparticle gaps.

RESULTS

The dependence of brightness on position defines the cross section profile which is given in the form of a diagram or numerical data. Figure 2 presents an example of the profile of 0.16-60 μm dolomite granule intersection area, referring to the image located at a distance of 0.25L from the intersection edge.

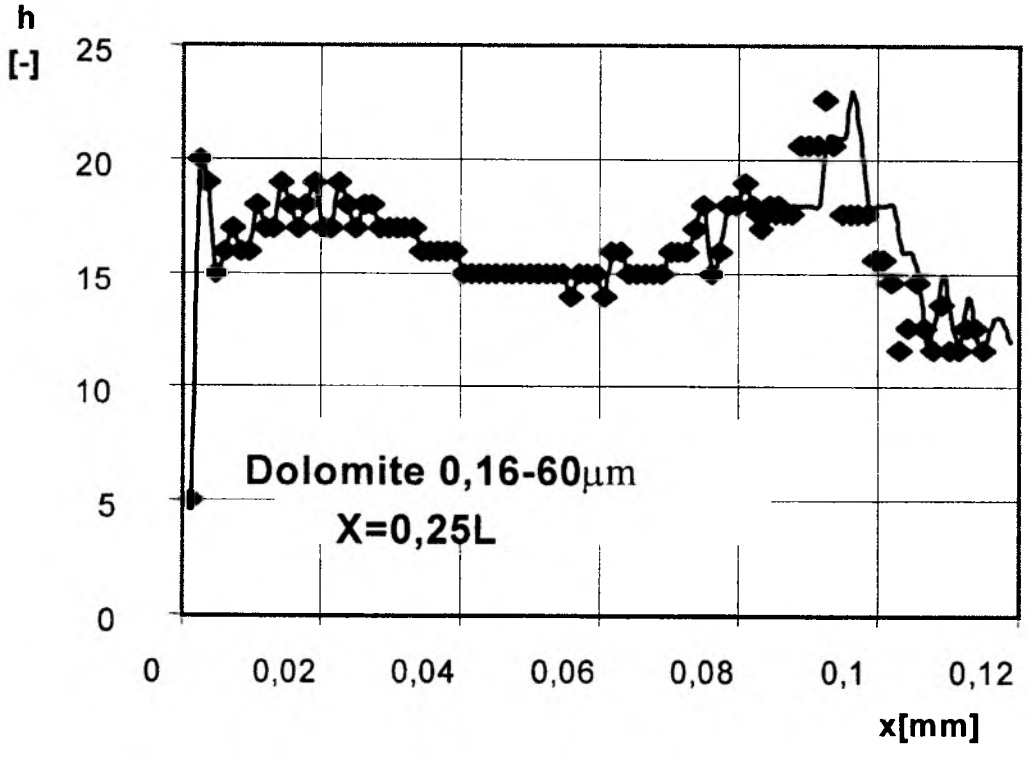

Fig. 2. Profile of 0.16-60 mm dolomite granule intersection area

The profile of glass ball granule intersection drawn for axis x is shown in Fig. 3. On the basis of these data the distances between peaks of a profile curve were determined. Each peak of the profile curve corresponds to the local brightness maximum and, in fact, provides an evidence of the presence of the next solid grain in this place. Diagrams of the dependence of interparticle distances on the position of solid particles along measuring axes x, y were drawn. Examples of these dependences are illustrated in Fig. 4.

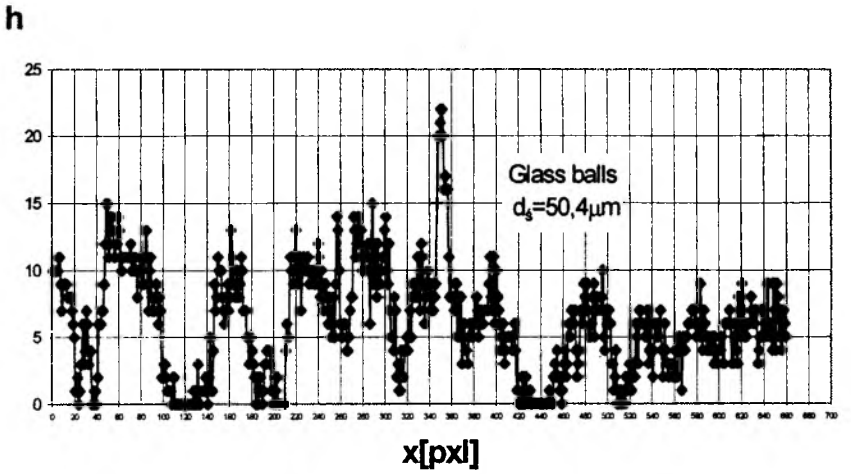

Fig. 3. Profile of granule intersection along the horizontal axis of the image

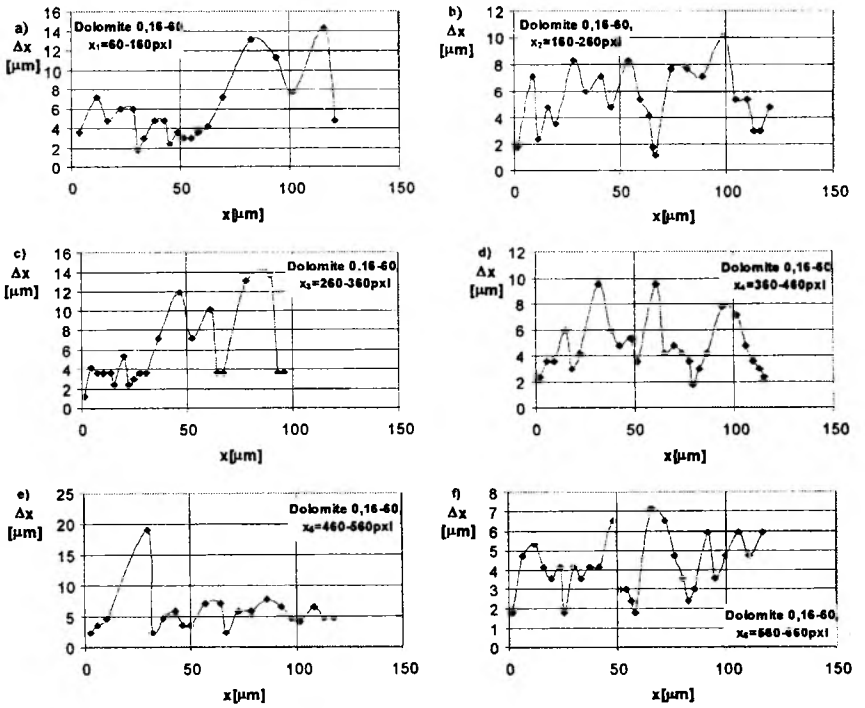

Fig. 4. Dependence of the interparticle distance on the position for particular measuring lengths

For a given measuring length the mean interparticle distance $\Delta x_{\acute{s}}$ was calculated:

$$\Delta x_{\acute{s}} = \frac{\sum_{i=1}^{n} \Delta x_i}{n} \tag{3}$$

standard deviation $s(\Delta x)$

$$s(\Delta x) = \sqrt{\frac{\sum_{i=1}^{n} (\Delta x_i - \Delta x_{\acute{s}})^2}{n-1}} \tag{4}$$

and density distribution $q(\Delta x)$.

$$q(\Delta x) = \frac{n_i}{\Delta(\Delta x)\sum_{i=1}^{n} n_i} \tag{5}$$

The dependence of mean interparticle distance in the tested granules on the position along the intersection axis is shown in Fig. 5.

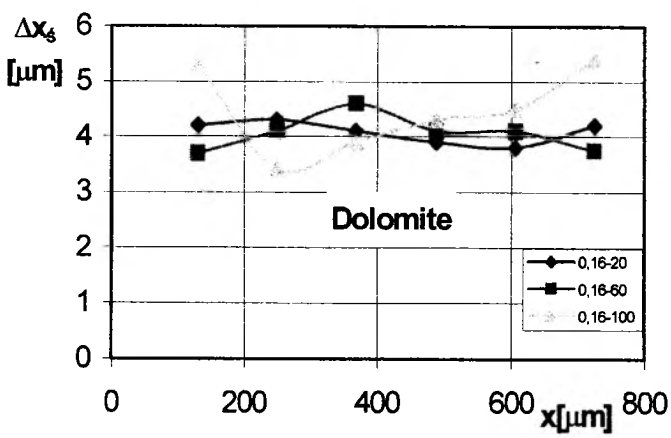

Fig. 5. Dependence of mean interparticle distance on the position of measuring length in the measuring field X = 0.5L

The mean distance between solid particles $\Delta_{\acute{s}}$ was calculated for particular measuring fields as follows:

$$\Delta_{\acute{s}} = \frac{\sum_{k=1}^{6}\sum_{i=1}^{n}\Delta x_i}{\sum_{k=1}^{6}\sum_{i=1}^{n} n_i} \tag{6}$$

The distribution of interparticle distances for various field in the granule intersection is illustrated in Fig. 6. The values of dimensionless distance of the measuring field from the intersection edge presented in the form of quotient X/L are represented on the axis of abscissae, and on the axis of ordinates there are mean values of interparticle distances.

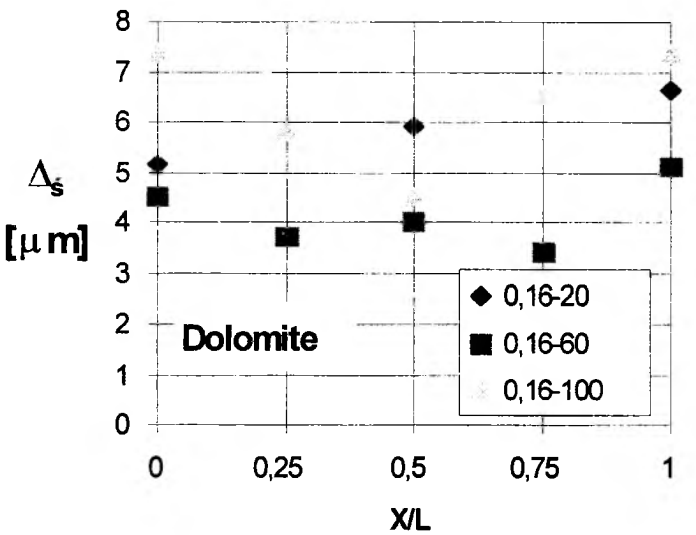

Fig. 6. Distribution of interparticle distances along the granule intersection axis

The functions of distance density distributions in the measuring fields X = 0.5L in the intersections of tested dolomite granules are shown in Fig. 7. Figure 8 shows the functions of density distributions for distances in the field X = 0.5L along its diagonals and axis *x* and *y* calculated for granules of glass balls.

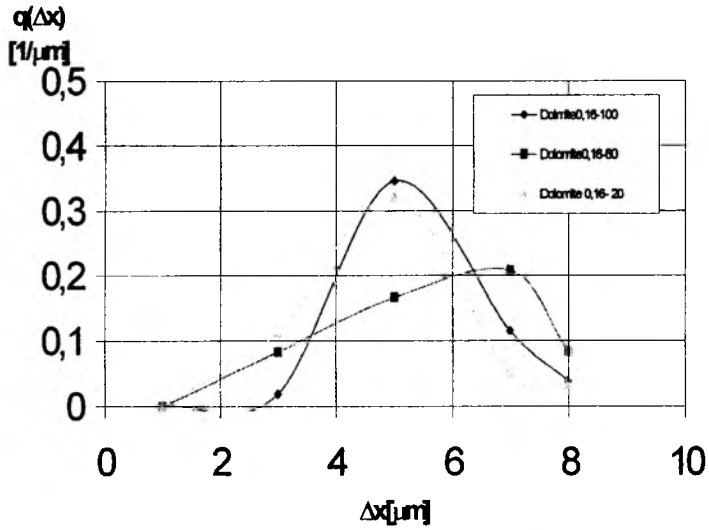

Fig. 7. Diagrams of density distributions of interparticle distances in dolomite granules

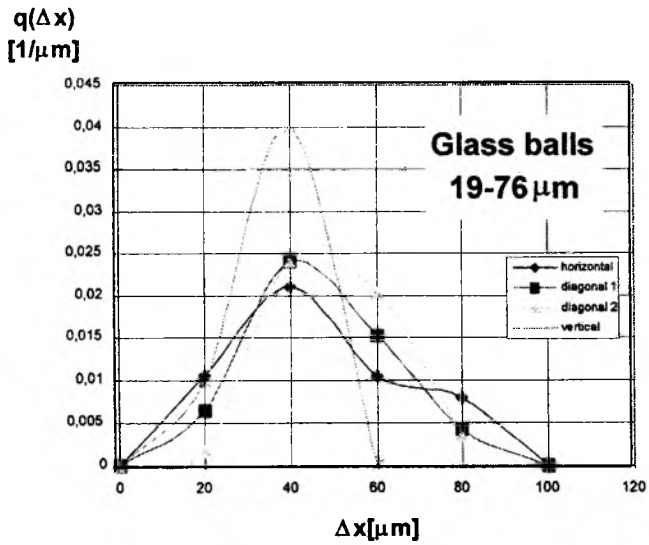

Fig. 8. Distance distributions on model granules made from glass balls

A comparison of density distributions of distances determined for particular measuring lengths of the field X = 0.5L for 0.16-60 dolomite granules is shown in Fig. 9.

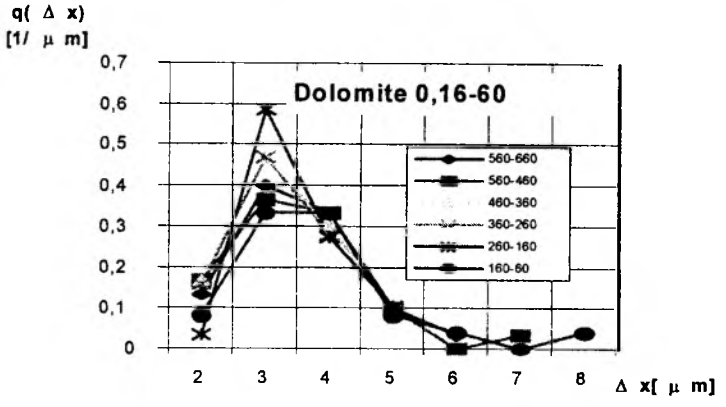

Fig. 9. Distributions of interparticle distances in measuring lengths of the field 0.5L in the 0.16-60 dolomite granule intersection

CONCLUSIONS

The following conclusions can be drawn on the basis of results obtained:

The profiles of surface brightness determined by the microscopic method suggest that granules have a discreet structure and can be used in the studies of microstructure.

A granule is formed as a results of coalescence of multilayer aggregates of particles (microgranules) which emerged at the stage of nucleation and after completing the process constitute local centres of particles concentration.

A multilayer (most frequently three or four peaks of the profile separate the brightest from the darkest point of the profile) structure of microgranules provides an evidence of a limited range of liquid penetration in the interparticle space.

The range of changes of interparticle distances is related to the range of grain size of the raw material. The largest distances occur in 0.16-100 dolomite, while the smallest in 0.16-20 dolomite.

The density functions of interparticle distance distributions for tested granules, similar to normal distributions, provide the evidence of a random character of their distribution in space.

The distance between particles changes periodically along the measuring field of the granule cross section and depends on the range of particle sizes of granulated material.

REFERENCES

STRELKOV S.P. (1982), *Mechanics*, Mir Publishers, Moscow.

BATTERHAM R.J., CRASS M., THURLBY J.A.(1990), *Review of Modeling in Agglomeration System*, ICHEME – 5th International Symposium on Agglomeration, Brighton, 569.

OUCHIYAMA N., TANAKA T. (1986). *Porosity estimation from particle size distribution*, Ind. Eng. Chem. Fundamentals 25, 125.

YU A.B., STANDISH N. (1987), *Porosity calculations of multi-component mixtures of spherical particles*, Powder Techn. 52, 233.

NOLAN G.T., KAVANAGH P.E. (1992), *Computer simulation of random packing ard spheres*, Powder Techn. 72, 149.

Gluba T., Kochański B., Odległości międzyziarnowe w przekroju granulek substancji o różnym składzie ziarnowym, Fizykochemiczne Problemy Mineralurgii, 34 (2000), 57-66, (w jęz. angielskim).

Badania struktury prowadzono na stanowisku pomiarowym wyposażonym w mikroskop światła odbitego Olympus SZ11 za pomocą komputerowego w systemu analizy obrazu „Lucia". Badano granulki utworzone z dolomitu o trzech zakresach wielkości cząstek (zawierającego ziarna 0,16-20, 0,16-60 i 0,16-100μm) oraz ze szklanych kulek (19-76μm) o średniej średnicy 50μm. Przeznaczone do badań granulki, ścierano na płaskiej siatce do mniej więcej połowy w celu utworzenia płaskiego przekroju średnicowego. Analizowano pięć obrazów (w kształcie prostokątów o długości 0,85mm i wysokości 0,65mm) położonych wzdłuż dłuższej osi pola przekroju. Dla stosowanej kalibracji odległość punktów pomiarowych wynosiła 0,00119mm. Jeden odcinek pomiarowy obejmował sto punktów. Określone wartości jasności poszczególnych punktów obrazu odpowiadały charakterystycznym miejscom. Na podstawie tych danych określano odległości między pikami krzywej profilu. Sporządzono wykresy zależności odległości pomiędzy cząstkami ciała stałego od ich położenia wzdłuż osi pomiarowych oraz funkcji gęstości rozkładów odległości w polach pomiarowych X=0,5L w przekrojach granulek badanych dolomitów i kulek szklanych. Stwierdzono, że granulka składa się z kilkuwarstwowych agregatów ziaren rozmieszczonych losowo w jej objętości. Zakres zmian odległości międzyziarnowych związana jest z zakresem wielkości ziaren surowca.

ACKNOWLEDGMENT

The work was carried out under research project no. 3T09C 032 12 financed by The Polish State Committee for Scientific Research for the years 1997-2000

Physicochemical Problems of Mineral Processing, 34 (2000), 67–75
Fizykochemiczne Problemy Mineralurgii, 34 (2000), 67–75

Andrzej HEIM*, Tadeusz GLUBA*, Andrzej OBRANIAK*

THE EFFECT OF PROCESS AND EQUIPMENT PARAMETERS ON THE DRUM GRANULATION KINETICS

Received March 15, 2000; reviewed and accepted May 15, 2000

Results of studies on agglomeration of powder material in drum granulators at drop-wise wetting of a bed with constant flow rate of supplied liquid are presented. The effect of process and equipment parameters, including drum diameter D, drum filling φ, rotational speed of the drum n, on granulation kinetics was determined. The effect of these parameters on mean diameter of granulated material d, and variability defined as the ratio of standard deviation of particle size distribution to the mean diameter (s/d) was discussed.

Keywords: drum granulation, granulation kinetics

INTRODUCTION

The process of agglomeration covers processing of dust and powder materials into a granulated form. One of the basic properties of a product obtained in such a process is its particle size distribution. Of importance is not only the mean particle size of granulated bed but also homogeneity of the product obtained. One of frequently applied methods of granulation is drum agglomeration which consists of forming and agglomeration of particles in a moving (tumbling) bed of fine-grained material. In this

* Technical University of Lodz, Department of Process Equipment, 90-924 Lodz, Stefanowskiego 12/16, Poland

process, the final product quality is affected by the following factors: granulation time, geometry of the drum, its operating parameters and bed wetting conditions.

The effect of operating parameters on granulation kinetics was studied by Newitt and Conway-Jones (1958) among the others. Kapur and Fuerstenau (1966) tried to find a relationship between particle size and process parameters (the absolute number of drum rotations n). They found that the process depended on water content in the agglomerate and particle size distribution of the raw material. That was confirmed by studies carried out by Linkson et al. (1973). Due to the range of studies, these investigations did not result in general solutions related, for instance, to the effect of several parameters on particle size of the product.

AIM OF THE STUDY

The aim of the present study was to determine the effect of some equipment and process parameters (drum diameter, its filling with raw material and rotational speed) on the granulation kinetics.

MEASURING EQUIPMENT AND METHODS

Investigations were carried out in a laboratory drum granulator. The drum was driven by motoreducer by means of a belt transmission and a gear. A smooth change of the drum rotational speed was achieved by means of inverter. The granular bed in the drum was wetted drop-wise by sprinkler, inserted axially to the equipment.

The wetting liquid was supplied from tank and its flow rate was controlled by rotameter. A constant level of liquid in the tank was maintained during the testing which ensured constant pressure of the supplied liquid. The wetting liquid was distilled water which was fed over the tumbling bed by means of a sprinkler which ensured a uniform supply along the entire drum length. The granular bed was wetted at a constant liquid flow rate ($Q = 10^{-6}$ m^3/s), until overwetting of material which caused sticking of the bed to the inner wall of the granulator. The process of granulation was carried out batch-wise, each time at a determined filling of the drum, rotational speed of the granulator and drum diameter.

For comparison, in the investigations the values of relative velocity n_w expressing the ratio of rotational speed n to critical speed of the drum n_{kr} were used. The relative velocity n_w was changed in the range which ensured a sudden motion of the bed tumbling in the drum. In time intervals equal to 60 s samples were taken from the drum to determine on this basis the particle size distribution in the bed. Owing to a constant rate and continuous feed of the wetting liquid, changes of the tested values

during granulation (wetting) were identical with the changes referring to the bed moisture content in the drum.

Tests were carried out in a batch drum granulator for the following range of parameters:

- drum diameter of the granulator D = 250-400 mm
- drum filling with granular bed φ = 5–20%
- the ratio of drum rotational speed to critical (relative) velocity $n_w = n/n_{kr} = 0.15–0.375$.

A testing material was casting bentonite of grain size ranging from 0 to 0.16 mm (mean diameter d_m= 0.056 mm) and batch density ρ_n = 0.865 kg/m^3.

RESULTS AND DISCUSSION

The effect of equipment and process parameters on the particle size of the final product obtained for different wetting times (moisture content of the granulated bed) was analysed. On the basis of the studies, the relationships of the effect of the tested parameters on mean particle size of the granulated material and on its size distribution were developed.

On the basis of results obtained during screen analysis some parameters of grain size distribution of the granulated material were calculated according to Kafarov (1979) and Achnazarova and Kafarov (1982):

ordinary moments of the first order (mean diameter)

$$d = m_1 = \sum_{i=1}^{n} x_{si} \cdot d_{mi} \tag{1}$$

–central moments of the second order (variances)

$$M_2 = s^2 = \sum_{i=1}^{n} x_{si} \cdot \left(d_{mi} - d\right)^2 \tag{2}$$

The variability coefficient defined as the ratio of standard deviation of particle size distribution to the mean diameter s/d (PN-90/N-01051) determining the spread of particle size of the obtained product in relation to mean diameter d, was proposed.

The dependence of mean particle diameter of the granulated product on wetting time is described by the equation:

$$d = C \cdot t + 0.056 \tag{3}$$

An example of the dependence of the increase of mean particle diameter of the granulated material during the process on different drum diameters is shown in Fig. 1.

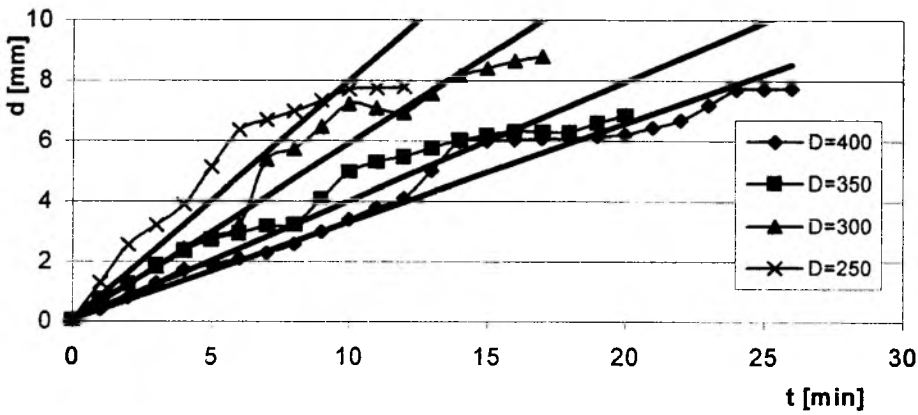

Fig. 1. The effect of wetting (granulation) time on the mean particle diameter of the product for different drum diameters at $n_W = 0.2$ and $\varphi = 15\%$

For other tested parameters of the granulator operation (drum filling φ and relative rotational speed n_W) similar relationships were obtained. They are presented in Figs. 2 and 3.

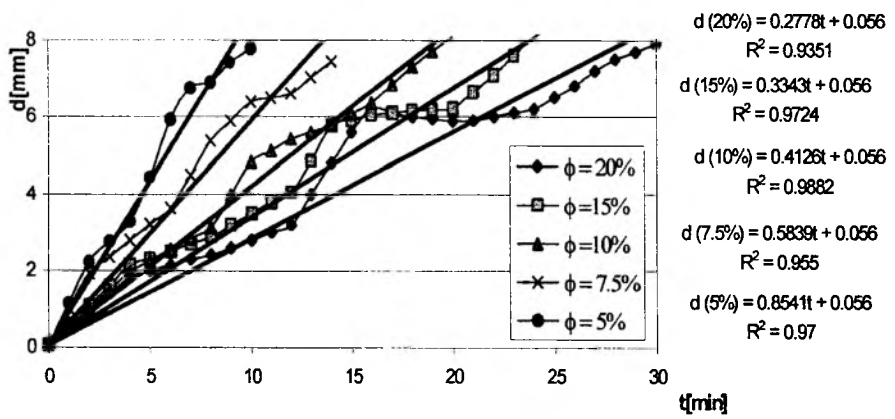

Fig. 2. The effect of wetting time on mean particle diameter of the product for different drum filling (D = 400 mm, $n_W = 0.15$)

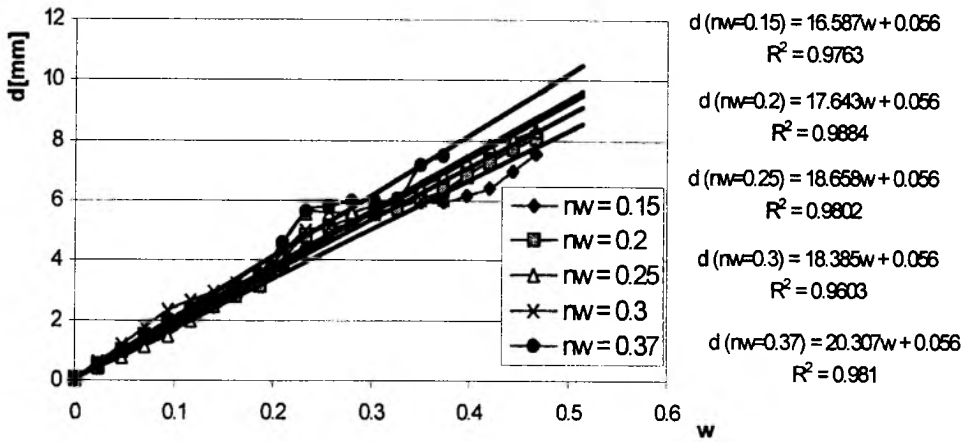

Fig. 3. The effect of moisture content (wetting time) on mean particle diameter of the product for different relative rotational speeds of the drum (D = 400 mm; φ = 20%)

These relationships allowed us to propose a general relation for the growth rate of granulated material in the form of the following correlation:

$$C = \frac{\partial d_{śr}}{\partial t} = 10^{-2} \cdot n_w^{\,0.144} \cdot D^{-2.06} \cdot \varphi^{-0.9} \tag{4}$$

The correlation coefficient in the above equation was R = 0.98.

The variability coefficient s/d was made dependent on the tested equipment and process parameters. The dependence of coefficient s/d on the wetting (granulation) time for all tested parameters is described by the equation:

$$\frac{s}{d} = A \cdot t^B \tag{5}$$

Examples of changes in the variability coefficient s/d during granulation for varying equipment and process parameters (drum diameter D, filling of the drum with material φ, relative rotational speed n_W) are presented in Figs. 4 - 6.

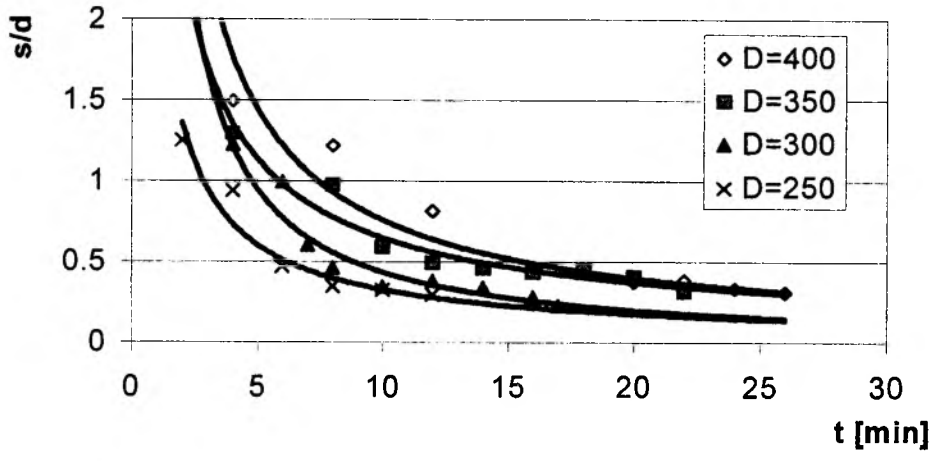

Fig. 4. The effect of wetting time on variability coefficient s/d for granulated material obtained at different drum diameters D (n_W = 0.15; φ = 0.15)

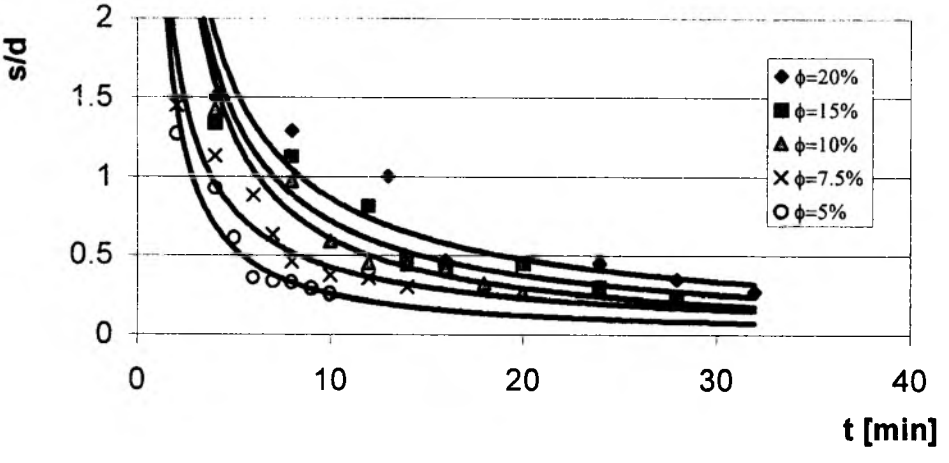

Fig. 5. The effect of wetting (granulation) time on variability coefficient s/d, for different values of drum filling φ (D = 400 mm; n_W = 0.2)

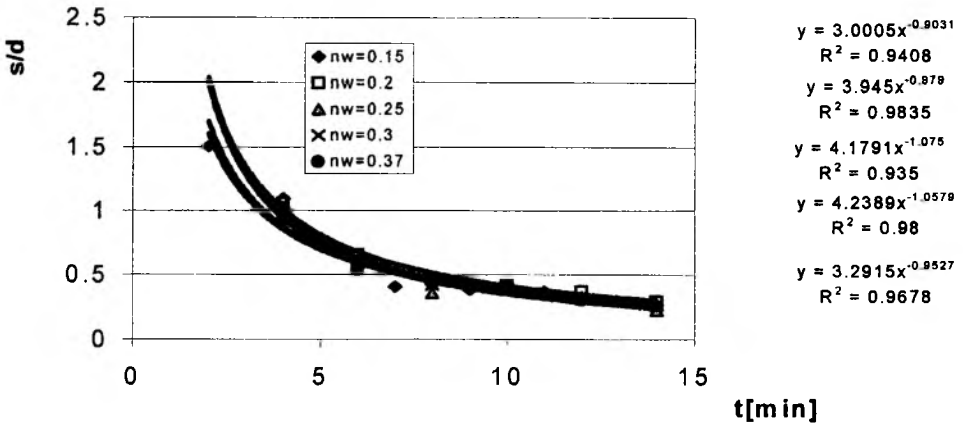

Fig. 6. The effect of wetting time on variability coefficient s/d of the product for different relative rotational speeds n_W of the granulator drum (D = 350 mm, φ = 10%)

For all tests the value of coefficient B in eq. (5) was close to -1, therefore the equation was simplified to the form:

$$\frac{s}{d} = A \cdot \frac{1}{t} \tag{6}$$

For all tests the coefficient A in eq. (6) was related to the parameters: drum diameter D, its filling φ and relative rotational speed n_w, obtaining the following equation:

$$A = 10^{-3.5} \cdot D^2 \cdot \varphi \tag{7}$$

The effect of relative speed n_W appeared to be insignificant and as such was omitted in the final form of the equation. Equation (7) was obtained at correlation coefficient R = 0.94.

CONCLUSIONS

1. The mean particle diameter of granulated product depends linearly on wetting time (moisture content of the granulated bed).
2. The rate of changes in the mean particle diameter of the granulated product can be related to the equipment and process parameters.
3. Variability coefficient s/d determining the scatter of grain size of the granulated product depends on the drum diameter and its filling. It is inversely proportional to the granulation (wetting) time.

REFERENCES

ACHNAZAROVA S. Ł., KAFAROV V. V. (1982), *Optymalizacja eksperymentu w chemii i technologii chemicznej*, WNT Warszawa

KAFAROV V.V. (1979), *Metody cybernetyki w chemii i technologii chemicznej*, WNT Warszawa

KAPUR P. C., FUERSTENAU D.W. (1966), *Size distributions and kinetic relationships in the nuclei region of wet pelletization*, Ind. Eng. Process Design Develop. 5. 5

LINKSON P. B., GLASTONBURY J. R., DUFFY G. J. (1973), *The mechanism of granule growth in wet pelletising*, Trans. Inst. Chem. Eng., Vol. 51

NEWITT D. M., CONWAY-JONES J. M. (1958), *A contribution to the theory and practice of granulation* , Trans. Inst. Chem. Eng., Vol. 36

PN-90/N-01051(1990), *Rachunek prawdopodobieństwa i statystyka matematyczna, Terminologia*

NOMENCLATURE

A, B, C – coefficients
D – drum diameter, m (in figures in mm)
d – mean particle diameter of the granulated material, mm
m_1 – ordinary moment of the first order
M_2 – central moment of the second order
d_{mi} – mean diameter of class i, mm
x_{s_i} – mass fraction of class i
n_w – relative rotational speed
φ – drum filling with material
t – granulation (wetting) time, s
s^2 – variance

Heim A., Gluba T., Obraniak A., Wpływ parametrów procesowo-aparaturowych na kinetykę procesu granulacji bębnowej, Fizykochemiczne Problemy Mineralurgii 34 (2000), 67-75 (w jęz. angielskim)

Jedną z podstawowych własności uzyskanego w procesie aglomeracji produktu jest jego skład granulometryczny. Istotny jest tu nie tylko średni wymiar charakterystyczny dla zgranulowanego złoża,

ale także jednorodność otrzymanego produktu. Jedną z częściej stosowanych metod wytwarzania granulatu jest bębnowa granulacja aglomeracyjna polegająca na formowaniu i narastaniu cząstek w ruchomym złożu materiału drobnoziarnistego (przesypowym). W procesie tym na jakość produktu końcowego wpływ ma wiele czynników takich jak czas granulacji, parametry geometryczne aparatu, parametry jego pracy oraz warunki nawilżania złoża. Celem pracy było określenie wpływu niektórych parametrów aparaturowo-procesowych na kinetykę procesu granulacji. Badania prowadzono w granulatorze bębnowym o działaniu okresowym dla następującego zakresu zmian parametrów:

-średnica bębna granulatora D=0.25–0.40m

-wypełnienie aparatu złożem ziarnistym φ=5%–20%

-stosunek prędkości obrotowej bębna do prędkości krytycznej: $n_w = n/n_{kr}$=0.15–0.375

Do badań zastosowano bentonit odlewniczy o średniej wielkości ziarna d_m=0.056mm, a jako ciecz zwilżającą wodę destylowaną, którą podawano na przesypujące się złoże równomiernie na całej długości granulatora, przy stałym natężeniu wypływu cieczy $Q=10^{-6}$ m^3/s. W odstępach czasu równych 60s pobierano z bębna próbki, na podstawie których określano skład granulometryczny złoża. Na podstawie uzyskanych wyników opracowano zależności dotyczące wpływu badanych parametrów aparaturowo-procesowych na średnią wielkość uzyskanego granulatu oraz współczynnik zmienności s/d określający rozrzut wielkości uzyskanego produktu względem średnicy średniej d. Zależność średniej wielkości ziarna granulatu od czasu nawilżania opisano równaniem, a jej przykładowe wzrosty w czasie procesu dla różnych parametrów aparaturowo-procesowych przedstawiono na rysunkach. Charakter uzyskanych zależności pozwolił na zaproponowanie ogólnego równania na szybkość wzrostu ziaren granulatu. Zależność współczynnika s/d od czasu nawilżania (granulacji) dla wszystkich badanych parametrów opisano równaniami.

Physicochemical Problems of Mineral Processing, 34 (2000), 77–94
Fizykochemiczne Problemy Mineralurgii, 34 (2000), 77–94

Kazimierz St. SZTABA*, Alicja NOWAK*

ASSUMPTIONS FOR MODELLING OF SEPARATION IN COIL CLASSIFIERS

Received March 15, 2000; revieved and akcepted May 15, 2000

The coil classifiers are flow classifiers in which the process of separation of grains into fractions differentiated by their grain size occurs in the stream of the medium and the separation feature is a characteristic velocity of grains movement in relation to the medium which is the function of their size. The multi-parameter capacity of the system of conditions of the classification process course makes up for serious difficulties in constructing of this model. The paper presents an attempt of identification of significant conditions out of these in which the process takes place. The authors separated groups of factors affecting the course and results of classification and described their role in forming the technological indicators and separation characteristics. Also a scheme of construction of a phenomenological model of classification which can be considered to be sufficient for practical purposes, especially for the tasks connected with the regulation and controlling of the operation of coil classifiers in industrial conditions.

Key words: flow classification, coil classifier, conditions of the classification process, process modelling

* Akademia Górniczo-Hutnicza im. St. Staszica, al. Mickiewicza 30, 30-059 Kraków

FLOW CLASSIFICATION

Essentials of flow classification

The coil (spiral) classifiers constitute a separate group of flow classifiers in which the characteristic velocity of grains (v_c) in the liquid medium, formed under certain conditions, constitutes the feature of grains separation. The extreme value of this velocity is constituted by the limit velocity (v_0) with which the grain moves when the forces acting on it are at equilibrium. The formulas for the characteristic velocity, especially the limit one, are widely discussed in the literature (Barskij et al. 1974; Budryk 1937; Höffl 1985; Ljaščenko 1935; Sztaba 1992, 1993, 1997; Tumidajski 1993; Collective work 1976, 1972, and others) though this problem has not been sufficiently worked out for the general case of characteristic velocity (Ljaščenko 1935). There are, however, many formulas and calculating methods which enable the values of limit velocity for certain ranges of basic conditions of the process course to be calculated (i.e. to evaluate more precisely with the practical accuracy). This velocity is also generally applied for technological calculations.

The characteristic (limit) velocity v_c depends on:

properties of the grains - classified solid phase (e.g. mineral grains):

- grain density - ρ_s, kg/m^3,
- grain size – d, m,
- grain shape (considered numerically in calculations),
- other less important factors ,

properties of the liquid phase – classification medium:

- density of the medium, ρ_c, kg/m^3,
- viscosity of the medium (e.g. determined by the dynamic viscosity rate) - μ, Pa.s,

basic characteristics of the external force field in which the system grain-liquid occurs:

- the acceleration of gravity force (g) or (and) centrifugal acceleration (Ω) – m/s^2.

There are many formulas for calculating the limit velocity having theoretically an unlimited range of applications. This is Budryk's formula (Budryk 1937; Collective work 1976):

$$v_0 = \frac{a}{d \cdot \rho_c}\left(\sqrt{1 + d^3 \cdot b \cdot \rho_c \cdot (\rho_s - \rho_c)} - 1\right) \text{ m/s} \qquad (1)$$

where: $a = 18 \cdot \mu$, $b = g/(162 \cdot \mu^2)$.

This formula can be applied for spherical grains.

A modified form (Sztaba 1992) of Budryk's formula was derived for non-spherical grains. The shapes of grains can be characterised the following coefficients:

- spherical coefficient, introduced by Wadell (Andreev et al. 1959; Sysło 1964) -

$$C_k = \frac{F_k}{F_z} \text{ and}$$

- coefficient introduced by A. Nowak (1979; 1981) - $C_{AN} = \frac{d_z^2}{d_r^2} \approx \frac{d_z^2}{d_p^2}$,

where: F_z, F_k – external surfaces: grains and a sphere of the volume equal to the volume of a grain, m^2, d_z, d_r, d_p – grain size: substitute, view, projection, respectively, m, (Sztaba 1964). This formula has the form:

$$v_0 = 18 \cdot \frac{C_{AN}}{\sqrt{C_k}} \cdot \frac{\mu}{d_z \cdot \rho_c} \cdot \left(\sqrt{1 + \frac{g}{162} \cdot \frac{C_k}{C_{AN}} \cdot \frac{(\rho_s - \rho_c) \cdot \rho_c}{\mu^2} \cdot d_z^3} - 1 \right), \text{ m/s} \qquad (2)$$

and contains all the above mentioned factors affecting the value of the limit velocity v_0. Substituting in the quoted and other formulas the acceleration due to gravity (g) and centrifugal force (Ω) allows, with certain simplifications, to apply these formulas for the calculations of grain movement under the influence of centrifugal force (Nowak 1981).

The application of flow classification

The operations of flow classification occur commonly in technological processes of processing and transforming solid materials that are medium and especially fine-grained. They are characterised by high efficiencies with a simultaneously lower precision of separation in comparison with the screen classification ("mechanical" – sieving). As far as the latter one is concerned, they are much cheaper, both from the point of view of machinery costs and exploitation expenditure. The finer material is separated, the larger are the differences. When the very fine grains are classified, the application of screen classification is economically nonviable, and in case of extremely fine grains, technologically impossible, except for some rare cases, occurring mostly in chemical technology, production of special abrasive materials, semi-products for electronic or medical ceramics and a few others.

Flow classifiers

The equipment for flow classification, i.e. flow (stream) classifiers, reveals extreme diversity of construction solutions, depending on numerous factors and also on technological assumptions (Barskij et al. 1974; Grzelak 1975; Hőffl 1985; Ljaščenko 1935; Nowak 1981; Razumov et al. 1982; Collective work 1976, 1972 and many others). Usually the attempts of detailed systematic classifications of these machines are given up in favour for determining of their certain classes, differentiated by certain groups of conditions of operation courses and certain types of construction solutions (Collective work 1976, 1972). The subject-matter of this paper comprises exclusively the classification operations, performed in coil classifiers.

COIL CLASSIFIERS

Figure 1 presents the schematic diagram of construction of the coil classifier.

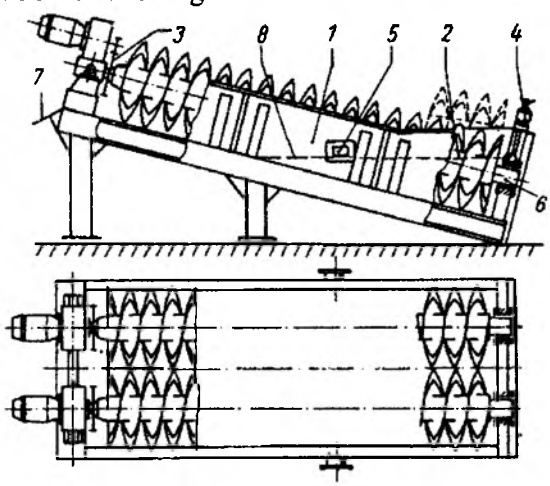

Fig. 1. Two-coil spiral classifier (according to Hőffl, 1985)
1 – chute, 2 – worm, 3 – drive, 4 – worm shaft lifting mechanism, 5 – suspension inflow, 6 – worm shaft bearing, 7 – underflow intake chute, 8 – suspension level

The spiral classifiers belong to the group of classifiers (Barskij et al. 1974):
- with the liquid medium of classification (hydraulic),
- gravitational,
- horizontal-current,
- with lateral intake of feed,
- with mechanical underflow (coarse-grained product).

The mechanical outtake of the underflow occurs by means of the worm (spiral, coil) conveyor, the presence of which makes the coil classifiers distinct among other flow "mechanical" classifiers (having mechanical parts for taking the underflow out). In high-efficiency classifiers two parallel conveyors are installed (spirals) (Fig. 1). Three-coil classifiers are almost exceptional.

The operation of the coil classifier is generally known and described in the literature, including the reference quoted in the introduction, therefore it is not discussed in this paper. To supplement the previous remarks about the range of applications of such classifiers, it should be mentioned that the occurrence of the zone of free water run-off from the underflow product (between the left edge – Fig. 1. – of the suspension surface (8) and the threshold of underflow intake (7), enables the use of spiral classifiers not only for the grain classification but also for dewatering of coarse-grained suspensions. The effect of dewatering occurs always as accompanying the classification in flow machines. In case of classifying the materials of heterogeneous mineral composition, especially density-like, there is also a side effect of enrichment, which, however, is a characteristic feature of all flow operations. These problems are not discussed in this work (Sztaba 1988).

IDENTIFICATION OF CONDITIONS OF THE SEPARATION PROCESS IN THE COIL CLASSIFIER

The above mentioned multi-parameter characteristics of the system in the course of the classification process is especially visible in case of mechanical classifiers (including the coil ones) which reveal a specific configuration of construction elements, including these which have movable elements, distinctly affecting the course and results of the process. The works of Sztaba (1992; 1993) and Sztaba et al. (1996, 1998) indicate difficulties which occur during the attempts of considering the values characterising the construction elements, in the construction of model descriptions of classification processes. The main reasons are the lack, in many cases, of technological justifications of direct assumption of numerical characteristics of values of construction elements in models, as opposed to the influence (most often indirect, in many cases confounding or even not fully univocal) of these values upon the technological effects of the process and also the lack, so far, an unanimous concept of considering, in such descriptions, the influence of the classifier on the process of construction configuration. The quoted works contain an attempt of systematic approach of such a configuration, yet the effects of their influence are not univocal, not mentioning even the joint effect of the set of these elements.

In this situation an attempt of identification of significant conditions was made in which the process occurs by means of the phenomenological description. The groups of

factors affecting the course and results of the process were differentiated (groups: 1. – construction characteristics of the classifier and 2. – movement characteristics of the process) and their role in shaping the process technological conditions of the process was described (group 3.). A similar influence on the separation characteristics is a separate problem (group 4.).

Factors describing the conditions of the separation process and the evaluation of its results

The title conditions of the process course and the parameters of description and evaluation of its results (Tichonov 1973; Sztaba 1988; Sztaba et al. 1990) can be grouped as follows. The list presents, respectively, the factor's name, denotation and dimension:

1. construction characteristics of the classifier
1.1. length of the classifier chute - L, m
1.2. width of the classifier chute – B, m
1.3. length of the overflow edge – b, m
1.4. diameter of the spiral – D, m
1.5. pitch of the spiral thread – S, m
1.6. number of spiral threads – Z,
1.7. number of worms (underflow conveyors) – N,
2. movement characteristics of the process
2.1. depending on the classifier construction parameters
2.1.1. number of spiral revolutions – n, min^{-1}
2.1.2. inclination angle of the classifier chute - φ, rad
2.1.3. height of the overflow edge – H, m
2.1.4. distance between the feed inlet and the overflow edge – l, m
2.1.5. area of the suspension level – P, m^2
2.2. depending on the feed properties
2.2.1. frequency function (distribution function of grain sizes of the feed) - $f_0(d)$
2.2.2. density of the solid phase - ρ_s, kg/m^3
2.2.3. coefficients of grain shapes – C_k, C_{AN},
2.2.4. density of the liquid phase - ρ_c, kg/m^3
2.2.5. viscosity of the liquid phase - μ_c, Pa.s
2.2.6. volume concentration of the solid phase in the feed - Θ_0, (%), or as a fraction
2.2.7. feed density - ρ_0, kg/m^3
2.2.8. suspension (feed) viscosity - μ_0, Pa.s
2.2.9. efficiency of the solid phase in the feed – Q_0, kg/h
2.2.10. efficiency of the inflow of additional water – Q_{wd}, kg/h
3. technological results of the process
3.1. efficiency of the solid phase in the overflow – - Q_p, kg/h
3.2. efficiency of the solid phase in the underflow – Q_w, kg/h

3.3. yield of the solid phase of the overflow - γ_p, (%), or as fraction
3.4. yield of the solid phase of the underflow - γ_w, (%)
3.5. volume concentration of the solid phase in the overflow - Θ_p, (%)
3.6. volume concentration of the solid phase in the underflow - Θ_w, (%)
3.7. overflow density - ρ_p, kg/m^3
3.8. underflow density - ρ_w, kg/m^3
3.9. frequency function (distribution function of grain sizes of the overflow) - $f_p(d)$
3.10. frequency function (distribution function of grain sizes of the underflow) - $f_w(d)$
4. characteristics of grain separation
4.1. separation boundary (division grain, cut size) – d_{50}, mm
4.2. probable deviation (quarter deviation) of separation – E_p, mm
4.3. absolute indicator of separation accuracy – r (dimensionless).

The values of groups 1 and 2 determine the course and results of separation. Further on, they are treated as *determining (variable) values.* The values of group 3 (first of all) and group 4 are *determined (variable) values.* In practice, their values (most often, only some of them) are assumed according to technological needs, resulting from the place and function of the described operation in the technological system (process).

The above listed determining values (groups 1 and 2) maintain this role in all aspects of evaluation of results of action of the classifier (functions: classification, dewatering, enrichment). The values of group 1 are connected with invariable elements of construction of the classifier and are not subject to regulations. Their possible changes would require appropriate changes in the construction of the machine, i.e. a construction of a new device. The values of subgroup 2.1 are as a rule also fixed by the construction features of the device but can, when needed, be changed with any significant construction alterations. This, however, happens only exceptionally. It then concerns first of all item 2.1.3 (H) and 2.1.4. (1). The change of the value of position 2.1.2 (φ) and (or) 2.1.3 (H) changes the values of the suspension mirror area (2.1.5 – P), connected with them and with appropriate values from group 1. (1.2 – B and 1.3 – b) a simple geometric dependence.[2] Among the values of subgroup 2.2 all these which characterise the material of the solid phase of the feed and the liquid phase of the suspension [2.2.1 - $f_0(d)$,[3] 2.2.2 - ρ_s, 2.2.3 – C_k and C_{AN}, 2.2.4 - ρ_c, 2.2.5 - μ], depend on the natural properties of these materials and are not subject to regulation, from the point of view of the process they are *disturbing (variable) values.* Out of the remaining values of this group, any assumption of values is possible in case of 2.2.6 - Θ_0, 2.2.9 – Q_0 and 2.2.10 – Q_{wd}. The others are connected with other values in the way presented roughly in the following part of this chapter. The value Θ - volume concentration of the solid phase in the suspension

---

[2] in classifiers provided for giving out an overflow of fairly fine grain sizes or (and) of fairly high efficiency of this product, B = b, as on Fig. 1.
[3] size of grains, d, a general feature, basic variable for the description of granulometric properties of grained materials

(occurring in the paper as Θ_0, Θ_p, Θ_w respectively, in relation to the feed, overflow and underflow) is a very important value characterising the suspension and allowing many its properties to be calculated, including these which directly affect the separation process in the classifier. It is described as a quotient of the volume of the solid phase (V_s, m^3) and the volume of the entire suspension ($V = V_s + V_c$, m^3; V_c, m^3 - the volume of the liquid phase in this suspension):

$$\Theta = \frac{V_s}{V_s + V_c} \tag{3}$$

For the sake of order, it should be mentioned that in industrial conditions often a similar value is applied, called the suspension *concentration* (α) and determined as a quotient of the solid phase (Q_s, kg) to the mass of the suspension ($Q = Q_s + Q_c$, kg; Q_c, kg – mass of the liquid phase of this suspension):

$$\alpha = \frac{Q_s}{Q_s + Q_c} \tag{4}$$

Both these important values are connected by dependencies

$$\alpha = \frac{\Theta \cdot \rho_s}{\Theta \cdot \rho_s + (1-\Theta) \cdot \rho_c}, \qquad \Theta = \frac{(1-\alpha) \cdot \rho_c}{(1-\alpha) \cdot \rho_c + \alpha \cdot \rho_s} \tag{5}$$

When the value Θ is known, it is possible to calculate the suspension density (ρ), its apparent viscosity (μ') and capacities of suspension (Q^z) and water in the suspension (Q^w). The role of these values in the flow classification process is described by Barskij et al. (1974), Ljaščenko (1935), Nowak (1981), Sysło (1964), Sztaba (1993, 1994, 1997), Tichonow (1973), Collective work (1972, 1976) and others.The density of the mixture of k components (in general case) is calculated by the formula:

$$\rho = \sum_{i=1}^{k} \rho_i \cdot \Theta_i \Bigg|_{\sum_i \Theta_i = 1} \tag{6}$$

where:
– ρ - mixture density, kg/m^3
– ρ_i - density of the i-th component of the mixture, kg/m^3
– Θ_i - concentration by volume of the i-th component in the mixture, (%).

For the two-component mixtures, e.g. suspensions which are, among others, the feed and classifier products (in case of classification of density-homogenous products, especially the monomineral ones, or in the conditions of omitting the occurrence of various components – "apparent homogeneity"), formula (6) is simplified to the form:

$$\rho = \rho_s \cdot \Theta_s + \rho_c \cdot (1 - \Theta_s) \tag{7}$$

where (as given before)
– ρ_s, ρ_c - density of the solid, liquid phase, kg/m^3
– Θ_s - volume concentration of the solid phase, (%),
($1 - \Theta_s = \Theta_c$ - volume concentration of the liquid phase of the mixture, in practice only the concentration of the solid phase is used – in the feed and classifier products Θ_0, Θ_w, Θ_p, respectively).

If, as in the case of hydraulic classification, water is the liquid phase ($\rho_c = 1000$ kg/m^3), then

$$\rho = \Theta \cdot (\rho_s - 1000) + 1000 \tag{8}$$

Apparent viscosity is calculated (formula given by Baczynski):

$$\mu' = \mu_c \cdot \left(1 + 4{,}5 \cdot \frac{\Theta}{1 - \Theta}\right) \tag{9}$$

where μ_c - coefficient of dynamic viscosity of pure liquid, Pa.s.

One of the most important applications of value Θ can be found in calculating the limit velocity in the conditions of *constrained settling*. The quoted formulas (1) and (2) concern the so-called *free settling* under the conditions of the lack of additional actions which are caused by the co-settling grains (and also, to some extend, geometry of the area in which the separation takes place) (e.g. Collective work 1972, 1976 and others). Formally, in a simplified way, the velocity of constrained settling (v_s, m/s) can be calculated substituting in Eqs (1), (2) and others, not quoted here, the value ρ instead of ρ_c and the value μ' instead of μ (μ_0 for the feed, analogically for the products, although calculating the apparent viscosity for them is not well-grounded.

Knowing the expenditure of the solid phase in the suspension stream (also in the tank, etc.) – Q_x, kg/h (x = 0, p,w), the capacity of the stream of the entire suspension can be calculated:

$$Q^z = \frac{Q_x}{\alpha} = \frac{Q_x \cdot \Theta \cdot \rho_s}{\Theta \cdot \rho_s + (1-\Theta) \cdot \rho_c} \tag{10}$$

and the expenditure of the stream of water in the suspension

$$Q^w = Q^z - Q_x. \tag{11}$$

It should be noted that: formulas (3) to (11) are general and some denotations do not form a self-consistant system with the system of denotations assumed before.

The values determined from the technological group (3) allow the process to be evaluated due to the implementation of both the function of classification and dewatering. A possible evaluation of effects of enrichment in the process of classification require first of all some additional data about the contents of the feed components which can be the subject of the evaluation.

Out of the values belonging to this group only the values of product density are obtained from direct measurements (ρ_p - 3.7. and ρ_w - 3.8.) and in a very limited range (only to the values of function $f(d)$[4] for single values of d) data about the grain composition ($f_p(d)$ – 3.9, $f_w(d)$ – 3.10, similarly as occurring in group 2, function $f_0(d)$ – 2.2.1). Also the measurements of the capacity of the suspension stream (Q^Z) of both products (though, practically, only the overflow). The other, technologically important, values are obtained in an indirect way or as a result of laboratory tests of samples taken from the streams of products ($f_p(d)$ and $f_w(d)$). The values of the yields of products:

$$\gamma_p = \frac{Q_p}{Q_0}, \qquad \gamma_w = \frac{Q_w}{Q_0} \tag{12}$$

expressed usually in percentage values, in industrial conditions practically impossible to be calculated directly from formulas (12), are computed most often from the balance of components (Stępiński 1964; Collective work 1976 and others) of the solid and liquid phases with the application of the measured values of ρ (ρ_0, ρ_p, ρ_w), or the grain classes with the application of functions $f(d)$ ($f_0(d)$, $f_p(d)$ and $f_w(d)$) and an appropriate calculation procedure, using usually the least square method – e.g. the formula given by Grumbrecht

[4] Here the frequency function $f(d)$ is used as the function of grain characteristics (Sztaba 1964, Collective work 1976); in practical applications almost always other functions are used, integer ones, of much higher utility advantages whereas the frequency function is more convenient in theoretical and general considerations.

(Tumidajski 1993) or others, for which the calculating programs have already been worked out.

The important value Θ (here $\Theta \equiv \Theta_s$ of the concentration of the solid phase) is calculated from the formula being the transformation of formula (7):

$$\Theta_S = \frac{\rho - \rho_C}{\rho_S - \rho_C} \tag{13}$$

The values Q_p and Q_w can be calculated knowing the given value Q_0 and the previously discussed values of yields of products (γ_p and γ_w or the feed density and products and Q^z at least for one product – transforming, among others, formulas (10) and (11)).

The listed values of the group of characteristics of grain separation (4) concern only the function of classification (separation of the feed into products of different grain size distribution, i.e. coarser *underflow* and finer *overflow*). These characteristics do not concern the function of dewatering or the effects of enrichment.

The characteristics 4.1 – d_{50}, mm and 4.2 – E_p, mm are taken off from the *separation curve* (Sztaba 1956; Mayer 1971), calculated and applied (the values of the *numbers of separation* - $\tau(d)$ for the overflow and T(d) for the underflow are calculated) in the way described (Sztaba 1956). The value 4.3, $r = E_p/d_{50}$. It is characteristic for a given classifier (Sztaba 1956). These values serve to estimate the process of classification as a random process. The value of d_{50}, the size of a grain of the same probability of transmitting into the overflow and underflow, determines the boundary between these products and E_p characterises the dispersion of values of these probabilities; thus characterising the separation accuracy (the higher the smaller the value of E_p).

In practice, it is not enough to obtain the separation of limit grains on the level of 50%. For example, one of the methods of calculation of sizes of coil classifiers (Razumov et al. 1982; Collective work 1976) uses the maximum overflow grain, determined as the grain of such a size that there are 95% of grains in the overflow which are under this size (the so-called 95%-grain). In such cases the separation curve has to be used (τ or T) together with the grain size distribution characteristics of the feed ($f_0(d)$) (Sztaba 1956).

For practical reasons the calculations of coil classifiers are mainly performed because of the sizes of: cut size (d_{50}), efficiency of the solid phase in the feed (Q_0) and in the underflow (Q_w), or (in case of the assumption of the use of the dewatering function) the overflow (ρ_p) and underflow (ρ_w) densities. For the sake of comparison mainly the values characterising the accuracy of separation (e.g. E_p, r) are evaluated (more seldom used).

The formerly discussed relations between the values applied for the description of course conditions and results of classification as well as limitations to the values practically useful in industrial conditions contribute to significant reduction of the number of values which should be taken under consideration when describing the mutual relations between them. According to the general rule assumed for the present paper, the values affecting the underflow characteristics are not differentiated.

The determining values to be considered are as follows:

1) area of the suspension level – P; P = P(B, b, φ, H),

2) distance of the feed inlet from the overflow edge – 1,

3) frequency function of the feed solid phase – $f_0(d)$[5],

4) efficiency of the solid phase in the feed - Q_0,

5) volume concentration of the solid phase in the feed, determining the conditions of grain constrained settling - Θ_0, (in general regulated by the expenditures of the solid phase and water, or calculated by formula (13),

6) joint efficiency of water in the feed - $\Sigma Q^w = Q^w_0 + Q_{wd}$; Q^w_0 - efficiency of water introduced together with the feed.

The remaining values of groups 1 and 2:

- the values of constant values for a certain group of processes: density of the solid phase (ρ_s) and the liquid (water) (ρ_c) and its viscosity; their influence on the classification conditions results clearly from formulas (1), (2), (5), (7), (10), (13); The coefficients of grain shapes of the solid phase (C_k, C_{AN}) are rarely significant for determining the limit velocity,

- the values influencing the characteristics and expenditure of underflow can be neglected (being important mainly for the function of dewatering): the length of the classifier chute (L), characteristics of the spiral and its movement (D, S, Z, N, n) – in case of evaluation of the grain characteristics of this product it is possible to use the relations between the grain size distributions of the feed, overflow, underflow and yields of the latter:

$$a_{wi} = \left. \frac{a_{0i} - a_{pi} \cdot \gamma_p}{\gamma_w} \right|_{\gamma_p + \gamma_w = 1} \tag{14}$$

[5] It is impossible to use such an entire function; the range of this work exemplifies it as a symbol of the feed grain size distribution; in case of the flow classification its most important feature is constituted by the content of extremely fine grains and, especially, the so-called primary muds (Razumov et al. 1982, collective 1976) whose presence significantly affects the rheological properties of the suspension, first of all increasing its apparent viscosity (over the value calculated, e.g., from formula (9) and thus decreasing the limit (characteristic) velocities of grains sedimentation.

where a_{0i}, a_{pi}, a_{wi} – contents of the i-th grain class in the feed, overflow, underflow, dimensionless.

It is enough to take into consideration the following values:

1) yield of the underflow solid phase – γ_p,
2) volume concentration of the solid phase in the overflow – Θ_p,
3) separation boundary (cut size) – d_{50},
4) probable deviation of the separation – E_p.

Additionally, it should be observed that the grain composition of the overflow ($f_p(d)$, a_{pi}) can be calculated, if necessary, applying the transformed formula (14) and the parameters of the separation curve (d_{50} and E_p). The qualitatively determined relations between the conditions of the process course and its results are listed in Table 1 in the cells of which there are symbols determining the character of the relation. These symbols determine the changes of the value denoted at growth of the variable determining value: + - determined value increases, - - determined value decreases. Moreover, it was assumed that apart from a few cases of clear strong non-linear dependence, denoted as ^+ or ^-, (increase or decrease, respectively), in case of the remaining relations the accurate character of the relation is not determined. It is also assumed that with the change of the value of a concrete determining value, the remaining values are not changed.

Dependencies of selected values determined from the basic determining values

$Z_{determining}$		$Z_{determined}$			
j	Symbol	γ_p	Θ_p	d_{50}	E_p
1	P	–	–	^–	–
2	I	+	+	+	+
3	$f_0(d)$[6]	+	+	+	+
4	Q_0	+	+	+	+
5	Θ_0	–	–	–	–
6	ΣQ^w	+	+	^+	+

[6] in fact, this is the formerly discussed (5) content of super-fine grains

Diagram of construction of the model of classification

In the simplest case of construction of the phenomenological model of the process it can be written, separately for each determined value, as:

$$Z_{\text{determined}} = \sum_{j} \pm b_j \cdot Z_{\text{determining},\,j} \tag{15}$$

where

– $Z_{\text{determining}}$, $Z_{\text{determined}}$ – input and output variables (values), (determining and determined), considered in Table 1,

– b – empirical coefficient with the symbol corresponding to the symbol in the Table 1.

Also other procedures of construction of such models can be applied. System (15) can serve also as an introductory scheme to determinist models, e.g. constructed with the application of principles of the dimensional analysis. Regardless of the presented dependencies, it should be reminded that two basic types of coil classifiers can be differentiated for which a distinguishing feature is constituted by the position of the lower end of the spiral in relation to the overflow edge (Razumov et al. 1982; Collective work 1976).

Numerically, this feature is determined by the difference D – H:

1) *classifiers with the non-immersed spiral* – (D – H) > 0 – are use for classification at larger values of d_{50} (size of 95% overflow grain usually > ~ 0.074 mm), obtained value of E_p is usually larger than in other constructions,

2) *classifiers with the immersed spiral* – (D – H) < 0 – are used for classification at lower values d_{50} (size of 95% overflow grain usually <~ 0.2), obtained value of E_p is usually smaller than in other constructions.

This variety of constructions should be taken into consideration when formulating conclusions which generalise the results of investigations carried out on the separation process in classifiers of differentiated construction features. The dependencies of Table 1 will be of the same character but in the model record the values of numerical coefficients will be different at respective values.The presented scheme of construction of models can be sufficient for practical purposes, particularly for the tasks connected with regulation and control of coil classifiers in industrial conditions. Having such models at disposal would make precise the principles of selection in comparison to the mentioned methods of designing of these machines, which, as a rule, do not consider the qualitative technological parameters of the process products (Razumov et al. 1982; Collective work 1972, 1976).

Such models cannot be considered satisfactory from the cognitive point of view. Maintaining only for selected determined values there are no grounds for determining a univocal model record, taking into account all these values. These difficulties will be enlarged by broadening their list. There are, however, some premises for a theoretical

proof, empirically stating an almost linear dependence (according the existing investigation results) between d_{50} and E_p which contributed to the introduction of the value r, approximately constant for a given classifier (Sztaba 1956), yet there are not enough data to state univocally this constancy for various items of machines of this type. The problem consists of large sampling of relatively numerous machines, apart from the execution of such samplings. The performed considerations and investigations allowed the results to be presented and confirmed a formerly formulated thesis (Sztaba 1993) about a significant effect of construction parameters on the operation of classifiers with numerous mechanical elements. Therefore, no possibilities of constructing the generalised models can be expected before a significant progress is reached in descriptions and quantifications of roles of mechanical elements in flow technological devices, including coil classifiers. On the other hand, the work on modelling of flow processes classification, carried out in other machines, without such strong participation of influences of mechanical elements on technological results (chamber and other simpler hydraulic and air classifiers, and also centrifugal devices of free vortex eg. hydrocyclones), can explain many details, important for flow classification processes and even the entire class of flow processes, necessary for solving the discussed problems. Strict determinist description of separation processes in machines of forced vortex (classifying sedimenting centrifuges), in spite of significant progress in modelling (Nowak 1981), must be confronted with problems, analogical to coil classifiers, with the description of the influence of mechanical elements on their operation and results. Nevertheless, no progress in solving them can be expected without such investigations which broaden the initial positions of further modelling of the process occurring in such complex conditions as coil machines.

The presented scheme of fraction modelling, sufficient for practical purposes, should be applied by means of using the collected industrial data and constructing phenomenological models for certain applications and simultaneously aiming at their gradual generalisation.

This work was completed as a result of implementation of the 1999 subject of statute investigations of Department of Mineral Processing, Environment Protection and Wastes Utilisation of University of Mining and Metallurgy in Kraków (contract no 11.11.100.238, task 1, stage 2) (Sztaba 1998).

REFERENCES

ANDREEV, S.E., TOVAROV, V.V., PEROV, V.A., (1959), *Zakonomernosti izmel'čenija i isčislenie charakteristik granulometričeskogo sostava* (*Essentials of Grinding and Numerical Characteristics of Granulometric Composition*) - Metallurgizdat, Moskva (in Russian).

BARSKIJ, L.A., RUBINŠTEJN, J.B., (1970), *Kibernetičeskie metody v obogaščenii poleznych iskopaemych* (*Cybernetic Methods in Mineral Enrichment*) - Izdatel'stvo „Nedra", Moskva (in Russian).

BARSKIJ, M.D., REVNIVCEV, V.I., SOKOLKIN, J.V., (1974), *Gravitacionnaja klassifikacija zernistych materialov* (*Gravitational Classification of Minerals*) - Izdatel'stvo „Nedra", Moskva (in Russian).

BUDRYK, W., (1937), *Przyczynek do teorii wzbogacania w ośrodku płynnym* (*Some Approach to the Theory of Enrichment in Liquid Medium*) - Przegląd Górniczo-Hutniczy nr 3 (in Polish).

COLLECTIVE WORK, (1972), *Sprawočnik po obogaščeniju rud*, (Handbook of Mineral Processing) vol. 1.- Izdatel'stvo „Nedra", Moskva (in Russian).

COLLECTIVE WORK,(1976), *Poradnik Górnika*, (*Miner's Guidebook*) vol 5 - edition 2., Wydawnictwo „Śląsk", Katowice (in Polish).

GRZELAK, E., (1975), *Maszyny i urządzenia do przeróbki mechanicznej surowców mineralnych* – (*Machinery and Equipment for Mechanical Enrichment of Minerals*) Wydawnictwa Naukowo-techniczne, Warszawa (in Polish).

HÖFFL, K., (1985), *Zerkleinerungs- und Klassiermaschinen* (*Crushers and Classifiers*) - VEB Deutscher Verlag für Grundstoffindustrie, Leipzig (in German).

LJAŠČENKO, P.V., (1935), *Gravitacionnye metody obogaščenija* (*Gravitational Methods of Enrichment*) - Gosudarstvennoe Ob'edinennoe Naučno-Techničeskoe Izdatel'stvo, Moskva – Leningrad (in Russian).

MAYER, F.W., (1971), *Berechnung des neuen Trennungschärfe-Kennwertes* (*Trennfehlermoment*) aus den Teilunszahlen, 1. und 2. Teil – (*The Evaluation of New Distribution Numbers*) Aufbereitungs-Technik nr 2 i 4 (in Germany).

NOWAK, A., (1979), *Kornformfaktor für die Bewegung in einem flüssigen Medium* (*The Shape Coefficient for the Application in the Wet Classification Processes*) - XXX Berg- und Hüttenmännischer Tag, Freiberg (in Germany).

NOWAK, A., (1981), *Charakterystyki rozdziału jednorodnych ziarn mineralnych w wirówkach klasyfikujących* (*Characteristics of Separation of Homogenous Mineral Grains in Classifying Centrifuges*) - PWN Warszawa – Kraków (in Polish).

RAZUMOV, K.A., PEROV, V.A., (1982), *Proektirovanie obogatitel'nych fabrik* – (*Designing of Processing Plants*) - Izdatel'stvo „Nedra", Moskva (in Russian).

STĘPIŃSKI, W., (1964), *Wzbogacanie grawitacyjne* (*Gravitational Enrichment*)- PWN Łódź - Warszawa – Kraków (in Polish).

SYSŁO, M., (1964), *Uogólnione prawo Stokesa dla brył spójnych* (*Generalised Stokes' Law for Compact Solids*) - Zeszyty Naukowe Akademii Górniczo-Hutniczej nr 94, Rozprawy z.33, Kraków (in Polish).

SZTABA, K., (1956), *Metoda statystyczna badania procesu klasyfikacji mokrej* (*Statistical Method for Investigating the Wet Classification*) - Archiwum Górnictwa, t.I., z.1 (in Polish).

SZTABA, K., (1956), *Krzywe rozdziału w procesie klasyfikacji mokrej* (*Separation Curves in Wet Classification*) - Archiwum Górnictwa, t.I., z.2 (in Polish).

SZTABA, K.S., (1964), *Niektóre własności geometryczne zbiorów ziarn mineralnych* (*Some Geometrical Properties of Mineral Grains Sets*) - Zeszyty Naukowe Akademii Górniczo-Hutniczej nr 85, Rozprawy z.25, Kraków (in Polish).

SZTABA, K., (1988), *Współwystępowanie efektów klasyfikacji i wzbogacania w procesach przepływowych* (*Co-occurrence of Effects of Classification and Enrichment in Flow Processes*) - Fizykochemiczne Problemy Mineralurgii z.20 (in Polish).

SZTABA, K., NOWAK, A., MAKARY, B., (1990), *Rozwój rozwiązań technologicz(nych i metod modelowania procesów klasyfikacji przepływowej* (*Development of Technological Solutions and Modelling Methods of Flow Classification*)- Zeszyty Naukowe Politechniki Śląskiej nr 1088, seria Górnictwo z. 190, Gliwice (in Polish).

SZTABA, K., (1992), *Problems of Taking into Account Shapes of Mineral Grains in Flow Classification* - The First International Conference on Modern Process Mineralogy and Mineral Processing, Beijing.

SZTABA, K., (1992), *Warunki i możliwości rozbudowy i ujednolicenia opisów modelowych procesów klasyfikacji przepływowej* (*Conditions and Possibilities of Development and Unification of Model Descriptions of Flow Classification Processes*)- Fizykochemiczne Problemy Mineralurgii z. 26 (in Polish).

SZTABA, K., (1993), *Directions and Development Trends of Model Descriptions of Flow Processes - Archives of Mining Sciences* (Archiwum Górnictwa) PAN, t.38, z.2.

SZTABA, K., (1994), *The Problems of Modeling of Technological Processes of the Mineral Processing* - IV Meeting of the Southern Hemisphere on Mineral Technology & III Latin American Congress on Froth Flotation, Concepcion (Chile), 20-23 November 1994.

SZTABA, K., (1994), *The Problems of Flow Classification of Very Fine Grained Materials* - IV Meeting of the Southern Hemisphere on Mineral Technology & III Latin American Congress on Froth Flotation, Concepcion (Chile), 20-23 November 1994.

SZTABA, K., TORA, B., TUMIDAJSKI, T., (1996), *Modelling of Processes of the Mineral Processing* - System Analysis, Modelling, Simulation (*SAMS*) 1996, Vol.24.

SZTABA, K., (1996), *The Problems of Modelling of Technological Processes of Mineral Processing* - International Conference Minerals & Materials '96, Somerset West, South Africa, 31 July - 2 August 1996, Volume I: Minerals.

SZTABA, K.St., (1997), *Możliwości uściślania opisów ruchu ziarn w ośrodkach płynnych* (*Possibilities of Precise Descriptions of Grain Movements in Liquid Media*) - Zeszyty Naukowe Politechniki Łódzkiej nr 780, Inżynieria Chemiczna i Procesowa z. 22, Łódź (in Polish).

SZTABA, K., TORA, B., TUMIDAJSKI, T., (1998), *Modelling of Mineral Processing Based on the Law of Mass Conservation* - 9th International Symposium on „System - Modelling - Control", Zakopane.

SZTABA, K., (1998), *Założenia metodyczne budowy wielostadialnych układów klasyfikacji przepływowej* (*Methodological Assumptions of Construction of Multi-stage Systems of Flow Classification*) - in *Kompleksowe wykorzystanie surowców a ochrona środowiska*, AGH - Uczelniane Wydawnictwa Naukowo-Dydaktyczne, Kraków (in Polish).

TUMIDAJSKI, T., (1993), *Zastosowanie metod statystycznych w analizie procesów przeróbki surowców mineralnych* (*Application of Statisical Methods in Mineral Processing*) - Śląskie Wydawnictwo Techniczne, Katowice (in Polish).

TICHONOV, O.N., (1973), *Vvedenie v dinamiku massoperenosa processov obogatitel'noj technologii* (*Introduction in Dynamics of Enrichment Processes*) - Izdatel'stvo „Nedra", Moskva (in Russian).

Kazimierz St. SZTABA, Alicja NOWAK, Założenia do modelowania separacji w klasyfikatorach zwojowych, Fizykochemiczne Problemy Mineralurgii 34, 77–94 (w jęz. angielskim)

Klasyfikatory zwojowe (spiralne) są urządzeniami służącymi do rozdziału średnio- i drobnouziarnionych zawiesin fazy stałej w cieczach (z reguły w wodzie) na produkty o zróżnicowanym uziarnieniu fazy stałej. Cechą ziarn decydującą o zachowaniu się ziarna w procesach przepływowych jest ich prędkość charakterystyczna – w praktyce tzw. prędkość graniczna. Oprócz podstawowego efektu klasyfikacji ziarnowej, w każdym jej procesie występują efekty różnicowania w poszczególnych produktach, stosunku fazy stałej do ciekłej, a w przypadkach klasyfikacji materiałów niejednorodnych pod względem składu mineralnego, występują ponadto uboczne efekty wzbogacania. Klasyfikatory zwojowe nadają się szczególnie do stosowania również w charakterze urządzeń odwadniających. Zespół cech konstrukcyjnych, ruchowych i eksploatacyjnych klasyfikatorów zwojowych obejmuje w związku z możliwościami różnorodnych zastosowań, kilkadziesiąt czynników wpływających na przebieg procesu i jego wyniki

technologiczne oraz wartości wskaźników służących do opisu procesu rozdziału. Wpływ większości owych cech na wyniki procesu nie jest w pełni rozpoznany. Uniemożliwia to budowę modelu deterministycznego procesu, a budowa modeli fenomenologicznych wymaga bardzo licznych badań, wykonywanych przy zmiennych wartościach wielu warunków. Ich realizacja, zwłaszcza w warunkach przemysłowych jest niezwykle trudna. W opracowaniu przedstawiono dyskusję wpływu warunków procesu na jego wyniki w odniesieniu do efektu klasyfikacji, a także w ograniczonym stopniu do efektów odwadniania. Przedstawiono propozycję sposobu postępowania w przypadku poszukiwania opisów modelowych o ograniczonej szczegółowości.

Physicochemical Problems of Mineral Processing, 34 (2000), 95–99
Fizykochemiczne Problemy Mineralurgii, 34 (2000), 95–99

Antoaneta BOTEVA*

TREATMENT OF SILICA FOR THE NEEDS OF THE ELECTRONIC INDUSTRY

Received March 15, 2000; reviewed and accepted May 15, 2000

The silica is one of the main raw material for the electronic industry. The requirement for silica are: high purity and fragment size. Usual native quartz is not of sufficient qualitative. This article proposes method for quartz processing. After processing the quartz can be used in electronic industry.

Key words: silica, electronic industry, defects, treatment

INTRODUCTION

The requirements for silica as a raw material for the electronic industry are related both to its purity and fragment size. The latter is necessitated in a view of certain hindrances in the operation of a silica smelting furnace. The silica concentrates contain monocrystal quartz or quartzites of purity higher than 99%. The Al_2O_3 content is determined within the range of 0.15–0.20%. The Fe_2O_3 content has to be lower than 0.05%. The presence of As, P and S is undesirable because they create an adverse gas phase in the furnace. The silica has to be resistant to high temperature so that it can be reduced in size when heated in the furnace. It is not admissible to use finely crushed silica since it changes the furnace gas circulation thus leading to a local gas compensation which can cause explosion in the furnace. The energy consumption varies between 12,000 and 14,000 KWh/t of the feed. The process runs at a temperature of 1500–2000°C. The silica feed should have a grain size of 20–150 mm. Therefore,

* University of Mining and Geology "St. Ivan Rilski"-Sofia, Bulgaria

quartz sand cannot be used for Si production. Sand pelletization is also considered to be unprofitable. From all that has been said above it follows that the requirements for the silica feed for the electronic industry are as follows:

1. Purity within the necessary requirements
2. Absence of defects which can break down the fragments during the silica processing into Si thus disturbing the operating mode
3. 20–150 mm fragment size.

The optical properties of quartz depend mainly on its purity and the presence of different kinds of defects. The Frankel and Schottky defects are of particular importance. These defects occur as a result of the thermal motion of the atoms building up the lattice. At any temperature there are certain atoms whose energy is much higher than the average energy of the atoms. At a given moment, the higher energy atoms may not only move considerably away from their equilibrium position in the lattice but may also overcome the potential barrier created by the neighbouring atoms and move to the interstitial space. As a result, two point defects occur: "interstitial atom" and "vacancy". The combination of these two lattice defects is called Frenkel's defect. If the atom, which leaves the lattice site, comes from the crystal surface, then the slight mobility of the Frenkel defects can result in a redistribution in the crystal depth that cause vacancy inside the volume without the presence of an atom in the interstitial site. Such vacancies are called the Schottky defects. The quartz colour depends essentially on the Frenkel defects, on their distribution in the volume and on the charge (positive or negative) of the atoms located in the interstitial site. The Frenkel defects can also be created by preliminary treatment of the material with high energy particles. When radiated with electrons, the defects exhibit a local character because of their low penetrating capacity. The gamma rays interact slightly with the nuclei of the substance. The interaction occurs mainly with the electrons released by these nuclei. The gamma ray energy should comply with the particular substance with the view to increasing the effective gamma cross-section. The interaction takes place within the whole volume of the treated material and the defects are evenly distributed thus avoiding their local character in other types of interaction. The gamma quantum energy, required for dislocating the atom and forming the Frankel defects, is determined by the energy of the photoelectrons and Compton recoil electrons. Therefore, under the action of gamma rays it is possible to recharge the lattice site atoms which have formed Frenkel defects. This will lead to a change in the material colour and hence, to a change in its optical properties.

MATERIALS AND METHODS

The quartz raw materials are represented by both monocrystal quartz and quartzites. In both cases coarse and fine size fractions are obtained thus requiring further treatment. With the coarse size fractions there is also a problem of assessing their stability during heating.

EXPERIMENTAL WORK AND DISCUSSION

The laboratory experiments were performed on a monomineral quartzite sample. A monomineral fragment was crushed to a size under 150 mm. The size fraction under 20 mm was separated. It was passed through a 0.16 sieve mesh. The two quartzite size fractions thus prepared were subjected to radiation treatment with gamma rays from Co 60, which has an energy of 1.33 MeV. An average sample was preliminarily taken from the two size fractions, ground to powder and chemically analysed. The values obtained for the admixtures are presented in Table 1.

Tab. 1. Chemical composition of quartzite's subjected to radiation treatment

Size fractions, mm	Content, %				
	Al_2O_3	Fe_2O_3	Cu	Au	S
+16; -20;	1.05	0.27	0.01	slight	0.02
+20; -150	0.16	0.10	0.01	no	0.02

The chemical analysis showed that the fines require a subsequent treatment. The size fraction over 20 mm was subjected to radiation treatment and the fines under 20 mm were washed and analysed again. After washing, the fines were subjected to radiation treatment. The colour of the samples was checked successively after radiation treatment with the following doses 0.1; 0.2; 0.3; 0.4; 0.5; 1.0; M rad. A change was observed in the colour of some grains after 1.0 M rad. In coarse fragments this tarnishing occurred in spots whereas in fine grains it was complete. The tarnishing started as slight greying, which gradually changed its nuance. It was interesting to observe that the increased radiation on the coarse fragments did not cause equalisation of colour, but only affected sections which changed (darkened their colour). The results obtained enabled us to continue our investigations on the treatment of processing plant quartz concentrates and separation of ore samples from quartzite's.

Quartz sand was used in conducting the experiments which is obtained as a waste product during ore treatment from the Brutes ore deposit in the Burgas ore region. As

a waste product from flotation it has a size grading of +0.16; -0.25. The samples were subjected to radiation treatment with gamma rays from Co 60 which have an energy of 1.33 MeV. After homogenisation, the material was divided into 36 samples, which were grouped in 9 groups. Each group was subjected to radiation treatment with the following doses: 0.5; 1.0; 2.0; 3.0; 5.0; 8.0; 10.0; 25.0 M rad (1 rad = 10^{-2} Gy), respectively. 1000 grains of each sample were studied by means of a binocular magnifier. Fig. 1 shows the dependence of the ratio of tarnished to untarnished grains N_{untar}/N_{tar} on the radiation dose [D_r(M rad)].

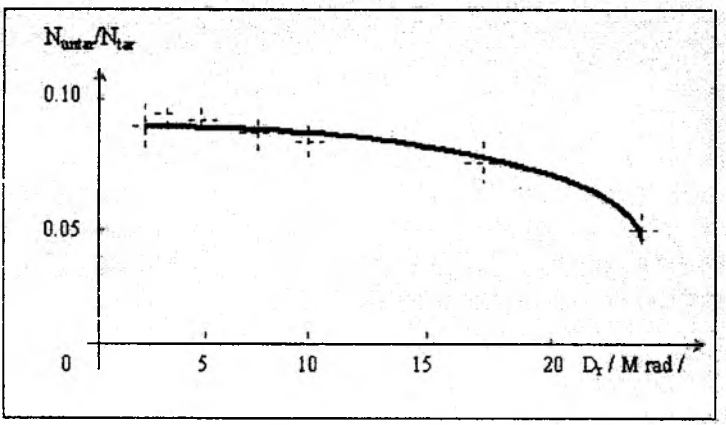

Fig.1. Dependence of the ratio of tarnished to untarnished quartz grains (N_{untar}/N_{tar}) on the radiation dose [D_r(M rad)]

The analysis of the sample shows that, as a whole, the tarnishing increases with increasing the dose. At doses 0.5 and 1.0 (M rad) a change is observed in the sample colour, though visually it is difficult to differentiate the individual grains by colour. From the differential analysis shown in Fig.1 it can be seen that the ratio of tarnished to untarnished grains remains relatively constant for the different radiation doses. It can be concluded that the tarnishing of the samples as an integral characteristic of the properties of the different doses, is due only to certain grains which change their colour at different doses. A smaller part of the grains preserve their qualities regardless of the radiation doses. Part of each sample was subjected to dry roll electric separation. Separation in size fractions depending on the radiation dose was not observed. Since the electric separation proved to be unusable for separating the tarnished from the untarnished grains, a laboratory optical separator, constructed on the laser beam principle, was used. The separation of the untarnished quartz grains was effected by using this separator. These proved to be the grains without defects. On this basis, a standard optical separator was proposed to be used for separating quartz with grain

sizes +15 mm; -20 mm. This separator managed to separate single spotted grains from the unchanged ones, which proved to be high quality quartz. The latter was established by analysis. A well-coloured (purple) amethyst was subjected to radiation treatment with gamma rays. The amethyst lost its colour bur remained dull.

CONCLUSIONS

The results of the studies showed the possibility for increasing the quality of quartz concentrates used for special applications by their preliminary radiation treatment with definite gamma ray doses.

REFERENCES

PIKE G. F., SEAGER C.H 1982, *Grain Boundaries in Semiconductors*. Materials Research Society, Symposia proceedings, Volume 5, H. J. Leamy (Ed.) North Holland

AJNSPRUKA N., UISSMENA U. 1988, *Аренид галка в микроелектронике,* Moscow, Mir.

BALAKSHIJ W.I., PARYTIN, W.N., CHIRKOW A.I. (1985), Физические основы акустооптики. Moscow.

ORMO B.F. (1968), *Введение в физическую химию и кристало химию полупроводников,* Moscow

Boteva A., Przeróbka krzemionki dla potrzeb przemysłu elektronicznego, *Fizykochemiczne Problemy Mineralurgii* 34, 95–99 (w jęz. angielskim)

Krzemionka jest jednym z głównych surowców stosowanym w przemyśle elektronicznym. Wymagania stawiane krzemionce są następujące: wysoka czystość i odpowiedni kształt. Najczęściej mineralna krzemionka nie spełnia tych jakościowych wymogów. W pracy przedstawiono proces przeróbki krzemionki przez jej naświetlanie promieniami gamma. Po przeprowadzenie procesu napromieniowania krzemionka była wzbogacana w laboratoryjnym separatorze optycznym, a uzyskany materiał może być użyty przez przemysł elektroniczny.

Physicochemical Problems of Mineral Processing, 34 (2000), 101–110
Fizykochemiczne Problemy Mineralurgii, 34 (2000), 101–110

Jan DRZYMAŁA*, Janusz KAPUSNIAK**, Piotr TOMASIK***

AMINO ACID DEXTRINS AS SELECTIVE DEPRESSANTS IN FLOTATION OF CHALCOCITE AND GALENA

Received March 15, 2000; reviewed and accepted May 15, 2000

A series of biodegradable, proecological depressants for selective flotation of galena and synthetic chalcocite was tested. These depressants, originating from dextrinization of potato starch with biogenic α-amino acids such as alanine, arginine, asparagic acid, cysteine, glutamic acid, glycine, histidine, isoleucine, leucine, lysine, methionine, proline, serine, threonine, tryptophane, tyrosine, phenylalanina and valine, appeared to be effective depressants. Among them dextrins from starch modified with asparagic acid, glutamic acid and threonine were superior as they provided good recovery of galena and significant depression of synthetic chalcocite at a concentration of 2-4 kg/Mg of minerals when sulfides were subjected to microflotation separately. Subsequently, threonine dextrin was tested as a copper mineral depressant for Polish industrial copper concentrates containing 18.28% Cu and 3.63 % Pb. The test was carried out in a laboratory flotation machine and it was found that threonine dextrin was highly selective but the results were opposite to the microflotation tests since it depressed lead mineral more efficiently than the copper minerals.

Key words: separation, flotation, upgrading, copper minerals

INTRODUCTION

Separation of lead minerals from Polish copper concentrates is a difficult task (Łuszczkiewicz et al., 1995) because it contains unusual pair of sulfides: chalcocite

*Technical University of Wroclaw (I-11), Wybrzeze Wyspianskiego 27, 50-370 Wroclaw, Poland
**University of Education, Armii Krajowej 13/15, 42-201 Częstochowa, Poland
*** University of Agriculture, Mickiewicza Ave. 21, 31-120 Krakow, Poland

and galena at a ratio of 10:1. Separation of those sulfides involving purely physical methods conducted by means of hydrocyclones, concentrating tables, high field magnetic separators and other has been unsuccessful (Kubacz et al., 1984: 1985). Application of selected depressants such as thioglycolic acid (Łuszczkiewicz and Drzymala, 1996) and ammonium acetate (Sanak-Rydlewska et al., 1999) was more promising. In other countries polymers are frequently used depressants in selective flotation of complex ores. Among them polysaccharides evoked particular interest (Lin and Burdick, 1988; Pugh, 1989; Liu and Laskowski, 1999; Rath, 1999). Recently, preparations from dextrinization of potato starch under ammonia (Wiejak et al., 1991; Sychowska and Tomasik, 1997), hydrogen sulfide (Sychowska et al., 1998), and with gluten (Sychowska and Tomasik, 1996) were tested as depressants in flotation of individual galena and chalcocite samples and their mixtures. Only dextrins prepared from starch under ammonia proved to be suitable (Drzymała et al., 2000).

All compounds mentioned above constitute a group of reagents called first generation depressants. They provide, to a certain extent, separation of lead minerals from copper minerals. However, there is a need for a second generation depressants leading to copper concentrates and tailing in form of lead concentrates. For this sake, special novel dextrins were prepared. They resulted from the thermolysis of potato starch with α-amino acids (Kapuśniak et al., 1999). These biodegradable and proecological preparations were used for model flotation studies involving chalcocite and galena.

MATERIALS

Dextrins resulted from thermolysis of potato starch with one of the following amino acids: alanine (ALA), arginine (ARG), cysteine (CYS), glycine (GLY), histidine (HIS), isoleucine (ILE), asparagic acid (ASPA), glutamic acid (GLUA), leucine (LEU), lysine (LYS), methionine (MET), phenylalanine (PHE), proline (PRO), serine (SER), threonine (THR), tryptophane (TRP), tyrosine (TYR), and valine (VAL). In the text they are denoted as ALA-dextrin, ARG-dextrins, and so on, respectively. Preparation of these dextrins was described by Kapuśniak et al. (1999) and their properties were reported in a paper by the same authors (1999a). Prior to flotation 0.2 g of any dextrin was dissolved in 100 cm^3 of water at 70-80°C. Although dextrins did not solubilize completely non-filtered solutions were used. A 10^{-4}mol/dm^3 solution of potassium butylxanthate (KBUTX) was used as collector. Synthetic chalcocite was provided by the Copper Metallurgical Enterprise in Legnica, Poland. Trzebionka Zinc-Lead Ore Mine, Poland, supplied us with galena. Prior to flotation samples of these minerals were identified by means of powder x-ray analysis in the Department of X-Ray Analyses in the Institute of Cryogenics and Structural Studies of the Polish Academy of Sciences in Wrocław, Poland.

METHODS

Minerals were crushed and pulverized in an agalite mortar followed by separation into fractions on the sieves. Only the 0.16-0.20 mm size fraction was used in the flotation tests. The period between crushing and beginning of flotation did not exceed 30 min. Microflotations were carried out in monobubble Hallimond apparatus equipped in calibrated receiver providing a continuous recording of the recovery as a function of time. Galena and chalcocite have different density therefore, standard weight of the samples of each mineral introduced into the apparatus was different. They were 1.10g for galena and 0.65 for chalcocite. Each mineral was subjected separately to flotation. The solid particles (0.2 cm^3 i. e. either 1.1 g of PbS or 0.65 g of Cu_2S) were suspended in 120 cm^3 of aqueous solution of depressant, then agitated for 5 minutes. The pH of the solution was usually between 6.4 and 7.2 unless otherwise stated. Amount of butyl xanthate subsequently added to the solution provided its final concentration of 0.0001 $kmol/m^3$. After 5 min. agitation, the suspension was transferred to the Hallimond tube and floated for 15 minutes with the air flow of 0.625 cm^3/s. Microflotation carried out at 20±2°C lasted 15 min. Recovery of minerals was calculated in form of volume of floated particles related to the original volume of particles. Kinetic output – time curve was determined for every test. From the recovery - time diagram recoveries after 15 min were taken and relationships in respect to the concentration of depressant were derived. Flotation tests were also carried out in a Mechanobr laboratory flotation machine, equipped with a 500 cm^3 cell. A sample of 150 g of industrial concentrate was used in the experiment. Flotation was carried out in distilled water in the presence of 50g/Mg potassium ethyl xanthate, 50g/Mg α-terpineol and 1500g/Mg threonine dextrin. The solids were introduced to water followed by dextrins, collector and finally the frother. The pH of flotation was 7.99. During flotation of the sample three concentrates, after 1, 2 and 4 minutes of flotation, were collected and the solid remaining in the cell were labeled as tailing.

RESULTS AND DISCUSSION

Fig. 1a-s shows results of microflotation in a small Hallimond tube of chalcocite and, separately, galena in the presence of the investigated dextrins. It can be seen from that Figure that results of depression of sulfides varied from one dextrin to another. To show the results on one graph and compare the results an index, denoted here as index I, was designed. Index I is measure of a difference between the dose of a dextrin necessary for 95 % recovery of galena and 5% of chalcocite related to the dose of dextrin required for 5% of chalcocite and has a form:

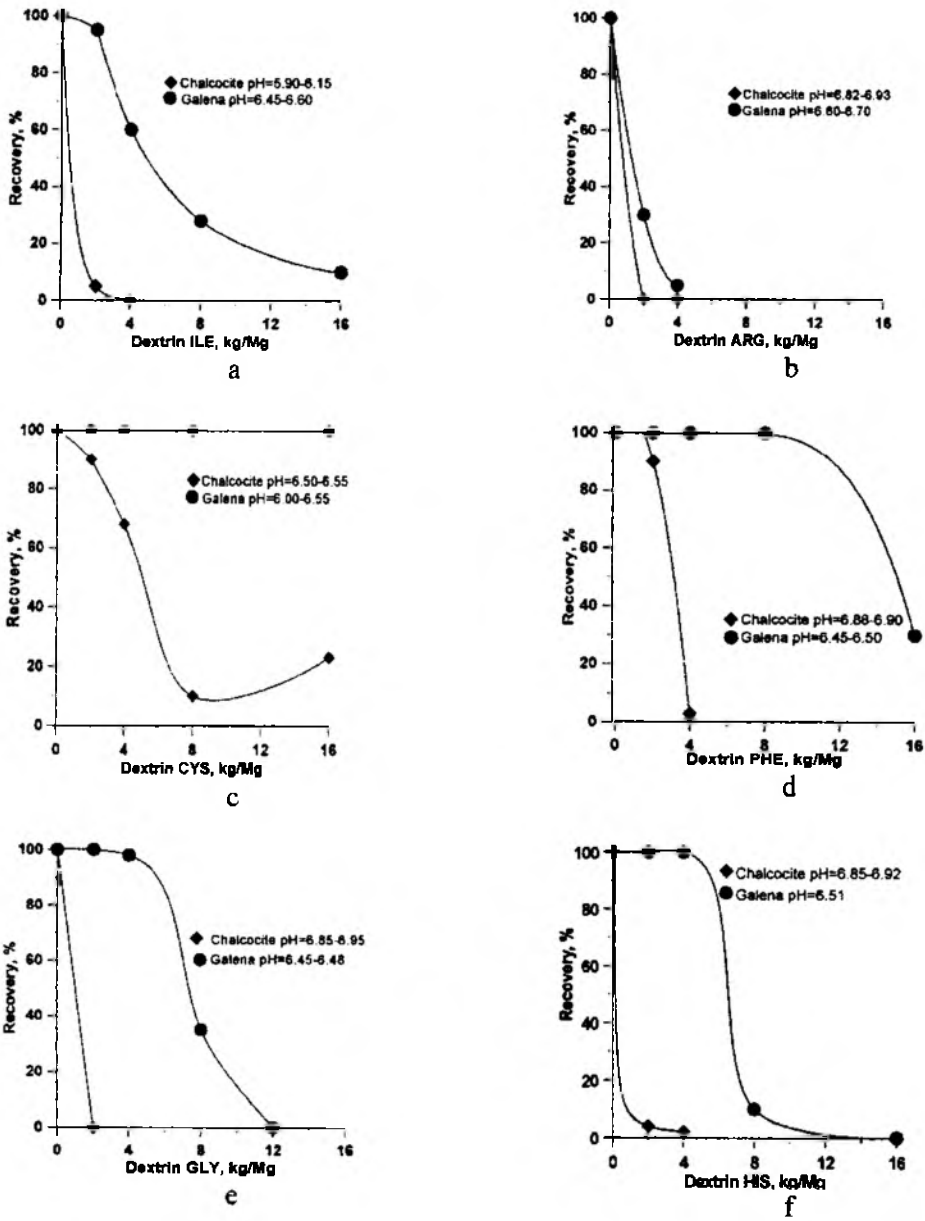

Fig. 1a-f. Results of flotation of galena and separately synthetic chalcocite in the presence of butyl xanthate and various amino acid dextrins: a) ALA (alanine), b) ARG (arginine), c) CYS (cysteine), d) PHE (phenylalanine), e) GLY(glycine), f) HIS (histidine)

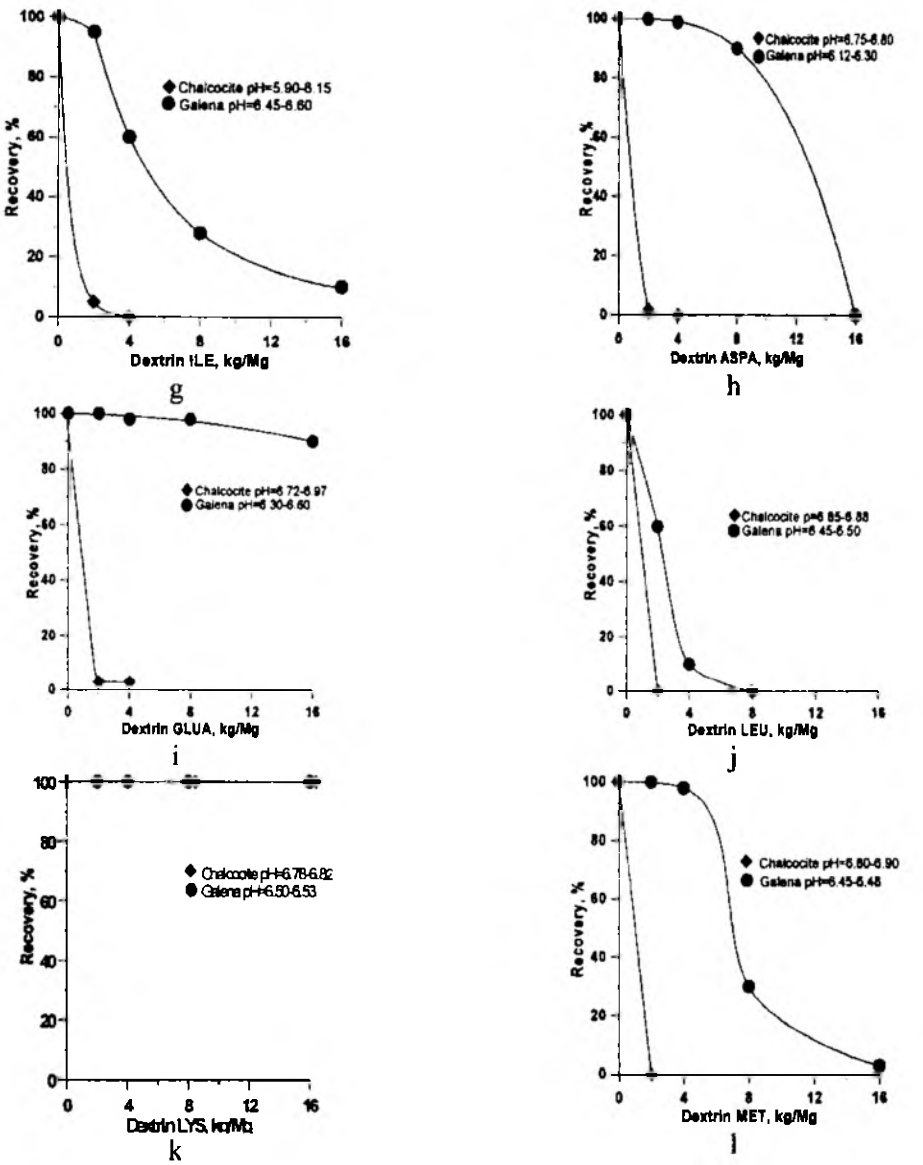

Fig. 1g-l. Results of flotation of galena and separately synthetic chalcocite in the presence of butyl xanthate and various amino acid dextrins: g) ILE (izoleucine), h) ASPA (aspargic acid), i) GLUA (glutamic acid), j) LEU (leucine), k) LYS (lysine), l) MET (methionine)

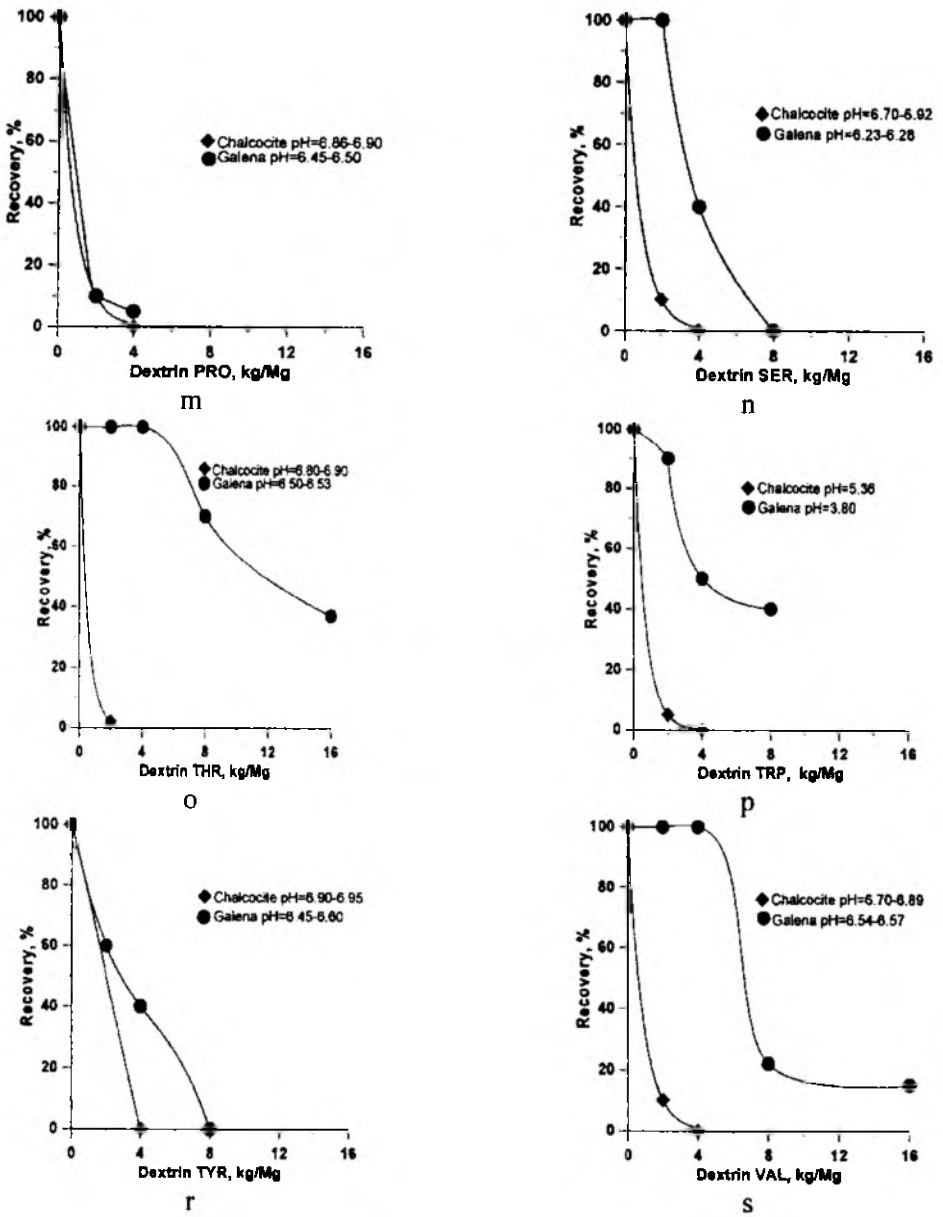

Fig. 1m-s. Results of flotation of galena and separately synthetic chalcocite in the presence of butyl xanthate and various amino acid dextrins: m) PRO (proline), n) SER (serine), o) THR (threonine), p) TRP (tryptophane), r) TYR (tyrosine), s) VAL (valine)

$$I = \frac{C_{\varepsilon Pb95\%} - C_{\varepsilon Cu2S5\%}}{C_{\varepsilon Cu2S5\%}} \quad (1)$$

where $C_{sCu2S5\%}$ is the dose of the dextrin (kg/Mg of solids) required for 5% recovery of Cu_2S, and $C_{\varepsilon Pb95\%}$ is the dose of the dextrin (kg/Mg of solids) required for 95% recovery of galena.

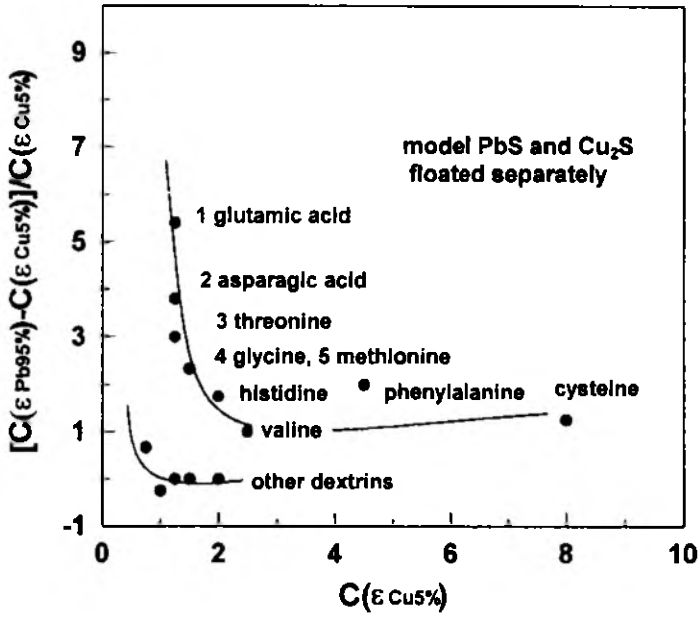

Fig. 2. Selectivity index I (Eq.1) vs $C_{\varepsilon Cu2S5\%}$ for the investigated amino-acid dextrins. Five most promising dextrins are labeled with numbers from 1 to 5

A higher value of index I at a lower value of $C_{\varepsilon Cu2S5\%}$ (Fig.2) points to a more efficient separation. Index I is helpful in selection of the most promising dextrins. It appears that the first five most promising selective dextrins are GLU-dextrin, ASP-dextrin, THR-dextrin, GLY-dextrin, and MET-dextrin. To check this finding a flotation test was performed in a laboratory flotation machine with a sample of an industrial copper concentrate from Lubin. The concentrate contained galena together with chalcocite apart from other sulfide minerals. THR-dextrin was used as the

depressant in the flotation test. The results involving industrial sample are shown in Table 1 and Fig. 3.

Table 1. Flotation of industrial copper concentrates in the presence of 1500 g of THR-dextrin per one megagram of solids. Other chemicals: KEtX 50 g/Mg, α-terpineol 50 g/Mg, pH 7.99. Flotation in a laboratory flotation machine

Product	Yield,%	Cu		Pb	
		content, λ%	recovery, ε%	content, λ%	recovery, ε%
Concentrate 1	21.34	43.40	50.65	1.53	9.09
Concentrate 2	9.52	33.75	17.58	2.09	5.58
Concentrate 3	8.97	22.75	11.17	3.10	7.58
Tailing	60.17	6.25	20.60	4.69	77.78
Feed	100	18.28	100	3.63	100

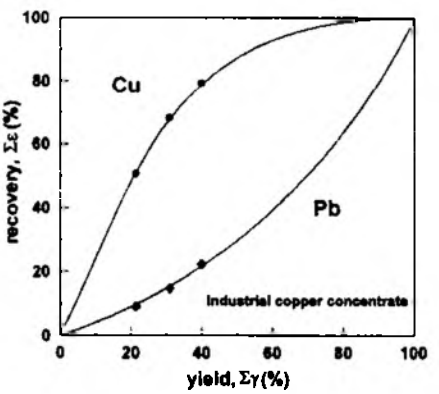

Fig. 3. Results of flotation from Table 1 in a graphical form.
Good separation of lead and copper minerals is well visible from the figure

Surprisingly, the flotation results for the industrial concentrate are inverted in relation to the results obtained from experiments with model samples, that is starch modified with threonine was a more powerful depressant towards synthetic chalcocite than for galena while for the industrial concentrate flotation of lead minerals was much more depressed than the copper minerals. The reason of the observed discrepancy is not clear and this calls for additional testing. A similar reversion of the selectivity of separation was observed by Liu and Laskowski (1999) in the galena - chalcopyrite system floated at pH 6 and pH 12. They explained the observed reversion

by the difference in the isoelectric point (iep) of oxidation products of sulfides that is $Cu(OH)_2$ (pH_{iep} 7.6-9.0) and $Pb(OH)_2$ (pH_{iep}=10-11). This and other possible reasons have to be checked by additional flotation tests.

PODZIĘKOWANIA

Autorzy dziękują KGHM-Polska Miedź S.A. za udostępnienie próbek koncentratu.

REFERENCES

Drzymała J., Tomasik P., Sychowska B., 2000, Dextrins as selective flotation depressants for sulfide minerals, in preparation

Kapuśniak J., Kozioł J., Tomasik P., 1999, Reaction of starch with α-amino acids Z. Lebensm. Unters. Forsch., A209, 325

Kapuśniak J., Kozioł J., Tomasik P., 1999a, Starch based depressors for selective flotation of metal sulfide ores. Starch/Die Staerke, 51, 416

Kubacz N., Bortel R., Grzebieluch Z., 1984, Institute of Nonferrous Metals, Gliwice, Poland, Report 2969/III/84, in Polish

Kubacz N., Bortel R., Grzebieluch Z., 1985, Institute of Nonferrous Metals, Gliwice, Poland, Report 2969/IV85, in Polish

Lin, K.F., Burdick, C.L., 1988, Polymeric depressants, in: Reagents in mineral technology (P. Somasundaran and B.M. Mondgil edytors), Marcel Dekker Inc., New York, Ch. 15, 471-518

Liu, Q., Laskowski, J.S., Adsorption of polysaccharides onto sulfides and their use in sulfide floatation, 1999, w: Polymers in mineral processing, J. Laskowski (edytor), Proc.3rd UBC-McGill Bi-annual Inter. Symp. on fundamentals of mineral processing, Met. Soc. CIM Montreal, 71-88

Łuszczkiewicz A., Drzymała J., 1996, Institute of Mining, Technical University of Wrocław, Report 1-11/S-29/96, Wrocław

Łuszczkiewicz A., Drzymała J., Grotowski, 1995, Problemy flotacyjnego rozdziału siarczków miedzi i ołowiu, Rudy i Metale Nieżelazne, 40, (8), Wroclaw, 315-318

Pugh R.J., 1989, Macromolecular organic depressants in sulphide flotation - a review. 1. Principles, types and applications, Int. J. Mineral. Process., 25, 101-130

Rath, R.K., Subramanian S., 1999, Effect of guar gum on selective separation of sphalerite from galena by flotation, Trans. IMM., Sec. C., 108, C1-C7

Sanak-Rydlewska S., Małysa E, Spalińska B., Ociepa Z, Konopka E., Kamiński S., 1999, Lowering lead content in copper concentrate, V Intern. Conf. on Mineral Proces. of Nonferrous Metals, Szklarska Poręba, KHGM- Cuprum- IMN

Sychowska B., Tomasik P., 1996, Thermolysis of starch with gluten, Pol. J. Food Nutr. Sci., 5/2, 53

Sychowska B., Tomasik P., 1997, Thermolysis of starch under ammonia, Pol. J. Food Nutr. Sci., 6/4, 27

Sychowska B., Tomasik P., Wang Y.J., 1998, Thermolysis of starch under hydrogen sulfide, Pol. J. Food Nutr. Sci., 7/2, 23

Wiejak S., Sychowska B., Tomasik P., Pałasiński M., 1991, Thermolysis of starch in the atmosphere of ammonia, Acta Aliment. Pol., 41, 297

Jan Drzymała, Janusz Kapusniak, Piotr Tomasik, Amino Acid Dextrins as Selective Depressants in Flotation of Chalcocite and Galena, *Fizykochemiczne Problemy Mineralurgii*, 34, 101–110 (w jęz. angielskim)

Przebadano szereg biodegradowalnych i proekolgicznych depresorów pod kątem ich zastosowania do selektywnego flotacyjnego rozdziału galeny od chalkozynu. Depresory te otrzymano w wyniku dekstrynizacji skrobi ziemniaczanej α-aminokwasami (alanina, arginina, kwas asparaginowy, cysteina, kwas glutaminowy, glycina, histidyna, isoleucyna, leucyna, lizyna, metionina, prolina, seryna, threonina, tryptofan, tyrozyna, fenyloalanina i walina). Uzyskane depresory zastosowano do ksantogenianowej flotacji naturalnej galeny i osobno syntetycznego chalkozynu w celce Hallimonda przy pH około 6.5. Dla większości depresorów zaobserwowano silną depresję flotacji syntetycznego chalkozynu, podczas gdy zanik flotacji galeny obserwowano dopiero przy dużych stężeniach depresora. Największą różnicę stężeń niezbędną do depresji badanych siarczków uzyskano dla dekstryn modyfikowanych kwasem asparginowym, kwasem glutaminowym oraz treoniną. Do dalszych badań, przeprowadzonych w laboratoryjnej maszynce flotacyjnej Mechanobr o pojemności celi flotacyjnej wynoszącej 0.5dm^3, użyto dekstryny modyfikowanej treoniną. Depresor ten, zastosowany do flotacji końcowego koncentratu miedziowego z LGOMu, który zawierał 18.28% Cu i 3.63 % Pb. Uzyskano dobry rozdział minerałów miedzi od ołowiu, gdyż w produkcie pianowym uzyskano koncentrat miedzi, a w produkcie komorowym koncentrat ołowiu. Zatem, nieoczekiwanie, minerały miedzi flotowały lepiej niż ołowiu, co oznacza, że depresji ulegały minerały ołowiu. Nie jest znana przyczyna niezgodności badań modelowych z badaniami z udziałem materiału technologicznego, ale prace dla jej wyjaśnia są w toku.

Physicochemical Problems of Mineral Processing, 34 (2000), 111–131
Fizykochemiczne Problemy Mineralurgii, 34 (2000), 111–131

Levent ERGUN*, Salih ERSAYIN**

PERFORMANCE EVALUATION IN A SMALL SCALE GRAVITY CONCENTRATION PLANT

Received March 15, 2000; reviewed and accepted May 15, 2000

In this paper, the results of a performance evaluation study carried out in a chromite concentration plant are presented. The plant is a typical of the similar kind of gravity concentrators which are not equipped with basic control and measuring devices. Therefore evaluation of their performance appears to be a difficult task and requires unique methodology. The study commenced with sampling. A week long sampling surveys were repeated twice. First, the data was mass balanced then conventional parameters of equipment efficiency were determined. After detailed evaluation of the performance data, some modifications at the plant operation, i.e. changing screen aperture from 6 mm to 2 mm, limiting capacity for the plant and the possibility of using two rod mills in parallel, were proposed. Their effects on the performance were investigated by using computer simulation techniques. The results show that the performance and capacity could be improved by applying the proposed changes in the flowsheet.

Key words: gravity concentration, performance evaluation, rod mill, modelling, simulation

INTRODUCTION

Performance evaluation has vital importance in mineral processing plants. It is necessary to determine the existing plant performance to diagnose problems in

*Hacettepe University, Department of Mining Engineering, Ankara, Turkey
**Coleraine Minerals Research Laboratory, University of Minnesota, USA

individual equipment or circuit configurations and to investigate the alternatives for improving metallurgy and/or reducing costs.
Since modern plants equipped with instruments and control devices, it is relatively easier to obtain large amount of good quality data from them. Developments in computers and softwares have made it possible to calculate complex mass balances and to carry out simulations for many the modifications in operating conditions and flowsheets. Consequently, this type of modern tools is emerging to have routine use in modern plants.

However, most plants of small to medium capacity are in general poorly instrumented. Most of chromite ores are processed in this type of plants. It is highly questionable that they are operated at optimum conditions. In order to take engineering based decisions to improve their profitability, detailed performance evaluation should be carried out time to time. In these circumstances, sampling and data collection is difficult since operating variables could be changed considerably during a short period due to the lack of measuring and control devices. Therefore, the data deserves a cautious treatment. The methodology to be applied in these circumstances should take the undesirable conditions into account.

In this paper, the methodology used in the performance evaluation of Sori Plant which represents a typical chromite processing plant in Turkey, as well as problems encountered and experiences gained are presented. After evaluating the data gathered, some modifications in the plant flowsheet were proposed for improving the performance. In contrast to its backward nature, modern tools such as modelling and simulation were used for estimating plausible improvements. The ideas for a better performance were also outlined.

DESCRIPTION OF PLANT

Performance evaluation studies were performed at the Sori Plant where shaking tables are used for beneficiation. The plant is designed for a tabling unit capacity of 10 t/h to produce a chromite concentrate of minimum 48 % Cr_2O_3. The ore is massive Alpine type and occurres as several small deposits. The gangue mineral of high grade (38–45 % Cr_2O_3) and relatively coarse grained ore is serpentine.

The simplified flowsheet of the plant is exhibited at Figure 1. Run of mine ore is, first, screened from 25.4 mm. Then, the oversize is transported to hand sorting unit, while undersize undergoes another screening through 6 mm (2 mm in original design).

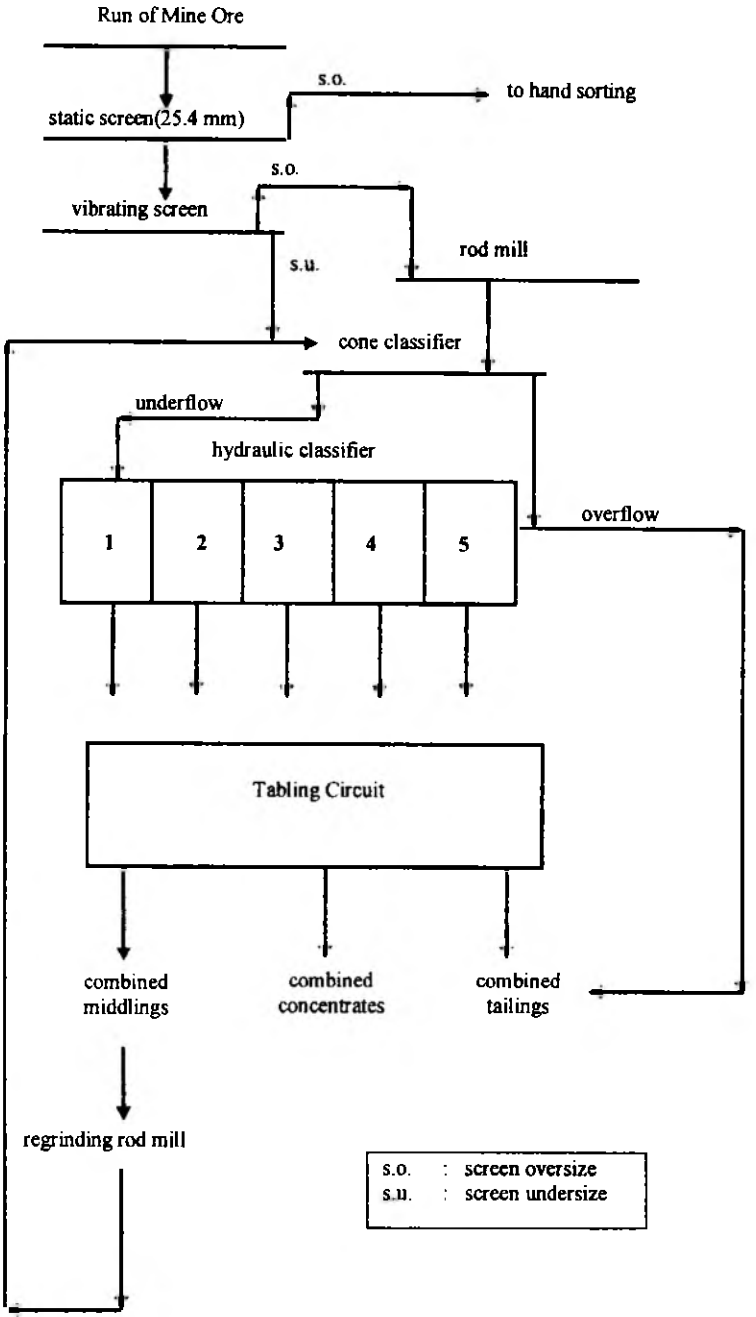

Figure 1. Simplified flowsheet of Sori plant

After rod mill grinding of -25.4+6 mm fraction, the rod mill product and screen undersize (-6 mm) are combined and fed to cone classifier for the separation of slime and excess water from the circuit. The slimes in the overflow of cone classifier is transported to tailing streams and the underflow is sent to a hydraulic classifier. Each classified product of hydraulic classifier is fed to a different set of shaking tables. The underflows from compartments 1, 2, 3, 4 and 5, are fed to 8, 3, 2, 2 and 1 shaking tables each having 8 m^2 deck surface, respectively. The middling obtained from the shaking tables concentrating the classified products of compartment 1 and 2 are sent to a regrinding rod mill and ground to -0.42 mm. The regrinding mill discharge is recycled to the cone classifier.

Apart from the belt scale weighing the feed flow, no instrumentation is available in the plant. Even the hand sampling points designed in the original flowsheet were obstracted by the modification made during the years. The daily metallurgical balance is based on the assays of three samples, namely feed, combined concentrate and tailings. Operators maintain the manual controls in the plant.

SAMPLING AND EXPERIMENTAL STUDIES

The lack of sampling devices in the plant rendered sampling very difficult. The overflows of the cone classifier and hydraulic classifier could not be sampled, since these two were transported in closed pipes to a thickener which could not be sampled either. The flow rates and solid ratios of rod mill overflows could not be measured, since there was not sufficient space for sampling cans at these points. Similarly, the physical conditions did not permit taking of reliable samples for flow rate and solid ratio measurements from the hydraulic classifier. All the remaining points were sampled.

Since the flow rates and operating parameters were possibly fluctuating in a very short period, it was considered that regular sampling throughout a relatively large period could provide samples representing the average behaviour of the plant. After examining the available data about the performance of the plant, it was decided that the length of such period should be about a week.

Two sampling surveys of one week long were carried out at the plant. Samples were taken from each point every hour during two shifts in a day. At the end of the week long survey they were combined and dried. Then, the amount of sample was reduced by coning and quartering. Consequently, they were transported to the laboratory where they were sieved and assayed for Cr_2O_3. The Bond Work Index of the ore was determined in the laboratory.

MASS BALANCING

It is well known that, whenever the excess data is collected, it contains some errors. These may be due to system dynamism, sampling equipment, operator, aging, bias etc. Therefore, it is necessary to balance the data before doing any further evaluation (Houdin et al. 1980). There are several mass balance algorithms presented in the literature (Richardson et al. 1987). They use same principles i.e., the least squares constrained optimization problem. At the time of the study, the commercially available mass balancing softwares were not in the reach of authors.To simplify the problem, a sequential methodology for mass balancing was followed. Starting from the first separator, i.e., screen, the best fit flow rates and corrected assays were calculated by using a house made program written for this purpose. For the following separators, the assays and flow rates of streams coming from previously calculated and adjusted streams were assumed to be the true values. The hydraulic classifier was the most problematic unit of the circuit in terms of calculations, since there were three incoming and five outgoing stream. A unique program was written for this unit. A constrained simplex approach (Carpenter et al. 1965) is used for the calculation of the flow rates around it. In the calculations, particle size of two unsampled stream, the overflows, was assumed to be 100 % -74μm. Although the reliability of the method used for mass balancing can be argued, it was the most practical approach available at the time of study. Later, the raw data were also inputted to a commercial mass balancing program and very similar results were obtained. However, the hydraulic classifier data from the first sampling period could not be balanced by either of the two probably due to large errors in assay values. Therefore the study was mainly based on the data obtained from the second sampling survey.

CALCULATION OF PERFORMANCE CRITERIA

After the calculation of best fit flow rates and adjusted assay values, the performance of individual equipments were examined by using conventional criteria. The equipments were screen, rod mills, hydraulic classifier and shaking tables.

The criterion used for measuring screen efficiency was imperfection (I). The partition curves were drawn and imperfection was calculated for each period using the equation below.

$$I = \frac{d_{75} - d_{25}}{2d_{50}} \qquad (1)$$

d_{25}, d_{50}, d_{75}: sizes at which 25, 50 and 75 % of feed reported to the coarse product, respectively

The performance of rod mills was examined by taking account of feed and product size distributions, Work Index of the ore, the dimensions of the mills and the powers of their drives.

The hydraulic classifier was symbolized by a series of simple separators having one feed and two product streams. This enabled the calculation of partition coefficients for each compartment. From the partition curve, imperfection, I, was calculated and used as an indicator of the quality of classification at different chambers.

Although ideally heavy liquid tests are required to assess the performance of gravity separators, performance evaluation of shaking tables was mainly based on their grade and recovery figures due to inavailability of high-density liquids. The length and frequency of stroke were also measured, whereas the measurement of wash water addition to tables was not possible.

PLANT PERFORMANCE

For the evaluation of plant performance, the design principles and methodology outlined by Ottley (1986) and Wells (1991). The design principles were found to be an excellent quide for both evaluating the existing flowsheet and proposing flowsheet modification. The methodology, however, could only be applied where the instrumentation and laboratory facilities permit its use.

The average grade of the feed was 41.90 % Cr_2O_3 with average flow rate of 10 t/h. The flow rate calculations of the remaining streams based on the measured flow rate of the feed. The flow rates and adjusted assays of main streams are presented at Table 1. The extend of data adjustment needed for mass balancing is illustrated in Figure 2.

Table 1. Mass flow rates and Cr_2O_3 assays of the main streams

stream →	plant feed	rod mill discharge	table feed	combined concentrates	combined tailings	overflow
weight (t/h)	10.00	4.84	11.60	7.47	2.53	0.23
Cr_2O_3 (%)	41.90	41.90	41.06	50.35	16.92	23.00

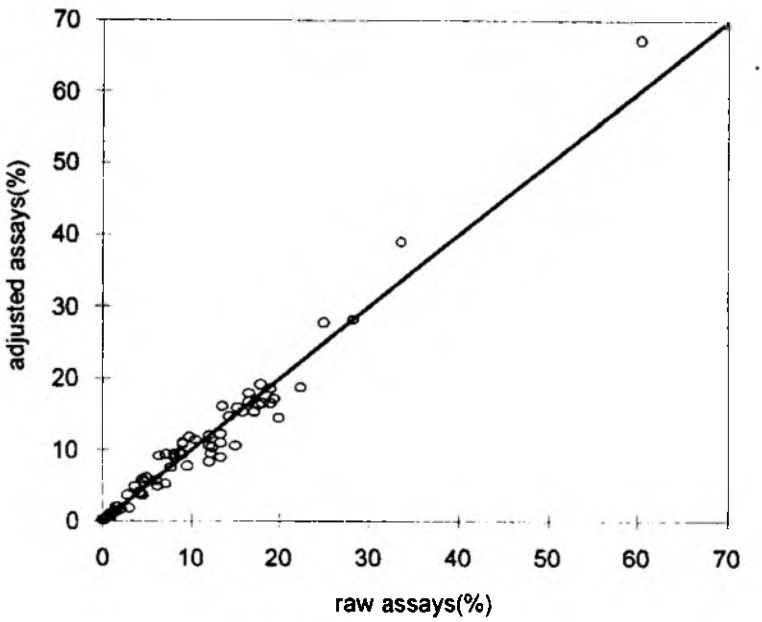

Figure 2. Raw vs adjusted assays

Partition curves of the screen for two sampling period are shown in Figure 3. The shape of the curves indicates screening operation was efficient. Imperfections and d_{50} values for the two sampling periods are presented at Table 2. These values also verify that screen was working properly. Significant difference between d_{50} values of the two periods aroused the question whether the screen aperture was different at each. Close examination of size distributions revealed that this was only due to the changes in feed size distribution.

Table 2. d_{50} and imperfection values of the screen

	period I	period II
d_{50}(μm)	2830	3813
Imperfection	0.226	0.189

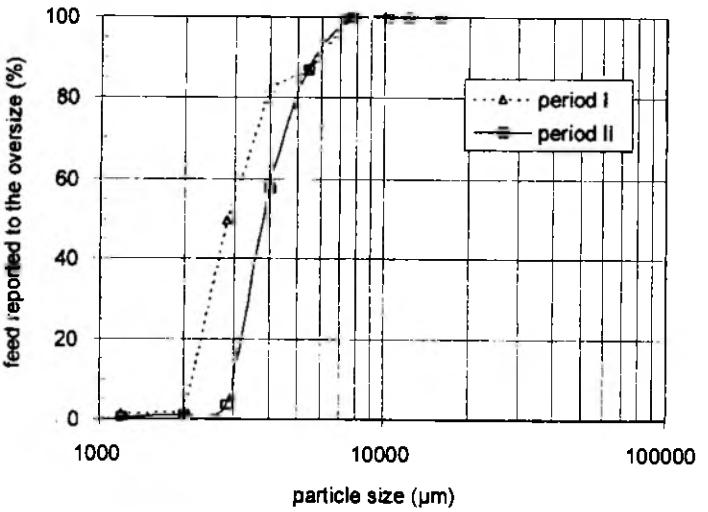

Figure 3. Partition curves of screen for two sampling periods

The partition curves for each hydraulic classifier compartment are presented in Figure 4. Imperfections and d_{50} values of each compartment are given at Table 3, excluding Compartment 5 whose product was finer than 100μm. Compared to the data available in the literature (Wells 1991; Burt 1984) both imperfections and d_{50} values indicate that the classification within hydraulic classifier was not efficient. d_{50} values are too close to each other and imperfections are too high. This was expected since the control system of the hydraulic classifier was not operational.

Table 3. d_{50} and imperfection values of hydraulic classifier compartments

	Compartment			
	1	2	3	4
d_{50}(μm)	330	135	125	80
Imperfection	0.58	1	0.76	0.72

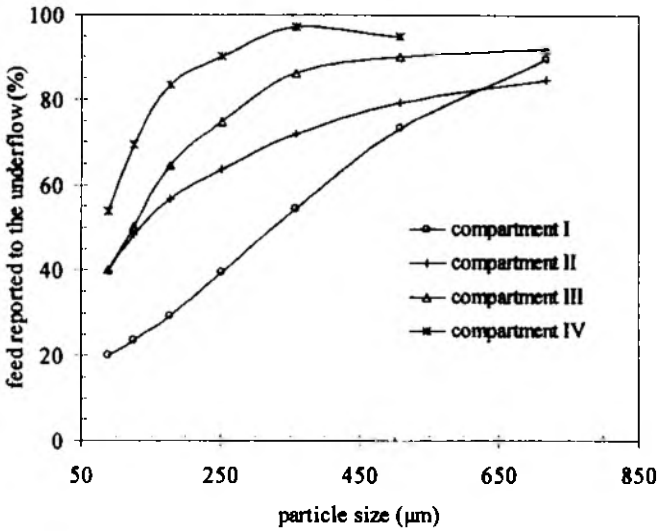

Figure 4. Partition curves of hydraulic classifier compartments

Variation of Cr_2O_3 contents with particle size for different chambers of hydraulic classifier are shown in Figure5. Preferential settling of chromite particles in the first chamber is clearly seen. This is also apparent in the second chamber, but in a much lesser extent. Since 95% of total Cr_2O_3 is in particles coarser than 74μm (Figure 6), very favourable metallurgical performance could be expected from tables treating the product of chamber I.

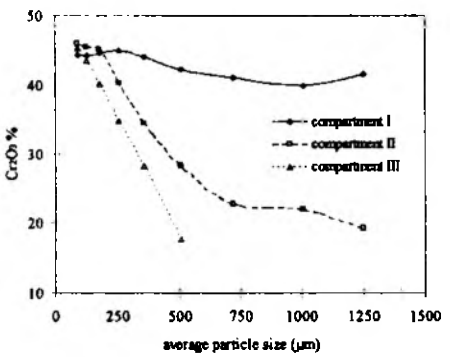

Figure 5. Variation of Cr_2O_3 contents with particle size at each compartment of hydraulic classifier

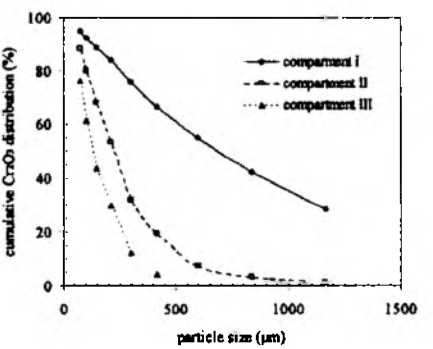

Figure 6. Variation of cumulative distribution of Cr_2O_3 with particle size at each compartment of hydraulic classifier

The properties and operating parameters of rod mills are presented at Table 4.

Table 4. Properties of rod mills and their operating parameters

	Rod Mill	Regrinding Mill
Diameter (cm)	91	61
Length (cm)	183	183
Rod Diameter (cm)	10	5
Number of Rods	36	28
Power (kW)	22	7.5
F_{80} (μm)	16470	865
P_{80} (μm)	1660	850

Feed and product size distributions of primary rod mill and regrinding rod mill for two sampling period are shown in Figure7 and Figure 8, respectively. Bond Work Index of the ore was determined to be 11.5 kWh/ton. From the available information, the following comments could be drawn:

a) Slime production is at acceptable levels.
b) The regrinding mill is not operating efficiently. The desired level of size reduction, 80% -0.42 mm, is not accomplished, despite the fact that only small fraction of available grinding power appears to be utilized. It is also arguable that a rod mill rather than a ball mill should be used for regrinding.

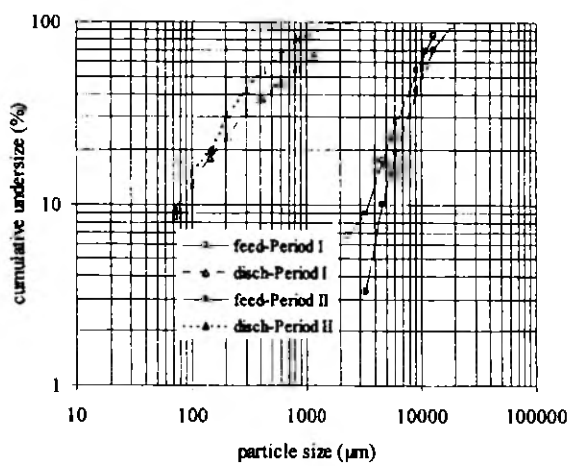

Figure 7. Particle size distributions of feed and discharge of primary rod mill

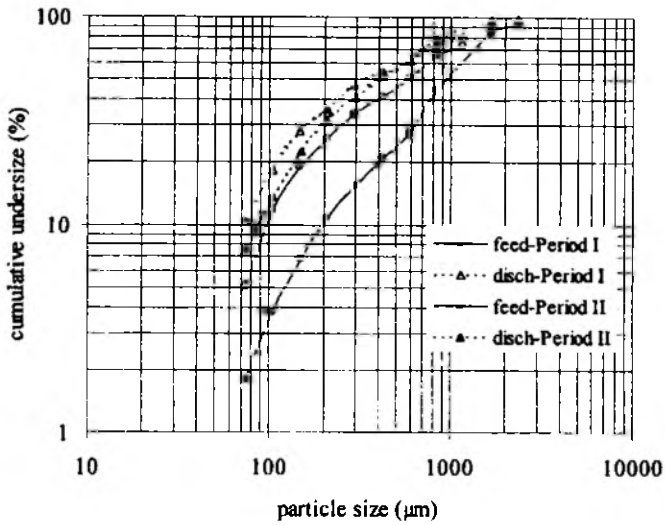

Figure 8. Particle size distributions of feed and discharge of regrinding mill

The performance values of shaking tables are presented at Table 5. The following conclusions were drawn:

a) While high grade concentrates with high recoveries were obtained from the first two sets of tables, the third, fourth and fifth sets did not perform so well both in terms of grade and recovery. However, the overall recovery and grade were satisfactory, mainly due to the fact that 87.8 % of total concentrates were recovered from the first set of tables.
b) The differences between the performance values of tables with and without middling product indicates that the performance of the third, fourth and fifth sets of tables could be improved by taking middlings from them and circulating directly to the cone classifier.
c) The measured capacities varied between 0.2 and 0.875t/h/deck indicating that, particularly at coarse size range the full capacity of tabling circuit is not utilized (Kelly et al. 1982, Burt 1984).
d) Microscopic examinations indicated that middlings are made of mainly liberated particles. Therefore, the necessity of regrinding was found to be questionable. The middling from the first set of tables may be combined with its concentrate. Then, the combined concentrate grade would only be reduced to 48.86 % Cr_2O_3. The circulation of middling from the second set of tables to cone classifier would be more suitable treatment for this product.

e) The length of stroke was varied between 30–60mm with frequencies between 160–180 rpm. They do not appear to be the suitable values for this type of operation (Burt 1984).

Table 5. Mass balance of tabling circuit

name of the product	Cr_2O_3 (%)	flow rate(t/h)	recovery (%)
the first set of shaking tables			
concentrate	51.30	5.31	84.01
tailing	11.30	0.53	1.85
middling	38.08	1.20	14.14
feed	46.02	7.04	100.00
the second set of shaking tables			
concentrate	50.00	1.25	76.49
tailing	11.10	0.69	9.33
middling	29.93	0.40	14.19
feed	34.96	2.34	100.00
the third set of shaking tables			
concentrate	42.60	0.61	75.25
tailing	19.40	0.44	24.75
feed	32.87	1.05	100.00
the fourth set of shaking tables			
concentrate	49.00	0.17	45.73
tailing	26.30	0.36	54.27
feed	33.37	0.53	100.00
the fifth set of shaking table			
concentrate	53.00	0.14	56.49
tailing	20.80	0.27	43.51
feed	31.67	0.41	100.00
overflow	23.00	0.23	1.28
combined middling	35.80	1.60	12.05
combined concentrate	50.35	7.47	89.79
combined tailing	16.92	2.53	10.21
feed	41.90	10.00	100.00

Liberation characteristics of the ore was also determined by examining closely sized fractions of the feed to shaking tables under a binocular microscope. The results showed that the ratio of liberated chromite particles decreased sharply above 2 mm.

Below this limit, they were mostly liberated, the degree of liberation for the coarsest fraction in this range is 75%. Although this confirmed that the level of grinding achieved in the rod mill was satisfactory, it indicated that the use of 6mm aperture screen, as opposed to 2mm in the original design, prior to rod milling was creating a detrimental effect for the concentration circuit.

Although an overall concentrate grade of 50.35 % Cr_2O_3 with 89.79 % recovery gives impression that the plant is operating well, it seems that even better performance could be achieved by proper adjustment of the operating parameters of hydraulic classifier and shaking tables. However, as pointed out earlier, the additional improvements in terms of efficiency criteria and, particularly, plant economics could be achieved by making some changes in plant flowsheet. For this purpose, three modifications were found to be worth of further investigation. They were:

- Changing 6 mm screen aperture to its original size of 2 mm. In this case, the amount of oversize material passing through the screen would be avoided, however the amount going to the primary rod mill would be increased.
- The necessity of regrinding is questionable. Although some oversize materials were fed to the tabling circuit, they did not report to middlings which were mostly formed by liberated particles. Therefore, the circulation of middlings to the cone classifier without regrinding could be suggested.
- Since shaking tables treating the coarsest fraction have large ample capacity(8–9t/h), it seems that the capacity of the plant could increased by operating two rod mills, i.e. primary and regrinding mills in parallel.

The second modification could only be tested in the plant, but the other two could be investigated by computer simulation. Simulation would have an additional benefit of investigating the effect of variations in capacity.

MODELLING OF SCREEN AND ROD MILL

Simulation studies concerned with screening and grinding units. Although mathematical models for hydraulic classifier (Mackie et.al 1987) and shaking table [Manser et.al 1986, Razali et.al 1990, Tucker et.al 1991, Manser et.al 1991) were available in the literature, since pulp solids contents of the products and water flow rates could not be measured, the use of these models had not been possible. The objective was to obtain a product size distribution suitable for achieving better concentration performance. Therefore, only the mathematical models of screening and rod mill grinding were required. The model developed by Whiten (1972) (Eq. 2), was used for modelling of screen. The model included another parameter (k_3) to define the

carryover of the fines with oversize material. The model parameters k_1 and f were considered constant within the range of feed flow rates to be investigated.

$$E(x)=\left(1-\left(\frac{h-x}{h+d}\right)^2\right)^m \tag{2}$$

$E(x)$, the probability that a particle of size x which does not pass through the screen in m trials, where $m = k_1^2 \ell . f$.

x – particle size
h – screen aperture
d – diameter of screen wire
k_1 – efficiency parameter
ℓ – length of screen
f – load factor in screen model (1 for normal operation)

The efficiency parameter, k_1, was calculated by using a non–linear regression algorithm. Since there was significant differences in the partition curves obtained from the two sampling periods, screen aperture was also considered as a variable and its best fit value calculated separately for each set of data. The estimated values for screen aperture were 5.81 and 5.84 mm with k_1 values of 2.46 and 2.56 respectively for the first and second periods. These values verified the earlier views that nominal screen aperture was 6 mm in both periods and screening efficiency was satisfactory (on average k_1 should have a value around 2.6). The parameters of the second period were used in further simulation work. For the rod milling, matrix model given by Lynch (1977) was used.

$$p=\prod_{j=0}^{j=v} T_j \,.\, f \tag{3}$$

where $T_j = (I-C)(B.S+I-S)[I-C(B.S+I-S)]^{-1} \,.\, f$

p: product vector; T_j: transition matrix; f: feed vector; v: number of breakage stages; I: unit matrix.

The model based on the selective breakage of the coarsest fraction. The mill is divided into imaginary compartments and the coarsest fraction entering a compartment will be completely broken down into the finer fractions. The model consists of three functions, namely classification, breakage and selection. Classification function (C) defines screening effect of the rods, breakage function (B) primary breakage distribution and selection function (S) the proportion of size fraction selected for breakage. For each compartment, the value of classification function for the coarsest size fraction was chosen as one. Breakage function is defined by Broadbent and Calcott equation (Lynch 1977) (Eq. 4):

$$B(x/y) = \frac{1 - e^{\left(\frac{-x}{y}\right)}}{1 - e^{-1}} \tag{4}$$

where y is the maximum particle size.

For the selection, a function defined by three parameters was used (Lynch 1994, Napier–Munn et al. 1996). This is illustrated in Figure 9. The number of coarsest fraction disappearing at the discharge of a mill is defined as the number of stages of breakage and this parameter is used in simulating the effect of feed rate on the product size distribution. The relationship is defined as mill constant and given below (Napier–Munn et al. 1996).

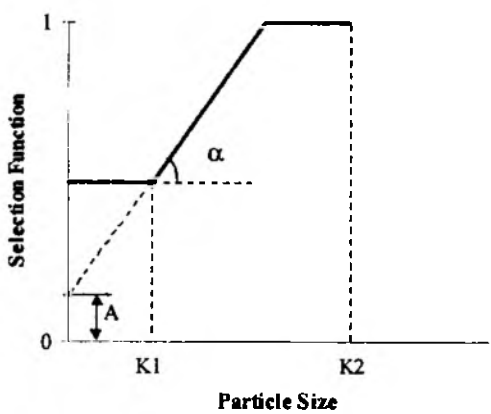

Figure 9. Schematic representation of selection function

$$(F.v)^{1.5}=MC \tag{5}$$

F – feed rate(t/h)
MC – mill constant
v – stages of breakage

For the simulation studies, calculation of three parameters of selection, and mill constant were required. A non–linear regression algorithm was used for this purpose. Both sets of data provided similar parameters and satisfactory fit to the data, and those of the second were used further studies.

Since regrinding rod mill was not operating efficiently, the use of data obtained its feed and product size distributions for the calculation of model parameters would be misleading. Then, model parameters of primary mill scaled down the using relationships developed at Julius Kruttschnitt Mineral Research Center of Australia (Napier–Munn et. al 1996). This approach provided reasonable simulation results. The expressions used for mill scaling, Eq. 6 and Eq. 7, are given below.

For scaling number of breakage stages, when feed rate and feed size distribution were changed.

$$v_{SIM} = \left(\frac{MC_{FIT}}{Feedrate_{SIM}}\right)^{2/3} + ln\left(\frac{F90_{FIT}}{F90_{SIM}}\right) / ln\sqrt{2} \tag{6}$$

Subscripts SIM and FIT denotes parameter values for simulated and fitted conditions respectively. For scaling the mill constant, for a mill of different dimensions and operating conditions:

$$\frac{MC_{SIM}}{MC_{FIT}} = \left(\frac{D_{SIM}}{D_{FIT}}\right)^{2.5} \cdot \left(\frac{L_{SIM}}{L_{FIT}}\right) \cdot \left(\frac{1-LF_{SIM}}{1-LF_{FIT}}\right) \cdot \left(\frac{LF_{SIM}}{LF_{FIT}}\right) \cdot \left(\frac{fCs_{SIM}}{fCs_{FIT}}\right) \tag{7}$$

where LF=mill load fraction (volume of mill occupied by charge and media after grinding out), fCs = mill speed (as fraction of critical speed).

The models for both screen and rod mill provided very good fit for the existing data and this is illustrated in Figure 10. However, it should be noted that fitting of rod mill model parameters requires some trial and error for initial estimates of the parameter values.

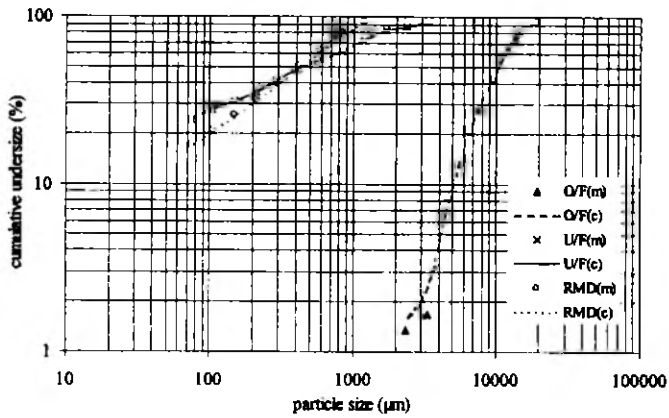

Figure 10. Model fits for screen and rod mill discharge (RMD);
(m and c refers to measured and calculated, respectively)

SIMULATION STUDIES

In simulation studies, the following three points were investigated:

i. The effect of changing screen aperture from 6 mm to 2 mm on the size distribution of circuit product.
ii. The limiting capacity for the plant.
iii. Possibility of using the two rod mills in parallel to increase grinding capacity for utilizing full capacity in the tabling circuit.

Separate house made computer programs were written for the simulation of each type of circuit configuration

Since the liberation size of chromite was around 2 mm and a product low in slimes was desired, the amounts of +2 mm and -74μm sized material in the circuit product were selected as main evaluation criteria. The effect of feed rate on product size was investigated in a range between 8 and 16t/h.

As expected, the results indicated that changing screen to its original aperture, 2 mm, would be beneficial in terms of the proportion of -2mm material in the circuit product (Figure 11), since there would always be some oversize material in the circuit product when 6 mm screen aperture was used. Screen aperture did not have any significant effect on the amount of slimes produced (Figure 12). Decreasing screen aperture to 2 mm results in an increase in the rod mill feed rate. Therefore, the rod mill discharge rapidly becomes coarser with the increase in feed rate. Independent of screen aperture, the fraction of +2 mm sharply increased with the plant feed rate

above 12 t/h. Since the fraction of slimes decreased with increased flow rate, it would be suggested that the plant should be operated with feed rate as high as possible.

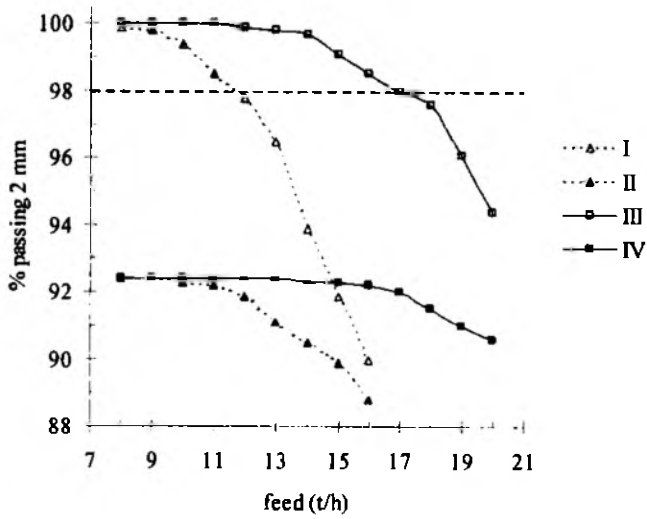

Figure 11. Variation of % passing 2 mm with the simulated plant feed rate(I and II for the primary rod mill with 2 and 6 mm screen apertures respectively;III and IV for the two mills in parallel with 2 and 6 mm screen apertures respectively)

Simulation results indicate that the optimum flow rate would be a good compromise between the two. Under these condition 98 % of the circuit product will be finer than 2 mm, when a screen with an aperture size of 2 mm is used. The same flow rate with a screening size of 6 mm would produce about 8 % oversized material. Such modification would also result in decreased middlings from tabling circuit. Before simulating the case with two mills in parallel, the ratio of rod mill circuit feed to be sent to the regrinding mill estimated by using the second period data so as to produce similar size distribution. It was found that the ratio should be 1 to 2.15.

Simulation studies were carried out with a feed rate ranging between 10–20 t/h. The results are summarized in Figure 11. It is shown that the capacity of the plant could be increased to 17 t/h. Above it, the proportion of oversize sharply increase. At this capacity, the amount of feed to the primary mill and regrinding mill would be 7.15 and 3.32 t/h, respectively. It should however be pointed out that running two mills in parallel increases the proportion of slimes and further deterioration in the performance of the hydraulic classifier is expected due to increased capacity (Wells

1991). Therefore, it would be recommended that they should only be used if the extra capacity created was fully utilized.

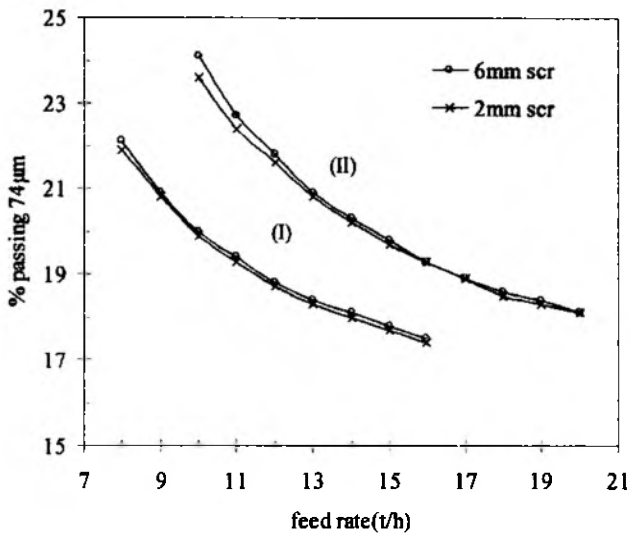

Figure 12. Variation of % passing 74 µm with the simulated plant feed rate
(I the primary mill only; II the two mills in parallel)

CONCLUSIONS

The performance evaluation study carried out at Sori Plant indicated that hydraulic classifier, shaking tables and regrinding rod mill were not operating properly, despite of the fact that a concentrate of 50.35 % Cr_2O_3 with recovery of 89.79 % was produced. It was also found that the full capacity of tabling circuit was not utilized.

Simulation studies indicated that the plant performance could be improved and the capacity could be increased by making some modification in the plant flowsheet only.

It is also shown that modern tools such as mathematical models and computer simulations could be used under the circumstances experienced in a plant with a very limited measuring and control devices. It appears that proper sampling is the key for success. It should however be coupled with detailed and accurate laboratory studies.

REFERENCES

BURT R.O. (1984), *The shaking table*. Chapter 14 in Gravity Concentration Technology, Elsevier Science Publishers B.V., Amsterdam, 288–316.

CARPENTER B.H. and SWEENY H.C. (1965), *Process improvement with "Simplex" self-directing evolutionary operation*. Chem. Engng., July, 117–126.

HODOUIN D. and EVERELL M.D. (1980), *A hierarchical procedure for adjustment and material balancing of mineral processes data*. Int.J. Min.Pro., 7, 91–116.

KELLY E.G. and SPOTTISWOOD D.J. (1982), *Introduction to Mineral Processing*, John Wiley&Sons, p252.

LYNCH A.J. (1994), *Design, Optimization and Simulation of Mineral Processing and Coal Preparation Plants*, Seminar notes, 14–16th Nov., Istanbul–Turkey.

LYNCH A.J. (1977), *Mineral Crushing and Grinding Circuits*, Elsevier Scientific Publishing Co., Amsterdam, 51–60.

MACKIE R.I., TUCKER P., WELLS A. (1987), *Mathematical model of the Stokes hydrosizer*.Trans. Instn.Min.Metall.Sect.C., 96,130–136.

MANSER R.J., BARLEY R.W., WILLS B.A. (1986), *Development of a mathematical model of a shaking table concentrator*, Chapter 57 in 19th APCOM Symposium, ed. R.V. Ramani, SME, 631–636.

MANSER R.J., BARLEY R.W., WILLS B.A. (1991), *The shaking table concentrator– The influence of operating conditions and table parameters on mineral separation– The development of a mathematical model for normal operating conditions*, Minerals Eng., 4 (3/4), 369–381.

NAPIER–MUNN T.J., MORREL S., MORRISON R.D., KOJOVIC T. (1996), *Rod mills*, Chapter 8 in Mineral Comminution Circuits: Their Operation and Optimisation. JKMRC, 192–205.

OTTLEY D.J. (1986), *Gravity concentration in modern mineral processing*, Proc. of the NATO Advanced Study Institute on Mineral Processing, Falmouth, UK, 317–338.

RAZALI R., VEASEY T.J. (1990), *Statistical modelling of a shaking table separator–Part one*. Minerals Eng., 3 (3/4), 287–294.

RICHARDSON J.M. and MULAR A.L. (1987), *Metallurgical balances*, in Design and Installation of Concentration and Dewatering Circuits. eds. M.A. Anderson and A.L. Mular, AIME, 607–632.

TUCKER P., LEWIS K.A., WOOD, P. (1991), *Computer optimisation of a shaking table*, Minerals Eng., 4 (3/4), 355–367.

WELLS A. (1991), *Some Experiences in the design and optimization of fine gravity concentration circuits*. Minerals Eng., 4 (3/4), 383–398.

WHITEN W.J. (1972), *The simulation of crushing plants with models developed using multiple spline regression*. J.S.Afr.Inst.Min.Metall., May, 257–264.

Levent Ergun, Salih Ersayin, Ocena pracy niskotonażowego wzbogacania grawitacyjnego, *Fizykochemiczne Problemy Mineralurgii*, 34, 111–131 (w jęz angielskim)

W pracy przedstawiono wyniki badań dotyczące zakładu wzbogacania chromitu. Zakład nie jest wyposażony w aparaturę kontrolno–pomiarową. Dlatego ocena wzbogacania jest trudna i wymaga specjalnej metodologii. Badania rozpoczęto od opróbowania procesu, a tygodniowe pobieranie próbprzeprowadzono dwa razy. Po szczegółowej ocenie danych dotyczących procesu zaproponowano kilka modyfikacji, np.: zmiana rozmiaru sit z 6 do 2 mm, ograniczenie zdolności produkcyjnejoraz zastosowanie dwóch młynó prętowych ustawionych równolegle. Następnie zbadano wpływ tych zmian na pracę zakładu, dzięki symulacji komputerowej. Wyniki wzbogacania oraz przerób ulegną zwiększeniu po zastosowaniu proponowanych zmian.

Physicochemical Problems of Mineral Processing, 34 (2000), 133–140
Fizykochemiczne Problemy Mineralurgii, 34 (2000), 133–140

Mehmet YILDIRIM*

LEACHING AND CEMENTATION OF THE SULPHATING ROASTED LOW GRADE ERGANI COPPER ORE

Received March 15, 2000; reviewed and accepted May 15, 2000

Leach-cementation operations were applied to produce impure copper from the sulphating roasted ore. Effect of acid concentration and temperature on the extraction of copper from the ore into the leaching solution were studied. The cementation tests were conducted with two different stirring devices. One, mild steel disc and the second a propeller. The mild steel disc was used to provide a uniformly accessible surface for the kinetic study of cementation of copper with iron in sulphate solution.

Key words: leaching, cementation, copper ore

INTRODUCTION

High grade sulphide copper ores have been usually processed pyrometallurgically. However, in the past two decades, in order to eliminate emissions of sulphur dioxide, other approaches have been extensively investigated on both laboratory and pilot plant scales. Eventually, hydrometallurgy emerged as a very promising alternative technology for recovering of copper from the low grade sulphide ores.

The ore used in this study was taken from the low grade Ergani copper deposit that has 1,5 million tons of partly oxidized sulphide ore containing about 1–3% Cu (Canbazoglu, Cebeci and Kahriman, 1992). The ore was roasted to produce material

* Cukurova University, Mining Engineering Department, 01330, Balcalı, Adana, Turkey.

which can be readily leached in a diluted sulphuric acid solution. The conditions of roasting of the ore are given by Yildirim (1980). This paper now presents the result on treatment of the roasted low grade Ergani copper ore sample by leach- cementation operations.

MATERIALS AND METHODS

The original ore sample (unroasted) contains mainly FeS_2, $CuFeS_2$, ZnS, FeS and PbS while gangue minerals are chlorides and silicates. The ore was roasted at 575 ^{0}C in air for one hour. Particle size of the samples of the roasted ore used in the leaching experiments was (-147+44) microns. Contents of the basic components of the roasted ore are shown in Table 1.

Table 1. Chemical analysis results of the roasted ore

Elements	Weight (%)
Cu	1.48
Fe	29.66
Zn	0.22
Pb	0.28
S	10.50
Si	41. 78

Perkin- Elmer 303 Atomic Absorption Spectrophotometer (AAS) was used to determine the copper and iron concentrations in the examined solutions. Particle size of the iron powder used for cementation was within the range of one micron. Its composition was 95% Fe, 0,02% N, 0,001% As and 2% acid insoluble matter.

The absorbance readings from the AAS were treated with a programmable Hewlett Packard desk calculator. This led to the direct copper and iron recoveries. The effect of different variables on the leaching of copper were studied.

Acid concentration. Twelve grams of the ore was leached in 40 ml (0,3 gr/ml) of the sulphuric acid solutions 5% to 45%. Tests were carried out at ambient temperature (20^0 C) for 30 minutes. The wrist shaker was used for the agitation. After completion the leaching, the liquor was filtered and adequate amount of the filtrate was diluted up to 250 ml for the AAS analysis. The remaining acidic solution was used for titration with sodium hydroxide and methyl red. More concentrated acid solutions were diluted with distilled water prior to the titration. The results of the titration and the AAS are shown in Figures 1 and 2 respectively.

Temperature. Forty-eight grams of the ore was leached in 160 ml of the 15% sulphuric acid solution at temperatures varying from 30^0 to 70^0 C. Temperature was controlled and maintained at defined level with a water bath. The results of experiments are shown in Figure 3.

Cementation tests. Two different stirring devices (mild disc and propeller) were applied to make comparison. The tests were conducted at various concentrations of (Cu^{2+}), at constant temperature of 20° C, and for 20 minutes each. Concentrations of (Cu^{2+}) were changed from 0,05 to 0,4 gr/l for the both mixing mechanisms. At the end of the each tests, concentrations of (Cu^{2+}) were determined with AAS. The results are shown in Figure 4.

The use of mild disc. The steel rod between the disc and the main body of the stirrer was covered by a plastic pipe (Figure 1) in order to prevent the contact between the rod and the solution. After immersing the disc into the solution (400 ml) for cementation the stirring began at rate 800 rpm. After completion of the experiment the disc was removed from the solution and immersed into the acid solution to disvolve the cemented copper from the disc.

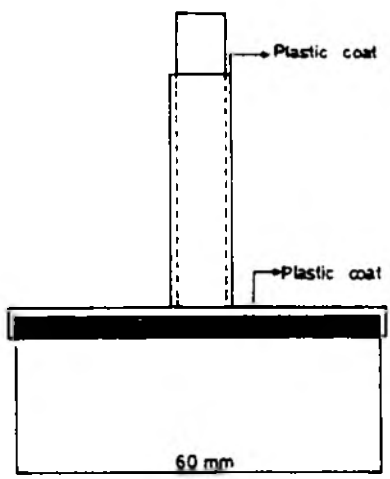

Fig. 1. Illustration of the disc

The use of propeller and iron powder. The same tests were repeated with iron powder introduced to the solution. Then the plastic covered rod with a propeller was used to mix the cementation mixture. No copper coverage on the propeller was observed.

RESULTS AND DISCUSSIONS

Consumption of acid during leaching of the ore studied at varying concentrations of acid is shown in Figure 2. The possible explanation of observed dependence is that the diluted acid preferentially attacks the more soluble copper and iron while the stronger acid attacks all of the species present in the ore.

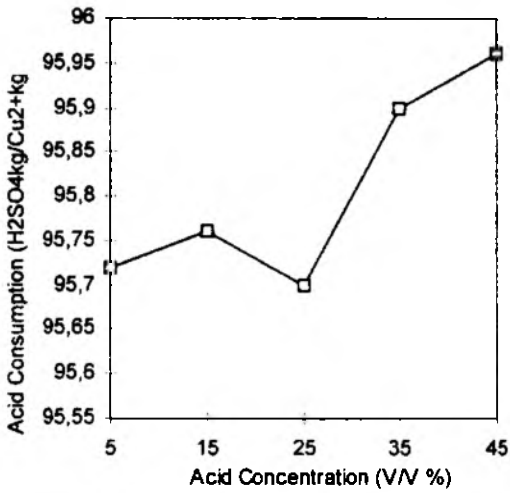

Fig. 2. Acid consumption against acid concentration

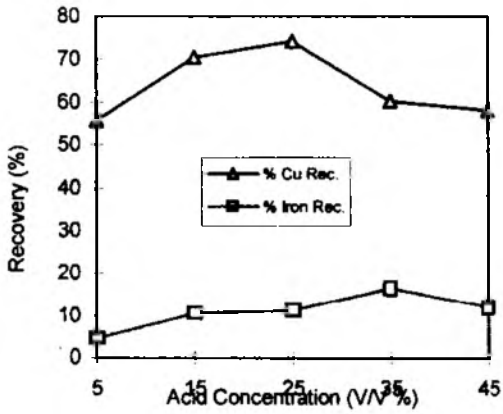

Fig. 3. Effect of the acid concentration on the leaching

However, Figure 3 shows that the copper recoveries are high throughout while the iron recoveries changes in the expected manner, i.e. the stronger the acid the larger the amount of leached iron. Copper recoveries in dilute acids might be more attributable to the temperature in contrary to the case of the stronger acids. Acid consumption results seem to reveal that the use of low acid concentration in beneficial.

An improvement in copper recovery is advisable at elevated temperatures (Figure 4). The amount of iron extracted increases too. High concentration of iron in the solution causes severe problems in solvent extraction process which would be ideal for concentrating copper prior to electrowinning. The following reactions involve the recovering of copper from the acidic solutions by cementation with iron (Biswas, 1972; Tilyard, 1973).

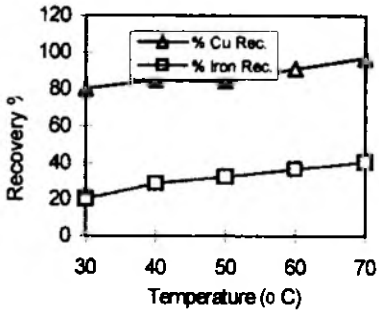

Fig. 4. Effect of the temperature on copper and iron recovery

$$Cu^{2+} + Fe^{0} \rightarrow Cu^{0} + Fe^{2+} \quad \Delta E^{0} = +777\ V \quad (1)$$

$$Fe^{0} \rightarrow Fe^{2+} + 2e \rightarrow \quad E_1^{0} = +0{,}440\ V \quad (2)$$

$$Cu^{2+} + 2e \rightarrow Cu^{0} \rightarrow \quad E_2^{0} = +0{,}337\ V \quad (3)$$

According to reaction (1) one mole of Fe precipitates one mole copper. This means that 0,88 kg iron is necessary to precipitate 1 kg of copper. Iron consumed in the practical operations is 2-3 times greater (Biswas, 1980).

Cementation tests were carried out in solutions at varying initial $CuSO_4$ concentrations. The percent recoveries of Cu increases with the decrease of copper concentrations (Fig 5). This was apparently caused by extremely rapid rates of copper precipitation at high solution concentrations, resulting in the formation of an almost impenetrable dense copper deposit on the steel disc. On the other hand, at high solution concentrations of copper, deposition of the cemented copper on the iron particles mixed with propeller caused low copper recoveries. However, as the concentration of copper decreases this effect ceases and therefore, the high copper recoveries are obtained.

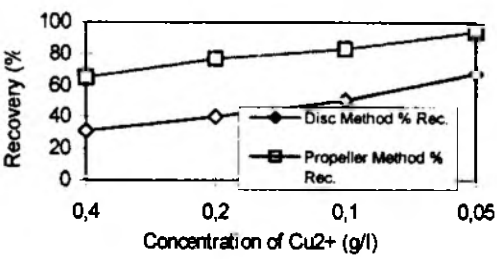

Fig. 5. Result of the cementation tests using the disc and propeller methods

The majority of previous investigations on cementation involved flow systems which were rather difficult to analyse allowing to interpret the data obtained qualitatively. Therefore, we chose the rotating disc by following Levich (1962) to provide information about the rate and activation energy. Effect of possible side reactions resulted from the presence of oxygen in the system were not considered.

Apparent rate constants of cementation in the experiments with mild steel disc were calculated for the each temperature using the heterogeneous first order rate equation. This equation may be written after Strickland and Lawson (1970) as follows:

$$J = kC \quad (4)$$

where, J–apparent mass flux based on the initial exposed precipitant area (kg $m^{-2}sec^{1}$), k–rate constant (m sec^{-1}), c–bulk concentration of (Cu^{+2}) ions at time t (kg m^{-3}).

The rate constants of cementation at varying temperatures are shown in Table 2.

Table 2. Rate constants of copper cementation at different temperatures

T (^{0}C)	(1/T)*10^3 (K^{-1})	k*10^{-2} (cm.min^{-1})	logk (-)	% Rec. (Cu^0/Cu^{2+}) *100
20	3.41	5.36	1.27	60.00
40	3.19	28.34	0.55	90.95
60	3.00	44.60	0.35	93.72
80	2.80	64.00	0.19	97.75

A – Frequency factor,
E – Activation energy (cal mole^{-1} K^{-1}),
R – the gas contant (1.987 kcal mole^{-1} K^{-1})
T – the present temperature
The equation (5) could be written as follows:

$$\log k = E/R \log_e(1/T) + \log A \quad (5)$$

It represents the plot in Figure 6 and its slope is: (logk)/ (-E/Rloge (1/T)), i.e., 0.90/ 1.50. Thus, the activation energy (E) equals to 2.747 (kcal mole^{-1} K^{-1}). Activation energy of this magnitude remains in a close agreement with the experimental values of other works.

CONCLUSIONS

High copper recoveries were achieved in the leaching test of studied ore with aqueous sulphuric acid. Therefore, extraction of the copper was efficient which indicates that required surface area of the particles for the leaching reactions is reached with applied granulation of ore. Copper present in the ore was readily soluble due to the roasting and leaching with the weakly acidic solutions. The leaching for 30 minutes was sufficient so that higher recoveries of copper can be reached only at elevated temperatures.

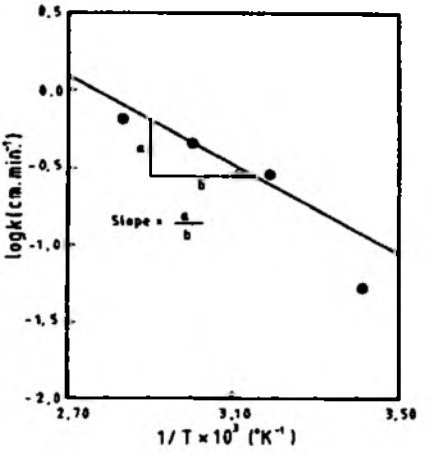

Fig. 6. Arrhenius plot for cementation of copper with iron (mixing device mild disc)

Better results of cementation of copper for the leach solutions were obtained at lower concentrations of solutions at room temperature. From comparison of the two different cementation systems, it might be concluded that the propeller method was more efficient than the steel disc. The first method gives an impure product. The copper cementation deposition rate per initial unit area of iron increases with increasing temperature. This rate depends on hydrodynamic conditions and viscosity of the solution.

REFERENCES

BISWAS, A. K. and J. G. REID (1972), *Investigation of the Cementation Copper on Iron,* Proc. Aust. Min. Met. No. 242, pp 37- 45.

BISWAS, A. K. and DAVENPORT, W. G.,(1980), *Extractive Metallurgy of Copper,* Pergamon Press, Oxford.

CANBAZOĞLU, M. ,CEBECİ, Y and KAHRIMAN, A. ,(1972), *Cementation of Copper from Leach Solutions and Cone Design.* 4th, Int. Min. Processing Symposium in Turkey, Proceedings, Vol. 2, pp 710- 719.

SHIRTS, M. B., et. al., (1975), *Double Roast- Leach- Electrowinning Process for Chalcopyrite Concentrates,* U.S. Bureau of Mines, RI 7996

STRICKLAND, P.H. and LAWSON F., (1970), *Cementation of Copper with Zinc from Dilute Aqueous Solutions,* Proc. Aust. Inst. Min. Met. No. 236 Dec.

TILYARD, P.,(1973), *Copper Cementation and Its Application in the Leach Precipitation Flotation Process,* Min. Sci. Eng. 5, pp 192- 206.

WOODCOCK, J.T., (1967), *Copper Waste Dump Leaching,* Aust. I.M.M. Proc. No. 277, pp 47-65.

YILDIRIM, M., (1980), *A study of Processing of a Low Grade Copper Ore by a Roast- Leach-Cementation Process,* M.Sc. Project, Dept. Min. Eng., Birmingham University, U. K.

Mehmet Yildirim, Ługowanie i cementacja prażonej siarczanująco rudy z Ergami o niskiej zawartości miedzi, *Fizykochemiczne Problemy Mineralurgii*, 34, 133–140 (w jęz. angielskim)

Zastosowano ługowanie i cementację do otrzymywania miedzi po prażeniu siarczanizującym rudy. Badano wpływ stężenia kwasu i temperatury na proces ekstrakcji. Cementację przeprowadzono w dwóch różnych urządzeniach mieszających tj. stalowym mieszadłem dyskowym oraz śmigłowym. Zastosowane mieszadło dyskowe zapewniło jednorodną powierzchnię do badania kinetyki cementacji Cu za pomocą Fe w roztworach siarczanowych.

Fizykochemiczne Problemy Mineralurgii, 34 (2000), 141–151

Cezary KOZŁOWSKI*, Małgorzata ULEWICZ*, Władysław WALKOWIAK**

SEPARATION OF ZINC AND CADMIUM IONS FROM AQUEOUS CHLORIDE SOLUTIONS BY ION FLOTATION AND LIQUID MEMBRANES

Received March 15, 2000; reviewed and accepted May 15, 2000

An experimental investigation is presented on zinc(II) and cadmium(II) ions separation from aqueous chloride solutions, containing equimolar mixture of both metals ions, by ion flotation (IF) and polymer inclusion membrane (PIM) processes. The IF experiments from dilute aqueous chloride solutions ($c_{Me} = 1 \cdot 10^{-5}$ M) with an anionic surfactant (sodium dodecylbenzene sulfonate) and a cationic surfactant (cetylpyridinium chloride) are shown. With a cationic surfactant, the flotation separation of Cd/Zn grows with Cl^- concentration increase. In addition, a selective transport of Zn(II) and Cd(II) from aqueous chloride source phase ($c_{Me} = 1 \cdot 10^{-3}$ M) through PIM containing cellulose triacetate (support), o-nitrophenyl pentyl ether (plasticizer) and tri-n-octylamine (ion carrier) is shown. The transport selectivity of Cd/Zn is decreasing with HCl concentration increase in source phase. In both studied separation methods zinc(II) and cadmium(II) are removed from an aqueous chloride solution in the form of $ZnCl_3^- + ZnCl_4^{2-}$ and $CdCl_3^- + CdCl_4^{2-}$, respectively. Results are discussed in terms of the stability of chloride complex species for zinc(II) and cadmium(II).

Key words: ion flotation, polymer inclusion membranes, zinc, cadmium

* Department of Chemistry, Technical University of Częstochowa, Poland
** Institute of Inorganic Chemistry and Metallurgy of Rare Elements, Wrocław University of Technology, Poland

INTRODUCTION

Selective separation of heavy metal ions from industrial and waste aqueous solutions is frequently required in hydrometallurgical processes (Davies 1987). In such technological processes, as CLEAR (Ochs et al. 1983) or EZINEX (Diaz et al. 1995) chloride solutions are used as aqueous leaching liquors and as the result those solutions contain zinc and cadmium chloride complexes. There are several methods of metal ions separation from aqueous solutions, i.e. solvent extraction, ion exchange, sorption, flotation methods, and liquid membranes (Davies 1987).

An effective and simple method of metal ions concentration and separation from dilute aqueous solutions ($c_{Me} \leq 1 \cdot 10^{-4}$ M) is an ion flotation, which involves the removal of surface inactive ions from aqueous solutions by the introduction of an ionic surfactant (called collector) and the subsequent passage of gas bubbles through the solution (Lemlich 1972). The selectivity of cationic surfactants for anions has been established in several ion flotation experiments including oxyanions of Re(VI), Mo(VI), W(VI), Cr(VI), and V(V) (Grieves and Charewicz 1974), cyanide metal complexes of Zn(II), Cd(II), Hg(II), Pd(II), and Pt(IV) (Walkowiak et al. 1976; Walkowiak 1992). Removal of zinc (II) in the presence of chlorides by ion flotation with cationic collector was also investigated by Jurkiewicz (Jurkiewicz 1990) as well as by Hualing and Zhide (Hualing and Zhide 1989).

The use of liquid membranes containing ion carriers offers as an alternative to solvent extraction for selective separation and concentration of metal ions from source aqueous phase, in which the concentration of metal ionic species is $> 1 \cdot 10^{-4}$ M. A variety of types of liquid membranes exits, i.e. bulk (BLM), emulsion (ELM) and supported (SLM) membranes (Bartsch and Way 1996). Moderate success in metal ion species separations with SLM was achieved using a porous polymer film, such Celgard or Accurel, and an organic solution of an ion carrier. On the other hand, a common problem for this system is loss of the carrier and membrane solvent to the contacting aqueous phases, which limits the long-term integrity of the membranes. Recently, a new type of membrane system, called polymer inclusion membranes (PIMs), has been developed which provides metal ion transport with high selectivity, as well as easy setup and operation (Sugiura et al. 1987). Casting cellulose triacetate from a solution to form a thin film forms the PIMs. The casting solution also contains a membrane plasticizer and an ion-exchange carrier. Since these membranes do not utilize an organic solvent to maintain this phase separation, PIMs are simpler to use than SLMs, and do not suffer from loss of the organic solvent. There are few papers, which deals with cadmium(II) removal and cadmium(II) over zinc(II) separation by supported liquid membranes. Breembroek et al. (1998) has reported on cadmium extraction through a flat sheet and hollow fiber supported liquid membranes using tertiary amines as ion carriers. Also Urtiga and Ortiz (1999) studied cadmium removal

from aqueous phosphoric acid by SLM. The separation of cadmium(II) from zinc(II) chloride media by a supported liquid membrane using quaternary ammonium salts as ion carriers was reported by Danesi et al. (1983) and Hoh et al. (1990). The only two papers on removal of cadmium(II) from chloride aqueous solutions by polymer inclusion membranes were published by Hayashita (1996).

Present work deals with the separation of zinc(II) and cadmium(II) metal ionic species from chloride aqueous solutions containing equimolar mixture of both metals by ion flotation ($c_{Me} = 1 \cdot 10^{-5}$ M) and polymer inclusion membranes ($c_{Me} = 1 \cdot 10^{-3}$ M).

EXPERIMENTAL

Ion flotation

The ion flotation experiments were carried out in a glass column 45.7 cm in high and 2.4 cm in diameter. Nitrogen gas was saturated with water and the flow rate was maintained at 12 cm^3/min. through a sintered sparger of 20–30 μm nominal porosity. The volume of each initial aqueous solution, prior to ion flotation, was 100 cm^3, and the temperature was maintained at 22 ± 2 ^{0}C.

The initial aqueous solutions were prepared with double distilled water and the salts $ZnCl_2$, $CdCl_2$, NaCl, HCl (all from POCh Gliwice, reagents of analytical grade). The surfactants, i.e. sodium dodecylbenzene sulfonate (DDBSNa) and cetylpyridinium chloride (CPCl), as analytical reagent grade, were utilized as 0.05 M standard solutions in water. The surfactants concentrations in the initial solutions were kept constant at $2.0 \cdot 10^{-4}$ M throughout this investigation. The gamma radioactive isotopes, i.e. Zn-65 and Cd-115m, were in the form of chloride acidic solution (0.1 M HCl). They were of sufficiently low specific activity to neglect the effect of carrier concentration (Zn-65: 9.2 GBq/g, Cd-115m: 2.2 GBq/g). These isotopes were from the Atomic Energy Institute (Świerk).

The time dependence of zinc(II) and cadmium(II) concentrations in the bulk solution (c) was recorded continuously during each ion flotation run by means of radioactive analytical tracer, and gamma radiation spectrometry, following a procedure described previously (Walkowiak and Ulewicz 1999). A single channel, gamma radiation spectrometer was applied as the detector of radioactive intensity of specific energy. The c versus time curves enabled the calculation of the percent removal (M):

$$M = [1 - (c_r/c_i)] \cdot 100\% \qquad (1)$$

where c_i is the initial metal concentration, c_r is the metal concentration in residual solution after foam ceased. Also selectivity coefficients (S) of Cd(II) over Zn(II) was calculated:

$$S_{Cd(II)/Zn(II)} = M_{Cd(II)}/M_{Zn(II)} \quad (2)$$

Polymer inclusion membranes

A solution of cellulose triacetate (as the support), tri-n-octylamine (as the ion carrier), and o-nitrophenyl pentyl ether (as the plasticizer) in dichloromethane was prepared. A portion of this organic solution was poured into a membrane mold comprised of a 9.0 cm glass ring attached to a plate glass with cellulose triacetate - dichloromethane glue. Dichloromethane, as the organic solvent, was allowed to evaporate overnight and the resultant polymer inclusion membrane was separated from the glass plate by immersion in water. The membrane was stored in water. Content of membrane (in weight percents) was: CTA - 41%, o-nitrophenyl pentyl ether - 37%, and TOA - 22%. The concentration of TOA was 1.28 M based on plasticizer.

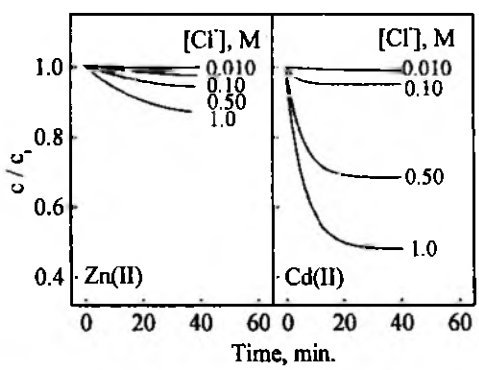

Fig. 1. Rate curves of zinc(II) and cadmium(II) concentration vs. time from aqueous solution containing equimolar mixture of both metals ($c_{Me} = 1.0 \cdot 10^{-5}$ M) in presence of chlorides with DDBSNa ($c_{surf.} = 2.0 \cdot 10^{-4}$ M)

Transport experiments were conducted in a permeation cell in which the membrane film (at surface area of 4.9 cm^3) was tightly clamped between two cell compartments. Both, i.e. the source and receiving aqueous phases (45 cm^3 each), were mechanically stirred at 600 rpm. The receiving phase was 0.10 M aqueous solution of ammonium acetate. The PIM transport experiments were carried out at the same temperature as IF

runs. Small samples (0.1 cm^3 each) of the aqueous receiving phase were removed periodically via a sampling port with a syringe and analyzed to determine zinc and cadmium concentrations by atomic absorption spectroscopy method (AAS Spectrometer, Solaar 939, Unicam).

The inorganic chemicals, their purity, and producer were the same as in ion flotation experiments. The organic chemicals, i.e. cellulose triacetate (Fluka), tri-n-octylamine (Serva), o-nitrophenyl pentyl ether (Fluka), and dichloromethane (POCh) were of analytical reagent grade. The percent removal and selectivity coefficients were calculated according to equations (1) and (2) in which c_i and c_r are the initial and residual metal concentrations in the aqueous source phase.

RESULTS AND DISCUSSION

First, the competitive ion flotations were studied to determine the chloride ions influence on flotation kinetic of both metals using an anionic (Fig. 1) and a cationic (Fig. 2) surfactant.

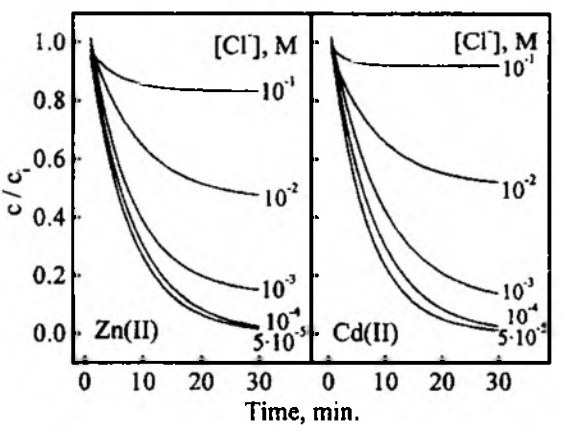

Fig. 2. Rate curves for competitive ion flotation of zinc(II) and cadmium(II) (c_{Me} = $1.0 \cdot 10^{-5}$ M) in presence of chlorides with CPCl (c_{surf} = $2.0 \cdot 10^{-4}$ M)

According to Fig. 1, with the increase of chlorides concentration rate and removal of both floated ions, i.e. zinc(II) and cadmium(II), decrease. At concentration of chloride ions equal to 0.10 M, percent removal of zinc and cadmium reaches 17 %, and 10 %, respectively. Contrary influence of chloride concentration on competitive ion flotation of zinc and cadmium is observed using a cationic surfactant, i.e. CPCl

(Fig. 2). In this case both flotation rate and percent removal of Zn(II) and Cd(II) increase with Cl^- concentration increase and partial separation of cadmium over zinc is observed (Fig. 3).

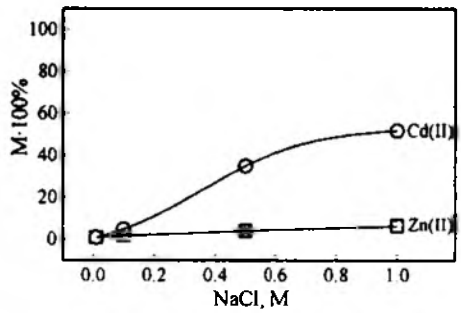

Fig. 3. Percent removal of zinc(II) and cadmium(II) in competitive ion flotation from aqueous solutions containing equimolar mixture of both metals vs. chlorides concentration. Conditions as in Fig. 2

The percent removal of cadmium(II) grows much faster than zinc(II) with chloride concentration increase.

Next, the competitive transport of zinc(II) and cadmium(II) ions from aqueous source phase ($c_{Me} = 1.0 \cdot 10^{-3}$ M) containing chlorides through polymer inclusion membranes into receiving aqueous phase was investigated. The kinetics of zinc(II) and cadmium(II) ions transport through PIM from aqueous source phase containing equimolar mixture of both metals is shown in Fig. 4.

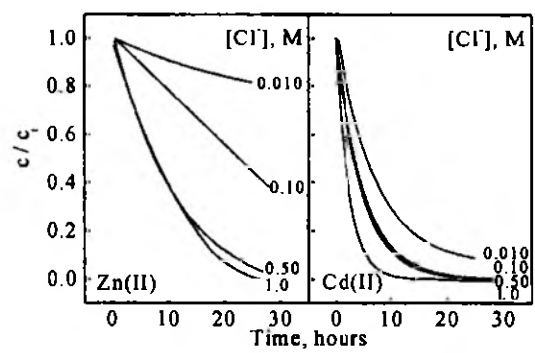

Fig. 4. Kinetics of zinc(II) and cadmium(II) transport through PIM from source aqueous phase ($c_{Me} = 1.0 \cdot 10^{-3}$ M) at different HCl concentrations

Comparison of both processes kinetics, i.e. IF and PIM (Figs. 2 and 4) shows that transport through polymer inclusion membranes is much slower than ion flotation of adequate metals, and it takes from 5 to 30 hours to remove more than 90 % of cadmium from source aqueous phase. Similarly to IF, in case of PIM transport of cadmium(II) goes faster than zinc(II). The dependence of percent removal of zinc(II) and cadmium(II) ions from a source aqueous phase as a function of HCl concentration for PIM is presented in Fig. 5.

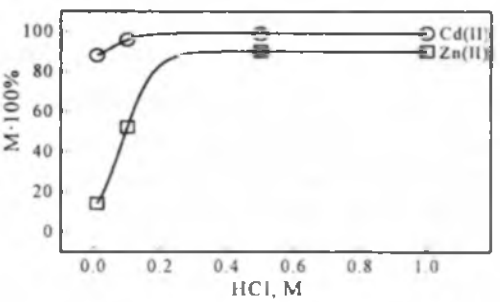

Fig. 5. Percent removal of zinc(II) and cadmium(II) ions from source aqueous phase containing equimolar mixture of both metals (c_{Me} = 1.0·10^{-3} M) vs. HCl concentration in source phase

Fig. 5 shows that the percent removal of both metals is increasing with HCl concentration increase and at acid concentration ≥ 0.5 M remains stable. This causes that separation of Cd/Zn coefficient is the highest for low concentrations of chlorides, i.e. 0.010 M.

To compare the separation of cadmium(II) over zinc(II) in ion flotation and in polymer inclusion membrane processes the bar plots of Cd/Zn separation coefficients are presented in Fig.6.

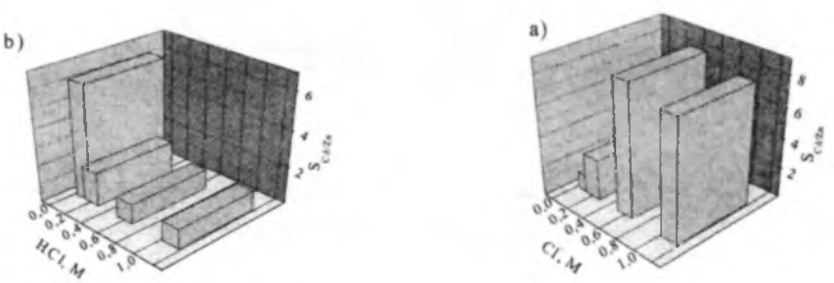

Fig. 6. Bar plots of Cd/Zn separation coefficients vs. chloride concentration in ion flotation (a), and polymer inclusion membrane (b) processes (conditions as in Figs. 3 and 5, respectively)

As it comes from this figure dependence of separation coefficients of Cd/Zn versus Cl^- concentration for both processes is different. For ion flotation, values $S_{Cd/Zn}$ are growing with Cl^- concentration increase while those coefficients values for polymer inclusion membranes are decreasing with HCl concentration increase. To explain IF and PIM experimental results, the contributions of formed complex species of zinc(II) and cadmium(II) in aqueous chloride solution are needed. The percent molar contributions of chloride complex species for those metals versus Cl^- concentration are presented in Fig. 7. α_0 is the percent molar contribution of uncomplexed cations (i.e. Zn^{2+} and Cd^{2+}); α_1, α_2, α_3 and α_4 are percent molar contributions of complexed ions with 1, 2, 3, and 4 ligands, respectively (i. e. $ZnCl^+$, $ZnCl_2$, $ZnCl_3^-$ and $ZnCl_4^{2-}$ or $CdCl^+$, $CdCl_2$, $CdCl_3^-$ and $CdCl_4^{-2}$). Values of stability constants for Zn(II) + Cl^- and Cd(II) + Cl^- systems were taken from Beck (1990).

In the presence of chlorides at concentration range from $5 \cdot 10^{-5}$ to 0.10 M zinc(II) and cadmium(II) exist as cations in 100 – 97 % and 100 – 62 %, respectively (Fig. 7). But percent removal of both metals in ion flotation process with an anionic surfactant is much lower than values of $\alpha_0 + \alpha_1$ molar contributions (Fig. 1). This is caused by interfering influence of sodium cations. Percent removal of zinc(II) in IF process with a cationic surfactant remains very low in the whole range of Cl^- concentration (Fig. 3).

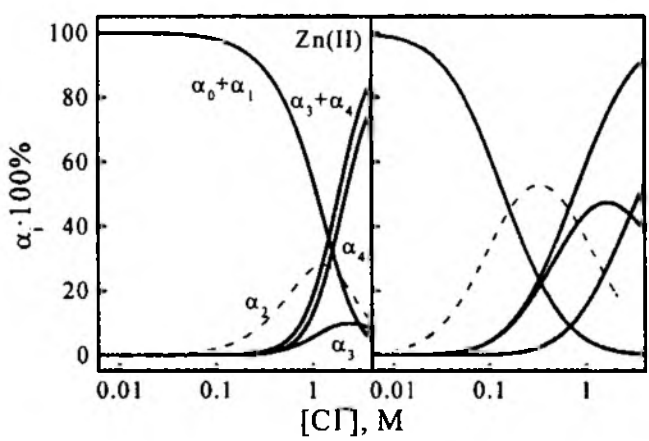

Fig. 7. Percent molar contributions ($\alpha_n \cdot 100\%$) of chloride complex species for zinc(II) and cadmium(II) vs. chloride concentrations

This correlates with low percent molar contribution of Zn(II) anionic forms (i.e. $\alpha_3 + \alpha_4$) which reaches 18 % at 1.0 M NaCl (Fig. 7). On the other hand cadmium(II) percent removal grows with Cl^- concentration increase and reaches 55 % at 1.0 M

NaCl (Fig. 3). This is in accordance with increase of percent molar contributions of anionic forms of Cd(II) up to 59 % at 1.0 M NaCl.

In case of polymer inclusion membranes the separation coefficients of Cd/Zn decrease with hydrochloric concentration increase. In addition, affinity of $CdCl_3^- + CdCl_4^{2-}$ anions to CPCl is higher than $ZnCl_3^- + ZnCl_4^{2-}$ anions to the cationic surfactant.

In case of polymeric inclusion membrane transport, which is significantly slower process (in comparison with IF), the main factor influencing the Cd/Zn separation is ratio of molar contributions of anionic forms for both metals. As it comes from Fig. 7, the mentioned ratio decreases with HCl concentration increase. Consequently the separation factor of Cd/Zn, which depends mainly on complexation reactions on source phase / membrane boundary, is decreasing with increase of hydrochloric acid concentration.

CONCLUSION

Zinc(II) and cadmium(II) can be effectively separated from aqueous chloride solutions in hydrometallurgical processes of ion flotation and polymer inclusion membranes. Ion flotation with a cationic surfactant (CPCl) allow to separate cadmium(II) from zinc(II) from dilute aqueous solutions ($c_{Me} = 1 \cdot 10^{-5}$ M) with separation coefficient increasing with Cl^- concentration increase. Competitive transport of zinc(II) and cadmium(II) from an aqueous chloride source phase ($c_{Me} = 1 \cdot 10^{-3}$ M) through polymer inclusion membranes containing tri-n-octylamine as ion carrier into aqueous ammonium acetate solutions also enables separation of cadmium over zinc. The selectivity coefficient of Cd/Zn for PIM decreases with HCl concentration increase in source phase. In both studied separation methods zinc(II) and cadmium(II) are removed from an aqueous chloride solutions in the form of $ZnCl_3^- + ZnCl_4^{2-}$ and $CdCl_3^- + CdCl_4^{2-}$, respectively. Results are discussed in terms of the chloride complex species stability for zinc(II) and cadmium(II).

ACKNOWLEDGMENT

Financial support of this work was provided by Polish Science Foundation Grants No. 3T09B08417 (for M. U.), No. 3T09B03516 (for C. K.) and No. 342285W-3 (for W. W.).

REFERENCES

BARTSCH R.A., WAY J., Eds. 1996, *Chemical Separation with Liquid Membranes*, ACS Symposium Series 642, Amer. Chem. Soc., Washington, DC.

BECK T. M., Ed. 1990, *Chemistry of complex equlibria*, Ellis Horwood Limited Publishers, Chichester.

BREEBROEK G.R.M., WITKAMP G.J., VAN ROSMALEN G.M. (1998), *Extraction of cadmium with trilaurylamine-kerosine through a flat-sheet-supported liquid membrane*. J. Membr. Sci., 147, 195-206.

BREEMBROEK G. R. M, VAN STRAALEN, A., WITKAMP G. J., VAN ROSMALEN G.M. 1998, *Extraction of cadmium and copper using hollow fiber supported liquid membranes*. J. Membr. Sci., 146, 185-195.

DANESI P. R., CHIARIZIA R., CASTAGNOLA A. 1983, *Transfer rate and separation of Cd(II) and Zn(II) chloride species by a trilaurylammonium chloride-triethyl-benzene supported liquid membrane*, J. Membr. Sci., 14, 161-174.

DAVIES G.A., Ed. 1987, *Separation Processes in Hydrometallurgy*, Ellis Horwood Ltd. Publ., Chichester.

DIAZ G., MARTIN D., LOMBERA C. 1995, *Zinc recycling through the modified Zincex process*. Recycling of Metals and Engineered Materials, P.B. Queneau and R.D. Peterson, Eds., Minerals, Metals and Materials Society, Warrendale, U.S.A., 623-635.

GRIEVES R.B., CHAREWICZ W.A. 1974, *Separation of the oxyanions of Re(VII), Mo(VI), Cr(VI), W(VI), and V(V) from a multicomponent solution at pH 6 by foam fractionation*, Anal. Letters, 7, 233-241.

HAYASHITA T. 1996, *Heavy metal ion separation by functional polymeric membranes*. ACS Symposium series 642, Chemical Separation with liquid membranes. R. A. Rartsch, J. D. Way, Eds., Washihgton DC, 303-318.

HAYASHITA T., KUMAZAWA M., YAMAMOTO M. 1994, *Selective permeartion of cadmium(II) chloride complex through cellulose triacetate plasticizer membrane containing trioctylmethylammonium chloride carrier*, Chemistry Letters, 37-39.

HOH Y.C., LIN C.Y., HUANG T.M., CHIU T.M. 1990, *Separation of cadmium from zinc in a chloride media by a supported liquid membrane*, Proc. of the International Solvent Extraction Conference. Solvent Extraction, Part B, 1543-1548, Ed. by A. Sekine, S. Kusakabe, Elsevier, Amsterdam 1992.

HUALING D., ZHIDE H. 1989, *Ion flotation behavior of thirty one metal ions in mixed hydrochloric/nitric acid solutions*, Talanta, 36, 633-637.

JURKIEWICZ K. 1990, *The removal of zinc solutions by foam separation. I. Foam separation of complex zinc anions*, Intern. J. Min. Process, 28, 173-188.

LEMLICH R. Ed., 1972, *Adsorptive bubble separation techniques*, Academic Press, New York.

OCHS L. R., FLETCHER W.A., WEBER H., NADEN D. (1983), *Metal sulphide extraction*, U.S. Pat. No S11464, 240-287.

SUIGRA M., KIKKAWA M., URITA S. 1987, *Effect of plasticizer in carrier-mediated transport of zinc ion through cellulose triacetate membranes*,. Sep. Sci. Technol., 22, 2263-2271.

URTIAGA M., ORTIZ I. 1999, *Comparison of liquid membrane processes for the removal of cadmium from wet phosphoric acid*, J. Membr. Sci., 164, 229-240.

WALKOWIAK W. 1992, *Mechanism of selective ion flotation technology, In: Innovation in flotation technology*, Edited by P. Mavros, K. A. Matis, *NATO ASI Series, Kluwer Academic Publishers, London*, 455-473.

WALKOWIAK W., BHATTACHARYYA D., GRIEVES R. B. 1976, *Selective foam fractionation of chloride complex of Zn(II), Cd(II), Hg(II), and Au(III)*, Anal. Chem., 48, 975-473.

WALKOWIAK W., GRIEVES R. B. 1976, *Foam fractionation of cyanide complex of zinc(II), cadmium(II), mercury(II), and gold(III)*, J. Inorg. Nucl. Chem., 38, 1351-1356.

WALKOWIAK W., ULEWICZ M. 1999, *Kinetics studies of ion flotation*, Physicochemical Problems of Mineral Process, 33, 201-214.

Kozłowski C., Ulewicz M., Walkowiak W., Rozdział jonów cynku i kadmu z roztworów chlorkowych w hydrometalurgicznych procesach flotacji jonowej i ciekłych membran *Fizykochemiczne Problemy Mineralurgii*, 34, 141–151 (w jęz. angielskim)

Zbadano selektywność procesu wydzielania jonów cynku(II) i kadmu(II) z wodnych roztworów chlorkowych zawierających równomolową mieszaninę jonów obu metali za pomocą flotacji jonowej (IF) i polimerycznych membran inkluzyjnych (PIM). Pokazano wyniki IF z rozcieńczonych roztworów wodnych (c_{Me}=1,0·10^{-5} M) za pomocą kolektora anionowego (dodecylobenzenosulfonian sodu) i kationowego (chlorek cetylopirydyniowy). Wykazano, że dla kolektora kationowego ze wzrostem stężenia chlorków selektywność flotacji Cd/Zn wzrasta. W pracy prezentowane są również wyniki transportu Zn(II) i Cd(II) z wodnej fazy zasilającej (c_{Me}=1,0·10^{-3} M) przez PIM zbudowaną z trójoctanu celulozy (nośnik), eteru o-nitrofenylopentylowego (pastyfikator) i tri-n-oktyloaminy (przenośnik jonów). Selektywność transportu przez PIM malała wraz ze wzrostem stężenia HCl w fazie zasilającej. Wyniki przedyskutowano w świetle zakresów trwałości poszczególnych form jonów kompleksowych Zn(II) i Cd(II). W obu procesach tj. IF i PIM wydzielane jony cynku i kadmu występowały w formie anionów tj. $ZnCl_3^- + ZnCl_4^{2-}$ oraz $CdCl_3^- + CdCl_4^{2-}$.

Physicochemical Problems of Mineral Processing, 34 (2000), 153–161
Fizykochemiczne Problemy Mineralurgii, 34 (2000), 153–161

Ashraf AMER*

PROCESSING OF EGYPTIAN BOILER-ASH FOR EXTRACTION OF VANADIUM AND NICKEL

Received March 15, 2000: reviewed and accepted May 15, 2000

Egyptian boiler ashes from thermal power stations contain up 20% vanadium and 22% nickel and thus they are valuable source for vanadium and nickel and their alloys as well as chemicals. The ash was directly leached with sulphuric acid under atmospheric pressure and in an autoclave. Atmospheric leaching leads to complete dissolution of vanadium and nickel together with iron. Separation of iron from vanadium is very difficult due to a narrow pH precipitation range of hydroxides of these metals, leaching under oxygen pressure leads to oxidation of iron and its precipitation as basic iron sulphate leaving vanadium and nickel in solution. Vanadium is thus precipitated as hydroxide by adjustment of pH value and then calcinated to vanadium penta-oxide. The leaching processes were thoroughly investigated and the optimum leaching conditions were determined.

Key words: boiler ash, pressure leaching, vanadium, nickel

INTRODUCTION

Egyptian crude oil contains considerable amounts of vanadium and nickel. These metals are concentrated in the heavy fraction obtained from the fractional distillation process. The heavy fraction is used as a fuel in electrical power stations and consequently the metals (vanadium, nickel) are concentrated in the ash. The standard method applied for recovery of vanadium from vanadium containing slag

* Department of Environmental Sciences, Faculty of Science, Alexandria University, Alexandria, Egypt.

consists of roasting the ash in a rotary kiln at 800 °C for 3 hr. followed by leaching with water to produced soluble sodium vanadate (Sastry, 1968; Solbodin, 1975; Cheng, 1987; Audin, 1988 and Chandra et al., 1998). The world consumption of vanadium increases in the last five years due to its utilization as special alloys such as ferrovanadium and special steels. Steel industry consumes about 90% of vanadium production (Ruhle, 1981; Pawlek, 1983; Campbell, 1999; Halikia, 1991; Martins, 2000). The present investigation aims at optimizing the conditions of extraction of vanadium and nickel by hydrometallurgical processing of Egyptian boiler ash using aqueous sulphuric acid under atmospheric and oxygen pressure to produce leach liquor of sulphates of both vanadium and nickel free from iron. The parameters affecting the leaching process such as temperature, sulphuric acid concentration, time and oxygen partial pressure were systematically studied.

EXPERIMENTAL

The Egyptian boiler ash samples were collected from different power stations which use fossil oil as fuel. The samples were crushed, ground and sieved to 100% (-250 μm). Chemical composition of studied sample is given in Table (1).

Table 1. Chemical analysis of studied boiler ash

Composition	%
V	20.0
Ni	22.0
Fe (total)	4.67
CaO	3.10
SiO_2	3.57
Al_2O_3	1.70
Cr_2O_3	1.50
MgO	1.10
ZnO	0.98
H_2O (100°)	10.00
H_2O (700°)	6.00

Atmospheric leaching was carried out in a glass reactor placed in a thermostatically controlled water bath. Pressure leaching experiments were carried out in a $2dm^3$ capacity vertical autoclave gas inlet/outlet. The container is made of titanium to resist acid corrosion. The feed is first placed in the titanium container, which is then placed in autoclave. The pressure vessel was closed and thoroughly flushed with oxygen gas. The autoclave was heated to the required temperature at

agitation maintained a 1200 rpm. Oxygen gas was then introduced upon the attainment of the desired temperature (Hahn, 1965 and Amer, 1987). Samples were collected at various time intervals, filtered and analyzed for vanadium and nickel.

RESULTS AND DISCUSSION

Dissolution of vanadium and nickel in sulphuric acid under the atmospheric conditions is explained as follows:

$$V_2O_3 + 3H_2SO_4 = V_2(SO_4)_3 + 3H_2O \quad (1)$$

$$NiO + H_2SO_4 = NiSO_4 + H_2O \quad (2)$$

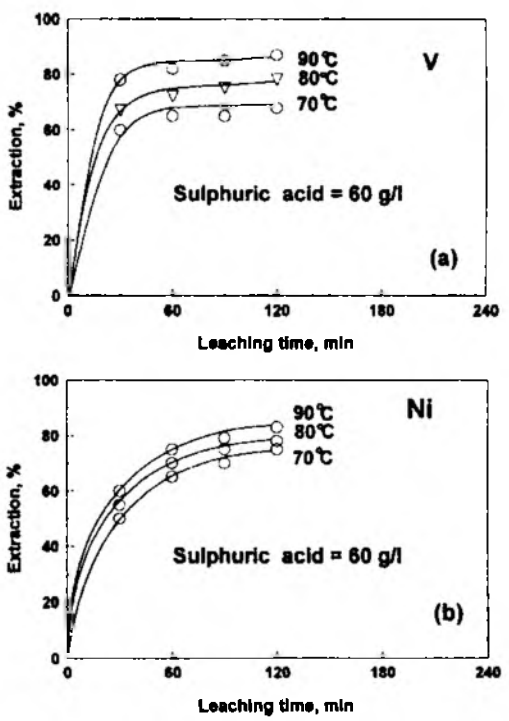

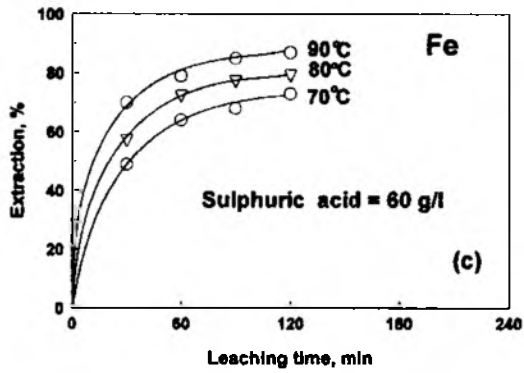

Fig. 1: Effect of leaching temperature upon the dissolution of vanadium nickel and iron under atmospheric conditions

Figure (1) shows the effect of temperature and time on leaching of boiler ash with 60 g/dm^3 sulphuric acid concentration at a solid-liquid ratio of 0.5. The degree of extraction of vanadium, nickel and iron increases with the increase of temperature. During the first 30 minutes, a sharp increase in recovery was observed, then the rate of dissolution becomes relatively slower till a constant recovery was achieved after 120 min.

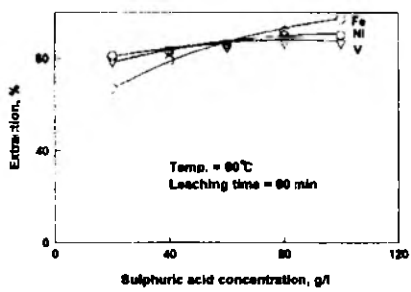

Fig. 2: Effect of sulphuric acid concentration upon dissolution of vanadium, nickel and iron under atmospheric conditions

Figure (2) shows the effect of sulphuric acid concentration on leaching of boiler ash at 90 °C and at solid-liquid ratio of 0.5 for 60 min leaching period. The percentage of vanadium, nickel and iron increases upon increasing acid concentration. Moreover, atmospheric leaching leads to 80% dissolution of iron. Separtation of iron from vanadium is very difficult due to narrow pH range of precipitation of hydroxides of these two metals (vanadium and nickel).

Leaching under oxygen pressure was recommended for oxyhydrolysis of ferrous sulphate and iron precipitation as iron oxide leaving vanadium and nickel in solution. The mechanism of iron oxidation was given by many authors (Sohn, 1979; Anand, 1988). The most important variables affecting the leaching process are: temperature (160-220 °C), oxygen partial pressure (5-20 bar) and sulphuric acid concentration (40-80 g/L).

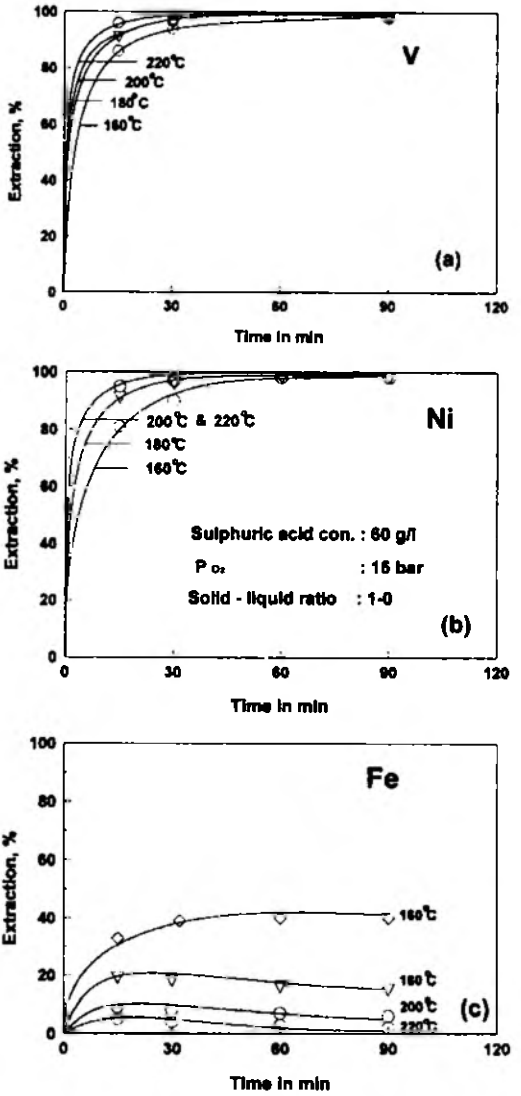

Fig. 3: Effect of temperature on the extraction of vanadium, nickel and iron under oxygen partial pressure

Figure (3) shows that the leaching rate of vanadium and nickel increases with increase of temperature in the range of 160-220°C. After 15 min at 220°C complete extraction of vanadium and nickel (97%) was reached with only 4% iron dissolution.

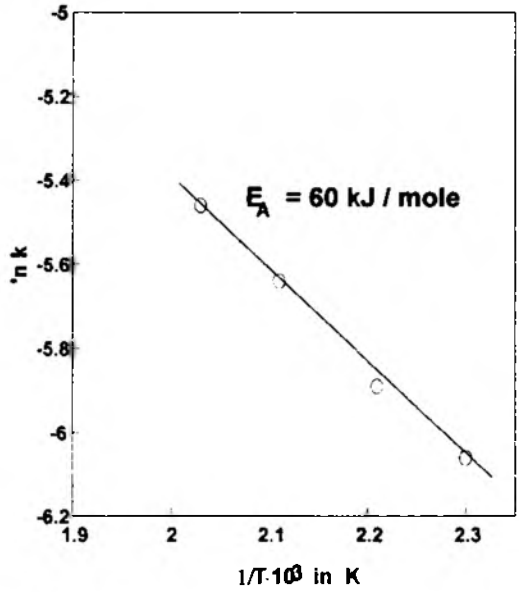

Fig. 4: Arrhenius plot for determination of apparent activation energy, data from Figure (3b)

From Arrhenius plot as shown in Fig. (4) the calculated value of apparent activation energy amounts 60 kJ/mole which is in good agreement with the value of 57 kJ/mole calculated from the oxidation of Fe (II) in aqueous sulphuric acid under oxygen pressure (Anand, 1989). The calculated value of apparent activation energy (60 kJ/mole) indicates that the reaction is chemically controlled (Sohn, 1979). The effect of partial oxygen pressure on the leaching rate is shown in Fig. (5). The leaching rate of both vanadium and nickel was slightly increased as the partial oxygen pressure increases from 5 up to 15 bar. The mechanism of oxyhydrolysis of iron sulphate is illustrated as follows:

$$2FeSO_4 + H_2SO_4 + 1/2\ O_2 = Fe_2(SO_4)_3 + H_2O \quad (3)$$

$$Fe_2(SO_4)_3 + 3H_2O = Fe_2O_3 + 3H_2SO_4 \quad (4)$$

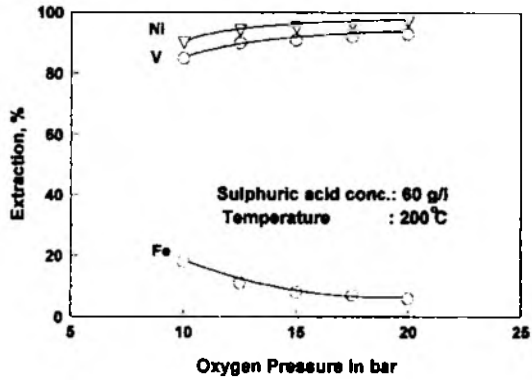

Fig. 5: Effect of oxygen partial pressure on the dissolution of vanadium, nickel and iron

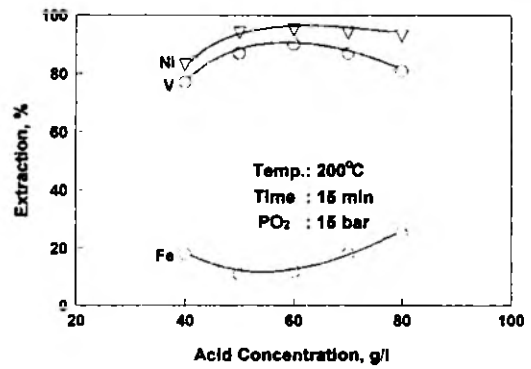

Fig. 6: Effect of sulphuric acid concentration on the extraction of vanadium, nickel and iron

The effect of sulphuric acid concentration on the leaching rate is shown in Fig. (6), the extent of vanadium and nickel recovery was about (95%) using acid concentration of 50 g/dm^3. The extent of iron dissolution was slightly increased at sulphuric acid concentration above 60 g/ dm^3, howeverm most of the iron (III) had precipitated as a result of hydrolysis. Vanadium and nickel were leached nearly completely at 50–60 g/dm^3 sulphuric acid concentration.

CONCLUSION

Direct H_2SO_4 processing of Egyptian boiler ash to produce both vanadium and nickel sulphate was achieved by pressure leaching under oxygen pressure. Iron is converted to basic iron sulphate which is then hydrolysed to iron oxide. The optimum conditions of pressure leaching process are; temperature 200 °C, partial

oxygen pressure 15 bar, sulphuric acid concentration 60 g/ dm^3 leaching period 15 min.

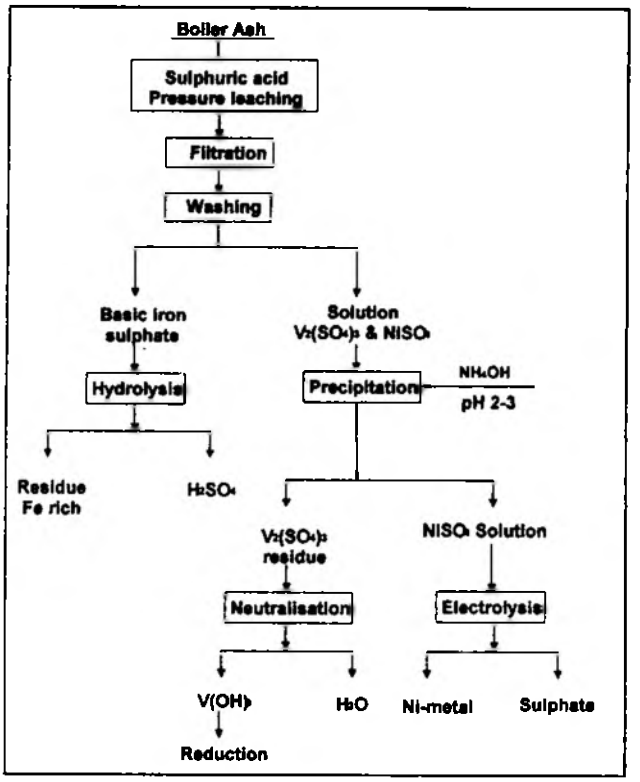

Fig. 7: Flow sheet of sulphuric acid pressure leaching of boiler ash

REFERENCES

CHENG, H. (1987), *Roasting of Vanadium Slag in Rotary Kiln and Extraction of Vanadium.* Faming Zhuanli Shenging gangkai Shuomingshu. CN 86, 108, 218 (CI. CO 1 31/02).

SASTRY, A.R (1968), *Parameters of leaching in the Soda Roasting Process for the Extracting of Vanadium from Titaniferous Magnetite Ores of Andh.* Chem. Age. India 3, pp. 195-201.

SOLBODIN, B.V. (1975), *The Extraction of Vanadium from Slag and Slag and Deposits from Power Stations. Russion Collection Publish., in Tr-Inst. Khim, Ural. Nauchn.* Tsentr. Akad. Nauk. Sverdlovsk 81.

AYDIN, A (1988), *Recovery of vanadium compounds from the slags and fly ashes of power plants, Chim.* Acat. Turc. 16(2), 153-82.

CHANDRA, K.S., SUBRAMANIAN, S. ET AL. (1998). *Removal of metal ions using an industrial biomass with reference to environmental control.* Int. J. Miner. Process. 53, pp. 107-120.

PAWLEK, F. (1983), *Metallhuttenkunde*, Walter Gruyter, Berlin. New York, pp. 737.

RUHLE, M. (1981), *Rohstoff profile Vanadium II.* Zolle, Preise, Nachfrageseite, Metall., 35, pp. 1282-3.

CAMPBELL, G (1999), *Recent Trends in World Metal Consumption.* Raw Mat. Rep. 14, No.1, pp. 15-26,.

MARTINS, A.H (2000), *Vanadium Precipitation from sulphate acid solutions acid solutions.* Can. Met. Quarterly. Vol. 39, No.1, pp. 15-22.

HALIKIA, L (1991), *Parameters influencing kinetics of nickel extraction from Greek laterite during leachin*, 20; pp. 155-68.

Ashraf AMER, Przeróbka egipskich popiołów po spalaniu oleju opałowego dla odzysku wanadu i niklu, *Fizykochemiczne Problemy Mineralurgii*, 34, 153–161 (w jęz angielskim)

Egipskie popioły z elektrociepłowni zawierają do 20% Vi 22% Ni. Popioły ługowano bezpośrednio pod ciśnieniem atmosferycznym araz w autoklawie. Ługowanie pod ciśnieniem atmosferycznym prowadzi do całkowitego rozpuszczenia wanadu i niklu razem z żelazem. Separacja wanadu od żelaza jest trudna z powodu wąskiego zakresu pH wytrącania się wodorotlenków tych metali. Ługowanie pod ciśnieniem tlenu prowadzi do utleniania się żelaza i jego precypitacji w formie zasadowego siarczanu żelaza a V oraz Ni pozostają w roztworze. Vanad ulega następnie wytrąceniu jako wodorotlenek przez regulację pH i dalej jest kalcynowany do pięciotlenku. Proces ługowania był dokładnie przebadany i określono optymalne warunki procesu.

Physicochemical Problems of Mineral Processing, 34 (2000), 163 - 170
Fizykochemiczne Problemy Mineralurgii, 34 (2000), 163 - 170

V.A.CHANTURIYA*, A.A.FEDOROV*, T.N.MATVEEVA*

THE EFFECT OF AUROFERROUS PYRITES NON-STOICHIOMETRY ON THEIR FLOTATION AND SORPTION PROPERTIES

Received March 15, 2000; reviewed and accepted May 15, 2000

The attempt to explain the differences in sorption and flotation properties of auroferrous pyrites of several deposits from positions of inconstancy of iron to sulfur proportion (non-stoichiometry) has been undertaken. The effect of natural pyrites non-stoichiometric composition on their surface ability to oxidation, as well as, on the correlation between sulfite- and sulfate-ions in liquid phase during pyrite flotation has been shown. It has been found, that the collector chemisorption on pirytes with a non-stoichiometric composition has increased. The sulfur/iron ratio in natural auriferous pyrites correlates with their flotation properties at the range of pH 9-12.

Key words: auroferrous pyrite, flotation, adsorption

INTRODUCTION

The study of geochemical peculiarities of great number of pyrites from various types of deposits (Korobeynikov et al. 1993) has shown, that the pyrites of any origin always contain gold. The gold content varies from $n \cdot 10^{-6}$ up to $n \cdot 10^{-3}$ %. The pyrites from gold ore deposits are characterized by a wide range of admixed elements. Gold, silver, copper, lead, zinc and arsenic are concentrated in the elevated amounts and differ by maximal inaccuracy of statistical distribution parameters. The basic reasons of mineral differences in both semi-conductive and physical characteristics are

* Institute of Comprehensive Exploitation of Mineral Resources (IPKON), Russian Academy of Sciences, Kryukovskiy Tupic 4, Moscow 111020, Russia, e-mail fedorov@ipconran.ru

isomorphous presence of these impurities in pyrite structure and the steoichometry deviation of the main components (iron and sulfur).

Flotation models (Avdochin and Abramov, 1989) without taking into account the crystal-chemical minerals singularities, elements-impurities, structural defects of natural sulfides are unsuitable to explain the flotation-depression conditions. The efforts to discover the relationships between physical characteristics and impurity composition of natural pyrites on one hand, and their flotability and sorption properties on the other were undertaken (Krasnikova, Krasnikov, 1978; Eliseev et al. 1979). However, the results of these studies were not completely conclusive. The studies of auroferrous pyrite and arsenopyrite selective flotation have shown that copper and gold isomorphous admixtures have the dominant effect on the mineral properties (Chanturiya et al. 1997, 1998).

The idea of the correlation of physicochemical solid-state properties of sulfide minerals with their flotability and electrochemical aspects of sulfide flotation has been studied by Woods and Richardson (1986), as well as, Hamilton and Woods (1984). The investigation of the surface compounds composition during the pyrite flotation showed, that dixanthogen is a main form of buthylxanthate adsorbed on the pyrite surface. However, the presence of metal-xanthate compounds and their formation conditions are not full accepted (Leppinen et al. 1995; Brandsaw 1997).

The influence of gold-content factor on the pyrite properties is connected with increasing the structural defects when gold is concentrated by a mineral. Raising the arsenic admixture contents and forming the acceptor sulfide vacancies when gold is introduced into the crystal lattice are next reasons (Tauson et al. 1996). The electro-physical characteristics of auriferous pyrite samples vary in broad range. The specific resistance and thermo-electromotive force can have different values inside of one mineral aggregate. The conductivity sign is connected with the "shut-off zone" formation.

It is considered that balance change at the S^{2-} vacancies formation causes an increase of n-type conductivity and on the other hand, the Fe^{2+} vacancies formation results in the p-type conductivity. The modification of pyrite crystalline structure is accompanied by transferring from the p to n conductivity. It is known, that the acceptor centers formation in hydrothermal pyrite, when substituting of divalent iron by univalent gold, causes its affinity to the electron. According to the Lewis acids and bases theory, the auriferous pyrites should reveal acidic properties.

Thus, all the gold-containing FeS_2 natural crystals in greater or smaller degree are defective. These crystals often contain cationic or anionic vacancies with non-stoichiometric composition. In the presented work on attempt to correlate the sulfur/iron ratio in natural auriferous pyrites with their flotation properties has been undertaken.

MATERIALS AND EXPERIMENTAL METHODS

Pyrites from five deposits have been examined. The data on the contents of iron, sulfide and free sulfur, donor (Cu) and acceptor (As) impurities in the samples are given in the Table 1. The true formulas of mineral pyrites have been calculated from the iron and sulfide sulfur analytical ratio.

Ground mineral samples were agitated in distilled water in the presence of pH regulator. The liquid phase within the range of pH 6-12 was analyzed for the content of sulfide and sulfite ions. The inverse iodimetric titration and lead nitrate titration at the presence of dithizon methods were used (Lurie, 1984). An amount of elementary sulfur at the mineral surfaces, quantities of adsorbed butyl xanthate under different pH values were analyzed by using UV-spectroscopy with Specord M 40.

Experimental conditions for determination of oxidized and reduced forms of sulfur compounds were as follows: 2 g of -0,16+0, 063 μm mineral sample was mixed with 40 ml of liquid phase than the suspension was conditioned by10 minutes. The suspension pH regulated with NaOH.

Table 1. Elemental composition and non-stoichiometry of pyrite samples

Sample No	Content % Fe	S Sulfide	Cu	As	g/t Au	mg/g S free	Real formula	Non-stoich-metry: ($S/S_{theoretic}$)
1	42,0	45,0	0,2	0,04	10	0,11	$FeS_{1.87}$	0,94
2	33,2	45,55	3,2	0,01	10	0,33	$FeS_{2.39}$	1,2
3	41,5	36,6	0,6	0,3	1	0,77	$FeS_{1.54}$	0,77
4	38,3	33,8	0,8	2,5	40	0,23	$FeS_{1.55}$	0,78
5	38,7	45,5	0,14	0,1	10	0,19	$FeS_{2.05}$	1,03

For flotation tests 1g of mineral samples were used. Mechanical flotation cell having 20 ml in a volume was used. Xanthate and frother dosages were 300 and 150 g/t respectively. The conditioning and flotation time was 2 minutes.

RESULTS AND DISCUSSION

The analysis of the studied pyrite characteristics (Table 1) has allowed to classify them according to types which reflects the relations between the structure and composition for non-stoichiometric compounds (Wadsley, 1964). The deviation from a multiplicity of cationic and anionic parts proportions in samples (1) and (5) is connected with the lack of sulfur and iron variable amounts in mineral structure

(deduction). Non-stoichiometry of sample (2) and sample(4) can be explained by admixtures (copper or arsenic) entering the mineral lattice (interpolation). Displacement dominates in the sample (3) which is rich in free sulfur. The iron atoms can be located in sulfur positions becoming vacant during oxidation of S^{2-} to S^0.

A comparison of the ration of substantial and stoichiometric of sulfide sulfur contents ($S/S_{theoretic}$) and free sulfur amounts on their surfaces has shown the following features. The deviation from a stoichiometry of mineral samples composition strongly influences their surface abilities to oxidation. Therefore, free sulfur is determined at pyrite surfaces (sample 1) and (sample 5) where small deflection from a stoichiometry (0,11 and 0,19 mg/g) existed. On the other hand, samples with considerable excess of sulfur (sample 2) and (sample 3) show a deficit of anionic parts (0,33 and 0,77 mg/g). Influence of gold content on pyrite surface oxidation is marked. Sample (3) (1g/t Au) and sample (4) (40 g/t Au) are characterized by approximately identical deviation from a stoichiometric sulfide sulfur content, however amount of free sulfur on an auriferous sample is 3 times less in this case.

It is known, that when increasing the oxygen concentration and sulfur contact endurance the further oxidation with liberation of mineral surface will be happen (Glazunov,1998).The peculiarity of such processes in the mineral suspension at non-stoichiometry pyrite positions, were observed. The curves in the Fig. 1 and 2 illustrate the variation of the sulfite and sulfate ion concentrations at the mineral suspensions in the range of pH 6-12. Pyrite, with an excess of anionic part is characterized by a formation of sulfites and sulfates in less degree (curve 5, Fig. 1 and Fig. 2). In the case of pyrite with a deficit of anionic components the sulfur is oxidized up to sulfates (curve 1, Fig. 2). Under the equal starting oxygen concentration in liquid phase of sample (1) and sample (5) it is possible to suspect, that pyrites with a shortage of sulfide anions are oxidized up to the highest sulfur oxidation degree (+6), and pyrites with an excess of sulfide anions oxidized up to intermediate degree (+4). This conclusion is correct at the values of pH>9, where the sulfites are rather stable only in alkaline conditions. An anionic part surplus in the sample (2) and its deficit in the sample (4), and also free sulfur amount on their surfaces are considerably higher than the same parameters at sample (5) and sample (1). However, sulfur oxidation in liquid phase is more gentle (curves 2 and 4). In this case a free sulfur surface film on the mineral surface is inconvertible enough and it is not removed during contact to fluid phase. The sample (3) is characterized by the greatest deficit of anionic part and free sulfur content and the sulfur surface is oxidized both to sulfites and sulfates (curve 3, Fig.1 and Fig. 2 respectively). Thus, at the deviation from a proportion multiplicity of cationic and anionic parts in pyrites as can be dedicated (sample 1 and sample 5) the free sulfur is removed from the surface and passes in a liquid phase as sulfur-containing ions with a degree of oxidation (+4) or (+6). The non-stoichiometry of pyrite which aroused by the interpolation of elements-admixtures (samples 2 and 4), causes the formation of an inconvertible free sulfur film on the mineral surface. The

failure of stoichiometry as a displacement (sample 3) is characterized by considerably major content of free sulfur, however, it dissolves partially as sulfites and sulfates at the fluid phase contact.

The deviation of pyrites composition from a stoichiometric iron to sulfur proportion with formation both cationic, and anionic vacancies testifies to partial crystal lattice destruction. This destruction effects on the adsorbed xanthate forms on the mineral surface. The relationship between chemisorbed form of collector and a proportion of a substantial and idealized content of sulfide sulfur is illustrated in Fig. 3.

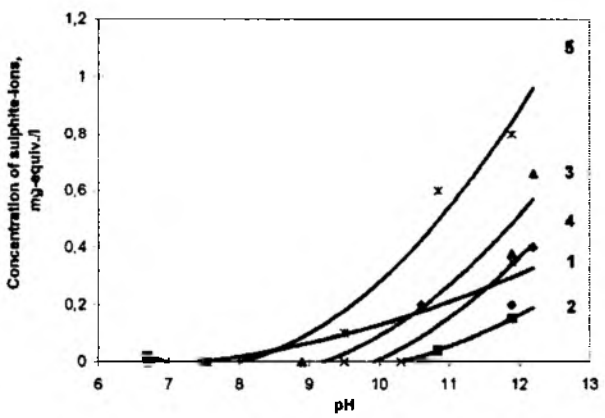

Fig.1. Sulfite-ions concentration in liquid phase of pyrite suspensions as a function of pH
1; 2; 3; 4; 5 – sample number

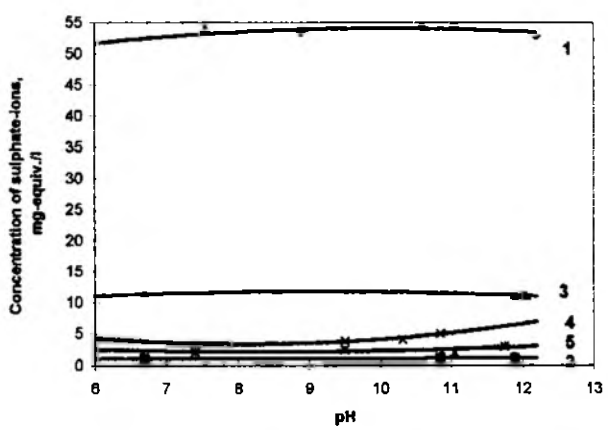

Fig.2. Sulfate-ions concentration in liquid phase of pyrite suspensions as a function of pH
1; 2; 3; 4; 5 – sample number

The non-stechiometry increase as a result of anionic part surplus or its shortage, results in the increase of chemical sorption. From the collected data such as free sulfur amount and its stability on the mineral surfaces, and a magnitude of the collector chemisorption, it is possible to suspect, that samples with a deviation in iron and sulfur ration will show a different behavior in flotation.

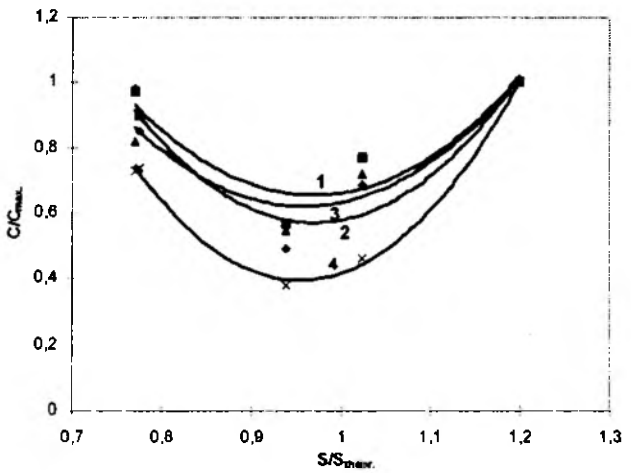

Fig.3. Xanthate chemisorption as a function of pyrites anionic part non-stoichiometry
1 – pH 9; 2 – pH 10; 3 – pH 11; 4 – pH 12

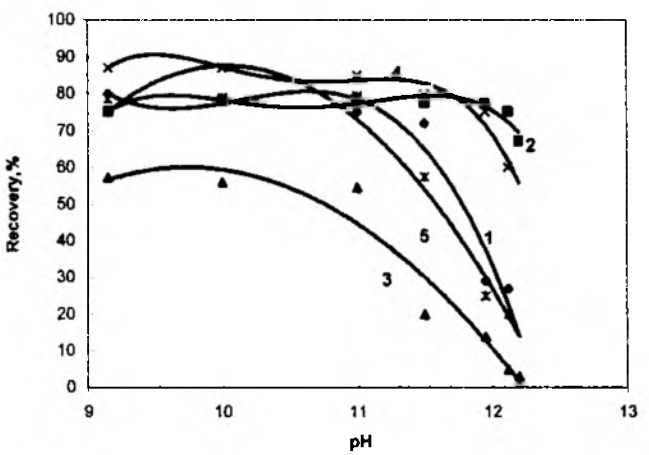

Fig.4. Floatability of pyrite samples as a function of pH, 1; 2; 3; 4; 5 – samples numbers

The analysis of pyrite flotation curves as a function of pH (Fig. 4) has shown, that sample (1) and sample (5) exhibit similar floatation properties. The pyrite recovery was about 80 % in a range of pH 9-11. The further raise of liquid phase alkalinity causes a partial depression. The pyrite recovery do not exceed of 25 % at pH equals 12-12,2 .

Sample (2) and sample (4), with high content of copper, arsenic and gold impurities and high values of non-stoichiometry, were effectively floated even in strongly alkaline conditions at pH 11,8-12,2.

Sample (3), which is rich in surface sulfur and has the most defective crystal lattice resulted in a displacement of sulfide vacancies by iron atoms, is the most responsive to the alkaline depression.

CONCLUSION

The experimental investigations onto geochemical differences and structural irregularities, as well as onto oxidizing, sorption and floatation characteristics of auroferrous pyrites have been performed. It was found, that the deviation from a stoichiometry of the basic components - iron and sulfur can be used for the forecasting technological properties of minerals under hard-to-benificate gold ores processing.

The relationship between pyrites non-stoichiometry and their oxidation ability is detected. The minerals having structure close to stoichiometric, are oxidized with transferring sulfide sulfur into sulfite and sulfate ions. Thus, oxidation of pyrite with an excess of anionic part occurs up to a stage of sulfites ions formation, and with a deficit - up to sulfates ions. A limiting stage of oxidation process of pyrite with a maximal deficit of sulfide part is the free sulfur formation.

Pyrites non-stoichiometry caused by the elements-admixtures intrusion results in formation as surplus (donor impurity of copper), and shortage (acceptor impurity of arsenic) of anionic part. The similar non-stoichiometry of iron/sulfur ratio essentially raises the chemisorbed collector content and ensures the pyrites floatability even in strong alkaline solutions.

REFERENCES

AVDOCHIN V.M. AND ABRAMOV A.A. (1989), *Oxidation of sulfide minerals in mineral processing*, Nedra, Moscow, pp. 98-170.

BRADSHAW D.J. AND O'CONNOR C.T. (1997), *The Synergism of thiol collection in a mixture used for the flotation of pyrite*, Proc. of XX IMPC, Aachen, pp. 343-354.

HAMILTON I.C. AND WOODS R. (1984), *A voltammetric study of the surface oxidation of sulfide minerals*, Proc. Intern. Symp. on Electrochem. in Miner. and Metal Processing, pp. 259-285.

CHANTURIYA V.A., FEDOROV A.A., BUNIN I.J. (1998), *The reports of Academy of sciences*, vol. 362, No.4, pp. 513-517.

CHANTURIYA V.A., FEDOROV A.A., MATVEEVA T.N. (1997), *Physicist-technical problems of mineral resources exploitation*, No.6, pp. 110-115.

ELISEEV N.I. et.al. (1979), *Modern conditions and prospects of flotation theory development*, Nauka, Moscow, pp. 232-237.

GLAZUNOV L.A. (1999), *On hydrophobization of minerals at flotation*, Tzv. Metallurgiya, No 8-9, pp. 21-24.

KOROBEYNIKOV A.F. et.al. (1993), *Pyrites from gold ore deposits (characteristics, zone properties, practical application)*, CNIGRI, Moscow, pp. 60-122.

Krasnikova T.I. and Krasnikov V.I., 1978, Mineral composition and mineral processing. Nauka, Moscow, pp. 99-105.

LEPPINEN J. et. al. (1995), *FTIR and XPS studies of surface chemistry of pyrite in flotation*, Proc. of XIX IMPC, vol. 3, pp. 35-38.

LURIE YU.YU. (1984), *Analytical chemistry of industrial sewages*, Chemistry, Moscow, pp. 197-210.

TAUSON V.YA., MIRONOV A.F., SMAGINOV N.V. (1996), *Gold in sulfides: state, problem of the forms of determination and prospects of experimental studies*, Geology and geophysics, Moscow, vol. 37, No. 3, pp. 3-14.

WADSLAY A.D. (1964), *Inorganic non-stoichiometric compounds*, Non-stoichiometric compounds, Academic Press, New-York, pp. 99-209.

WOODS R. AND RICHARDSON P.E. (1986), *The flotation of sulfide minerals – electrochemical aspects*, Adv. Miner. Process. Pros. Symp., New Orleans, pp. 154-170.

The work has been done under the support of Russian Fundamental Investigations Foundation, grant 99-05-65236.

V.A.Chanturiya, A.A.Fedorov, T.N.Matveeva, Wpływ niestechiometrii złotonośnego pirytu na właściwości flotacyjne i adsorpcyjne, Fizykochemiczne Problemy Metalurgii 34 (2000), 163 –170, (w jęz. ang.)

W pracy podjęto próbę wyjaśnienia różnic w właściwościach sorpcyjnych i flotacyjnych pirytów pochodzących z różnych złóż. Różnice we własnościach pirytu uzależniono od proporcji podstawień atomami żelaza i siarki czyli odstępstwami od stechiomerycznego składu pirytu. Wpływ tej naturalnej niestechiometryczności składu pirytu upatrywano w lepszej zdolności do utleniania, jak również, korelowano ten fakt z stężeniem jonów siarczanowych i siarczynowych w roztworze w trakcie flotacji. Zostało pokazane, że chemisorpcja kolektora wzrasta na pirytach o niestechimetrycznym składzie. Stosunek siarka/żelazo w naturalnych złotonośnych pirytach koreluje dobrze z wynikami flotacji w zakresie pH 9-12.

Wydawnictwa Politechniki Wrocławskiej są do nabycia w następujących księgarniach:
„Politechnika", Wybrzeże Wyspiańskiego 27,
50-370 Wrocław, budynek A-1 PWr, tel. (071) 320 25 34
„Tech", plac Grunwaldzki 13,
50-377 Wrocław, budynek D-1 PWr, tel. (071) 320 32 52
Prowadzimy sprzedaż wysyłkową

ISSN 0137-1282

Physicochemical Problems of Mineral Processing, 34 (2000)